

Rosnelo Fernandes

Design and Validation of a New Control Mechanism for PoLaRS SATA Multi-DOF Instruments



Design and Validation of a New Control Mechanism for PoLaRS SATA Multi-DOF Instruments

By

Rosnelo Fernandes

in fulfilment of the requirements for the degree of

Master of Science

in Mechanical Engineering (BioMechanical Design)

at the Delft University of Technology,
to be defended publicly on Thursday April 19, 2018 at 14:00 hr.

Internal Supervisor:	Prof. dr. ir. Jenny Dankelman, TU Delft Assistant Prof. dr. ir. Tim Horeman, TU Delft
External Supervisor:	Benno Groosman MScBA, Surge-On Medical B.V.
Thesis committee:	ir. J.W. (Jo) Spronck, TU Delft

This thesis is confidential and cannot be made public until April 19, 2019.

An electronic version of this thesis is available at <http://repository.tudelft.nl/>.

Preface

The Master Thesis “Design and Validation of a New Control Mechanism for PoLaRS SATA Multi-DOF Instruments” describes the development of a new system for controlling the SATA instrument for performing laparoscopic surgeries. It has been written in fulfilment of the graduation requirements for the master program Mechanical Engineering at Delft University of Technology (TU Delft). This is the final phase of my studies in the track of BioMechanical Design with a specialization in BioInspired Technology. The project was undertaken at Surge-On Medical B.V. and TU Delft under the external supervision of Benno Groosman MScBA CEO Surge-On Medical B.V. and internal supervision of Assist. Prof.dr.ir. Tim Horeman and Prof. dr. Jenny Dankelman from TU Delft.

The Master Thesis has been an interesting learning experience for me, not only in terms of technical knowledge but also in managing setback and delays. It also helped me grow in learning to work in co-operation with other colleagues, working on other components needed for this thesis. Another outcome of the master thesis was in learning to use the different machines in the workshop for making machining parts and learning about how different materials interact with each other.

I wish to thank Assist. Prof.dr.ir. Tim Horeman, for his input and help in development of this thesis and comments and corrections on this report. I would like to thank Prof. dr. Jenny Dankelman for her comments on my report. I also thank Ing. Arjan van Dijke, for the lab facilities and help in obtaining electronic components. I wish to thank the staff from the workshop for their help in providing the machines for use.

I also thank my friends, colleagues and my family for their constant support, not only during the thesis project but for the entire duration of my study.

*Rosnelo Fernandes
Delft, April 2018*

Contents

Preface.....	iv
Contents	v
Abbreviations List.....	vii
List of Figures	viii
List of Tables	x
Abstract	xi
1. Introduction.....	1
1.1. Laparoscopy	1
1.2. Robotic Laparoscopy	2
1.3. Laparoscopy in Low and Middle income countries.....	4
1.4. PoLaRS –Internship & Thesis Literature.....	4
1.4.1. Internship	5
1.4.2. Thesis Literature Study	5
1.5. SATA Instrument.....	6
1.6. Coupling Mechanism for SATA Instrument and Control Box	9
1.7. Goal.....	10
2. Analysis of Requirements	12
2.1. Requirements for ZTM	12
2.2. Requirements for Control Box.....	14
3. Methods.....	18
3.1. Design Approach	19
3.2. Concept Design.....	25
3.2.1. ZTM	26
3.2.1. Control Box.....	27
3.2.3. Mechanical/Strength Analysis	30
3.2.4. Calculations for the Design.....	33
3.3. Test Setup.....	36
3.3.1. Tests for Requirements Phase 1 and Phase 2.....	37
4. Results.....	46
4.1. Prototype	46
4.2. Component Selection	47
4.2.1. Motors for Rotation of the Rods	47
4.2.2. Motors for Translation of Middle CBC piece.....	49
4.2.3. Motors for ZTMo.....	49
4.2.4. Belt for ZTM.....	50
4.2.5. Belt for Control Box	50
4.2.6. Spring.....	51
4.3. Actuator Control	52
4.4. Requirement Check after Phase 1	53
4.5. Testing Phase 1 Analysis of Problems.....	56
4.6. Requirement Check after Phase 2	56
5. Discussion	60
6. Conclusion	64
Appendix A.....	65
Appendix B	71
Appendix C	75
Appendix D.....	77
Appendix E	80

Appendix F.....	83
Appendix G.....	86
Appendix H.....	92
Appendix I.....	95
Appendix J.....	99
Appendix K.....	103
Bibliography	140

Abbreviations List

Abbreviation	Abbreviation Term
PoLaRS	Portable Laparoscopy Robot System
SATA	Shaft-Actuated Tip Articulation
CBC	Control Box Coupling
IC	Instrument Coupling
FOS	Factor of Safety
LMIC	Low and Middle income countries
HIC	High Income countries
MIS	Minimally Invasive Surgery
RCM	Remote Center of Motion
DOF	Degree of Freedom
ZTM	Z-Translation Mechanism
ZTMo	Z-Translation Movement
PMA	The Pugh Matrix Analysis
FEA	Finite Element Analysis
LMMPH	Linear Movement Middle Pulley Holder

List of Figures

Figure 1: Laparoscopic Surgery	1
Figure 2: Hand Eye co-ordination in Laparoscopy	2
Figure 3: Operation Room with Robotic Surgical System	3
Figure 4: PoLaRS Master Device and Slave Cart.....	4
Figure 5: PoLaRS Slave Arm Design	5
Figure 6: Steerable Punch Cutter	7
Figure 7: Steerable Punch	7
Figure 8: SATA Instrument Laparoscopic Handheld	7
Figure 9: SATA Instrument Laparoscopic Handheld	8
Figure 10: Instrument Attachment/Removal Coupling.....	8
Figure 11: Gripper Opening/Closing	8
Figure 12: SATA Instrument Yaw	9
Figure 13: SATA Instrument Pitch	9
Figure 14: Coupling Piece	9
Figure 15: CBC (Left) and IC (Right)	10
Figure 16: Groove Design for Connections	10
Figure 17: Instrument DOF and Actuation	11
Figure 18: Operational Region of the CBC rods	16
Figure 19: The Design Process	18
Figure 20: Design Process	19
Figure 21: Morphological Chart	21
Figure 22: Concept 8.....	24
Figure 23: Concept 9.....	24
Figure 24: Concept 12.....	24
Figure 25: Complete Assembly on PoLaRS Arm.....	25
Figure 26: PoLaRS ZTM	26
Figure 27: ZTM Functioning	26
Figure 28: ZTM Back View.....	26
Figure 29: ZTM Orthogonal View.....	27
Figure 30: PoLaRS Control Box.....	27
Figure 31: Mechanisms in the Control Box.....	28
Figure 32: Instrument Control Box with CBC rods.....	28
Figure 33: Control Box Orthogonal View	29
Figure 34: Control Box Front View.....	29
Figure 35: Control Box Angled View.....	30
Figure 36: Motor Box Von Mises Stress	30
Figure 37: Motor Box Push Side	31
Figure 38: Motor Box Push Side Increased Thickness.....	31
Figure 39: Middle Pulley Holder Von Mises Stress	32
Figure 40: Leadscrew Von Mises Stress.....	32
Figure 41: ZTM Holder Von Mises Stress	33
Figure 42: Markers for CBC rods	37
Figure 43: Control Box with Markers for Inner, Middle and Outer CBC piece (left to right)	38
Figure 44: Range of Rotations of Inner, Middle and Outer CBC rods (left to right)	38
Figure 45: Horizontal Fixation for Middle Rod.....	40
Figure 46: Torque Test Setup	42
Figure 47: Horizontal Fixation for ZTM	43
Figure 48: ZTM Force Setup	44

Figure 49: Vertical Alignment of the ZTM	45
Figure 50: ZTM without the Control Box Attached	46
Figure 51: Prototype Complete Assembly of Control Box with CBC and IC rods	46
Figure 52: Control Box Internal Mechanisms	46
Figure 53: Emergency Removal Spring Mechanism	47
Figure 54: Belt Geometry	51
Figure 55: Circuit Diagram	52
Figure 56: Parts for the Control Box	80
Figure 57: Parts for ZTM	82
Figure 58: Method 1	86
Figure 59: Method 2	86
Figure 60: Experiment Setup	86
Figure 61: Test Setup for Cable Connections	87
Figure 62: Springs from Workshop	88
Figure 63: Test Setup	88
Figure 64: Timing Pulleys and Belts Prototyped	90
Figure 65: Timing Belt and Pulleys Selected	90
Figure 66: Setup for timing belt force test	91
Figure 67: Concept 1	92
Figure 68: Concept 2	92
Figure 69: Concept 3	92
Figure 70: Pulley with Cable Loop Holes	92
Figure 71: Beads for Cable Attachment	92
Figure 72: Timing Pulley Teeth, Timing pulley base, Timing pulley cover (Left to Right)	93
Figure 73: Timing Pulley Prototype Design	93
Figure 74: Completed Timing Pulley	94
Figure 75: Control Box Exploded View	96
Figure 76: Control Box Semi Assembly Exploded View	97
Figure 77: ZTM Exploded View	97
Figure 78: Cable Wrapping over Pulley	98
Figure 79: Motor Marker for Rotation	100
Figure 80: Encoder Step Plot in Serial Plotter	101
Figure 81: Encoder Step Count in Serial Monitor	101

List of Tables

Table 1: Values of Range of Motion Phase 1	38
Table 2: Values of Speed: Pitch, Yaw and Rotation Phase 1	39
Table 3: Values of Speed: Pitch, Yaw and Rotation Phase 2	39
Table 4: Distance Values Phase 1	40
Table 5: Distance Values Phase 2	40
Table 6: Pull/Push Force Values Control Box Phase 1	41
Table 7: Pull/Push Force Values Control Box Phase 2	41
Table 8: Torque Values at CBC Phase 1	42
Table 9: Torque Values at CBC	42
Table 10: Pull Push Force Values ZTM Phase 1	44
Table 11: Pull Push Force Values ZTM Phase 2	44
Table 12: Legend for Requirement Check	53
Table 13: Requirements for Control Box Check Phase 1	55
Table 14: Requirements for ZTM Check Phase 1	56
Table 15: Requirements for Control Box Check Phase 1	58
Table 16: Requirements for ZTM Check Phase 1	59
Table 19: Concept Ideas ZTM	66
Table 20: Concept Ideas Rotation of Cylinders	68
Table 21: Concept Ideas Middle Cylinder Translation	70
Table 22: Combined Concept Ideas	74
Table 23: PUGH Matrix	76
Table 24: List of Purchased Parts for ZTM	78
Table 25: List of Purchased Parts for Control Box	79
Table 26: Additional Purchased Parts	79
Table 27: Control Box Parts Method of Manufacture	81
Table 28: ZTM Parts Method of Manufacture	82
Table 29: Bead Pull Forces	87
Table 30: Spring Values	88
Table 31: Speed Conversion Table	89
Table 32: Timing Pulley and Belt Selection	90
Table 33: Motor Resolution and Error	102

Abstract

The use of robotic systems to perform MIS was given a boost in 2000, when Da Vinci Surgical system was granted FDA approval. Senhance surgical system by Transenterix, was the newest surgical system to be granted FDA approval in Oct 2017. The use of these systems is limited to high income countries due to its high costs and specialised components.

PoLaRs for laparoscopic surgery is being developed at Surge-On Medical B.V. with the goal of being cost effective, light weight, compact and portable making it easier to be accepted in high income and low and middle income countries. The Shaft Actuated Tip Articulation (SATA) Instrument being used in the PoLaRS can pitch and yaw when its tubes are rotated. Opening and closing of the gripper is activated when its middle tube is moved forward or or backwards linearly.

The 5-DOF controlled by the Control Box and the Z Translation Mechanism (ZTM) include opening/closing of the gripper, pitch, yaw, rotation and linear movement of the SATA instrument towards and away from the surgical site. The Control Box can be attached to the ZTM and this system is designed to fit on the PoLaRS slave arm, which provides additional 2-DOF and the result is; the SATA Instrument can be controlled in 7-DOF in total.

A leadscrew mechanism is used to move the Control Box attached to the rails of the slide in the ZTM. The rotations of the SATA instrument are controlled by a timing pulley and timing belt system inside the Control Box. A leadscrew mechanism is used to control the linear movement of the middle coupling piece. A mechanism to enable easy detachment of the coupling rods in case of an emergency is also designed in the Control Box.

A functional prototype was build and the results for the performed tests indicate that the prototype has the required rotational range and speed for the CBC and ZTM, but higher torque was needed to rotate the instrument coupling piece. The timing belts and pulleys used in the prototype were created by using 3-D printing and lasercutting techniques.

In this thesis, the functional mechanism for the control of the SATA instrument in 5-DOF was designed, prototyped and validated. There are still limitations in the design; higher torques are needed for the rotations of the SATA instrument cylinders, higher tolerances for the manufactured components and better materials are needed to improve the prototype further.

1. Introduction

With rapid rise in the field of Minimally Invasive Surgery (MIS), the MIS Market is predicted to reach 50.6 billion USD by 2019 and the Minimally Invasive Surgical Instruments Market will be worth 21.47 Billion USD by 2021 (Photonics Media, 2018). The rise in diseases which need surgical intervention like cancer and cardiovascular conditions, the increase in elderly population in developed nations, decrease in trauma to the patient etc. favor the use of MIS techniques instead of open wound surgeries. This can explain the increase in the use of MIS techniques and the predicted rise in the market (Marketsandmarkets.com, 2018).

MIS involves the use of long instruments that are inserted through small incisions in the body, the operation is carried out by using these long instrument tips inside the patient's body to manipulate tissue for surgery (Kuo, Dai and Dasgupta, 2012). MIS was introduced in late 1989 (Walker Reynolds, J., 2001.), the techniques of these type of surgeries were not new but this cholecystectomy in 1989 caused an increase in the interest of surgeons and public. The improved instrument designs, better light sources, high resolution video transfer and other improvements in MIS techniques were factors that pushed MIS even further (Vierra, M.D, 1995) (Jaffray, 2005).

MIS is a broad term, which includes procedures such as laparoscopy, thorascopy, arthroscopy etc. Generally this term is used to describe procedures that reduce the size or the invasiveness of the surgery, when accessing the surgical site. The reduced risk of infection, lower cost and shorter hospital stay make laparoscopy an attractive option for abdominal procedures (Fullum et al., 2009) (Guthart, G.S. and Salisbury, J.K., 2000).

1.1. Laparoscopy

Laparoscopic surgical procedure (Lawyer, 2017) (Fig.1) begins with pneumoperitoneum by the introduction of CO₂ through an insufflator. A flow rate of 6-15 liters/min is used to achieve a pre-decided intra-abdominal pressure of 9-18 mmHg. Following this, the trocar is introduced in the abdominal cavity after an initial incision using a sharp cannula (trocar or veress needle) is done blindly. A video camera located at the tip of a laparoscope is introduced in the abdominal cavity after the initial sharp cannula insertion, providing a view of the operation space in the operation room. Once the internal operation space can be viewed on the screen, other instruments are introduced in the abdominal cavity by observing the insertions on the video screen (Vierra, M.D, 1995).

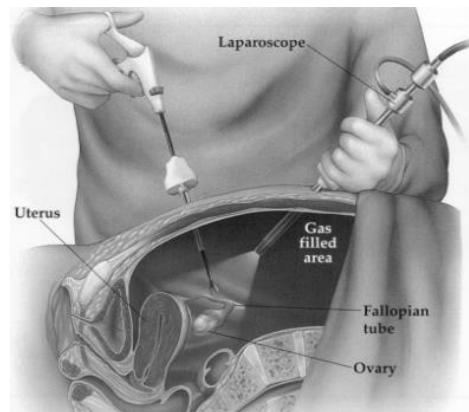


Figure 1: Laparoscopic Surgery

The initial access to the peritoneal space is achieved by 2 methods, open entry and closed entry (Pierre and Chapron, 2005). In closed entry technique, a veress needle is used to insufflate the surgical site and when full pneumoperitoneum is achieved, a sharp trocar is inserted blindly at an angle of 90 degrees to the abdominal wall. Once the trocar is inserted the valve is opened to confirm intraperitoneal placement. Then a camera is inserted to observe the surroundings and make sure that there is no injury and the remaining trocars are inserted under direct vision. In open entry, the skin, rectus, sheath and peritoneum are incised and a blunt trocar is inserted under direct vision (Jafari et al., 2015).

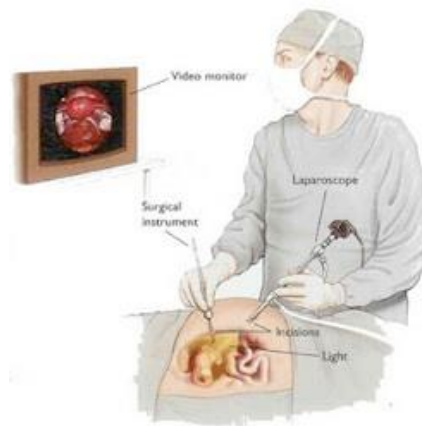


Figure 2: Hand Eye co-ordination in Laparoscopy

The advantages of laparoscopic procedures as compared to open procedures are (Prasad et al., 2010) (Harjai et al., 2015) (Benz et al., 2016):

- (a) Lower systemic stress
- (b) Lower rates of mortality
- (c) Decreased trauma
- (d) Small incision size
- (e) Reduced morbidity risk
- (f) Less pain etc.

However, laparoscopic procedures also have some disadvantages such as (Mack, 2001) (Hadavand et al., 2013) (Breedveld et al., 1999) (Hadavand et al., 2013) (Guthart, G.S. and Salisbury, J.K., 2000) (Wentink, 2001):

- (a) Surgeons need additional training for performing these procedures
- (b) There is a risk of puncturing the cavity walls or organs during the initial insertion of the trocar or veress needle
- (c) Since a gas is used to expand the cavity, there is a risk of haemodynamic and ventilator changes and gas embolus
- (d) It takes a longer time as compared to open surgery
- (e) Loss of haptic feedback
- (f) No direct vision to the surgery site.
- (g) Difficulty in hand-eye coordination (Fig.2) (Hernia.org, 2018) due to the different angles at which the video feed is seen and surgery is performed.
- (h) The movement of the instrument tip in the opposite direction to the surgeons hand can further decrease co-ordination.
- (i) Scaling of the movements of the surgeon depending on how deep the instrument is inserted inside the body.
- (j) The fulcrum effect.

1.2. Robotic Laparoscopy

In robotic laparoscopy there is a robotic interface between the patient and the surgeon. The surgeon controls the master device which relays the information to the slave device which performs the surgery (Hadavand et al., 2013). The slave device or robot is close to the patient and the instruments attached to the arms perform the surgery as directed by the surgeon at the master console (Bedem, 2010).

The use of Unimation Puma 200 robot for orienting a biopsy needle while performing neurosurgical biopsy in April 1985 was the first robotic system used (Kwoh et al., 1988). After this in 1988, the Puma 560 was used to carry out laboratory studies (Davies 2000). This was followed by the PROBOT designed for transurethral resection (Kwoh et al., 1988). Later, in 1991, the ROBODOC was used clinically on human patients for hip replacement procedure, this surgical system machined the femur (Davies 2000). SRI (Stanford Research Institute) began working on a master slave system for surgery in the 1990's on devices like the SRI telepresence systems (Taylor et al., 1995). During this time other systems like the surgical system at Politecnico di Milano in Italy (Rovetta et al., 1996), Black falcon at Massachusetts Institute of Technology and IBM Research Center/John Hopkins University surgical robot (Taylor et al., 1995) were developed. AESOP (Automated

Endoscope system for optimal Positioning) became the first robot to be approved by the FDA and was used to assist surgeons during surgery by holding the endoscope and allowing for repositioning as directed by the surgeon, this was later incorporated in Zeus Robotic Surgical System which was FDA approved in Oct 2001 (Lanfranco et al., 2004). The major competitor of the Zeus Surgical Robot was the Da Vinci Surgical Robot produced by Intuitive Surgical Inc. and was approved in July 2000. The three companies Zeus, AESOP and Da Vinci Surgical System merged under the Intuitive surgical Inc. and the production of Zeus and AESOP stopped. (Lum et al., 2009). Since then Da Vinci surgical systems have been dominating the surgical systems market. Transenterix was the most recent medical device company to receive FDA clearance for their surgical system called Senhance Surgical Robotic System in Oct 2017 (lr.transenterix.com, 2018).

For performing robotic laparoscopy, a preoperative planning carried which determines the attachments to be used on the robotic system, the placement of the patient, surgical system and the team positions(Fig.3)(Barrera, K., Chung, P. and Sugiyama, G., 2017) (Konietschke et al., 2004).

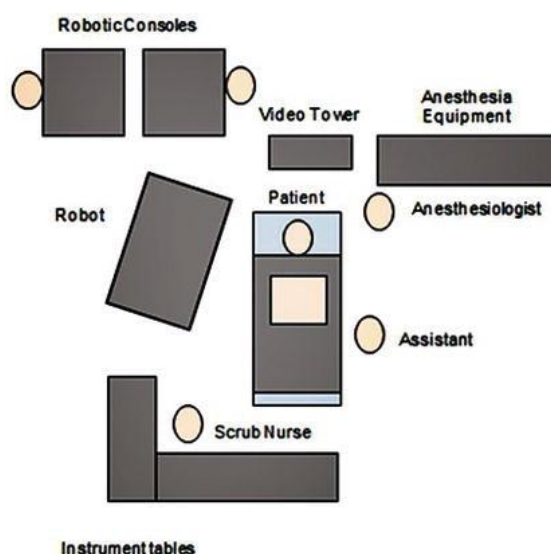


Figure 3: Operation Room with Robotic Surgical System

For example, in the case where laparoscopic surgical procedures were studied in Department of General Surgery, Misericordia Hospital, Grosseto, Italy; the Da Vinci Surgical System was used. A surgical team consisting of the surgeon, assistant surgeon, nurse and anesthetist were present in the operating room. The Da Vinci System runs a check on its functioning before the start of the procedure and then its arms are wrapped in nylon covers. Following this the mechanical supports for the trocars on the robot arms are fixed. Either 2-D or 3-D view is selected in the optical system after the frontal or inclined position of the scope is setup and then calibration of the optical system is carried out (Giulianotti, 2003). After these initial tasks are completed, the robotic surgical system is ready for use.

Robotic laparoscopy overcomes some of the disadvantages of conventional laparoscopy. Its advantages are (Lanfranco et al., 2004) (Ruurda, van Vroonhoven and Broeders, 2002) (Taylor and Stoianovici, 2003):

- (a) An ergonomic position for the surgeon as compared to conventional handheld laparoscopy
- (b) Provides precise and accurate movements and increases dexterity
- (c) Filters the tremors by using appropriate hardware and software features
- (d) Provides a 3-D view and can allow for scaling of movements to provide micro-movements at the surgical site
- (e) Provides a better hand-eye co-ordination for the surgeon
- (f) Provides data for training

There are also disadvantages associated with Robotic laparoscopy, such as (Ghanem et al., 2015) (Lanfranco et al., 2004):

- (a) The high cost of these systems limit their use in hospitals
- (b) The high costs associated with upgrading the systems and maintaining the system
- (c) These systems also have large sizes, which have large footprints and also large arms, which makes it difficult to fit in already crowded operation rooms
- (d) Lack of compatible instruments and equipment

- (e) Lack of haptic feedback
- (f) Risks due to the surgeon being away from the operating table

1.3. Laparoscopy in Low and Middle income countries

There is an increasing demand towards laparoscopic surgery in Low and Middle Income Countries (LMIC). However the adoption of this type of surgery has been low due to high cost of equipment and maintenance and lack of trained personnel. (Alfa-Wali and Osaghae, 2017) (Mir et al., 2008)

The use of robots in laparoscopic procedures has also seen a rise in recent years in developing nations. The benefits of laparoscopy in LMIC provide the same advantages as in High Income Countries (HIC) however the effects of these advantages can be of much higher importance there. The lower surgical site infections and faster recovery can be of a greater benefit, as less time in the hospital allow patients to return to work sooner maintaining the sustenance of the family (Alfa-Wali and Osaghae, 2017). Surgical mortality in developing countries is almost 10 times higher than developed countries (Morad Asaad and Ahmad Badr, 2016), which can be reduced by using laparoscopic surgeries.

The first robotic radical prostatectomy in India was performed in A.I.I.M.S. New Delhi in July 2006. Around 200 surgeries were performed from then until 2012. And in the year 2012, there were 8 Da Vinci Robots installed in India (Dogra, P.N., 2012). And the number is increasing further, with a US-based Vattikuti foundation's goal of installing 200 more robotic surgical systems by the year 2020 (The Economic Times, 2018).

The market for robotic surgeries is increasing in developing countries with the major drawback being the cost of these surgical systems and lack of trained surgeons (Dogra, P.N., 2012). The PoLaRS system has the goal of being affordable, modular and portable. The instruments used in the system can be cleaned by conventional sterilization techniques needing no expensive equipment for cleaning. Thus overcoming the challenges of the existing surgical systems in developing countries and providing an affordable surgery option in these countries.

1.4. PoLaRS –Internship & Thesis Literature

The PoLaRS robotic system overcomes some of the shortcomings of the existing robotic surgical systems. It uses a modular design, where the parts in the system are simple or off-shelf. The cost of the surgical system is significantly lower as compared to other systems. It is portable and weighs less as compared to other surgical systems. It is also easy to clean, maintain and has a small footprint (Surge-on Medical, 2018).

Before the start of the thesis, I worked for my internship on the arm for the PoLaRS Slave Device. Apart from that the literature study was carried out for the thesis to provide a strong base for the design and development of the thesis work.

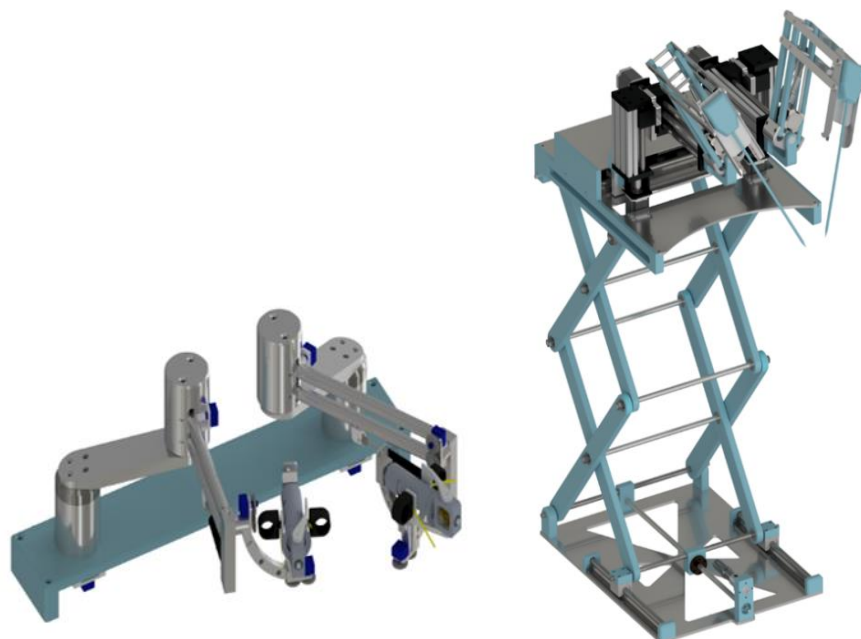


Figure 4: PoLaRS Master Device and Slave Cart

1.4.1. Internship

The internship was carried out at Surge-On Medical B.V. from 13 Feb 2017 until 13 May 2017. The core of the internship was working on the development and design of the new PoLaRS slave arm (Fig.5).

Summary

The internship at Surge-On B.V. was carried out with the aim of designing the robot arm for the PoLaRS (Fig.4). This robot arm will be supporting the movement system for the SATA instrument and providing additional 2 DOF. The goal of the internship was to design a new slave arm which can hold the instrument and the mechanisms that will be used to move the instrument. The slave arm also has to fit on the base plate designed by the students of LIS. There were other requirements such as 3 DOF actuation, RCM, weight below 5kg, distance from the base plate, dimensions of the arm below 200mmx200mmx400mm, decoupled actuation etc.

The internship began with a business case study where the market for the surgical systems was studied. The development of new systems and the trend of increased use of laparoscopic or MIS procedures instead of conventional open surgeries was seen during the research phase. The markets in different countries were also studied in this phase. Developed countries like North America are at the forefront of using this technology, with almost 60% of the share of this market being with USA. It was seen that the Asian market will also grow significantly due to the increase in GDP, rise in income and increased healthcare expenditure. Thus countries like China, India, Japan, Singapore, Thailand, Korea etc. will use the robotic surgical systems in the near future. The most common and widespread surgical system called the Da Vinci Surgical System, was the first system to be available commercially in 2004 and has a strong market position in EU, USA and Asia. However, this surgical system is expensive with the price ranging from 700,000 USD to 2.25 million USD per system. Which limits the LMIC from using these systems.

There was a comparison made between the systems that are currently in development stage or in the market in the internship report. Apart from that older systems were also included as it would be interesting to see how the systems have changed over the years. The comparison was made on the basis of cost, size, portability, force feedback, modularity, DOF, sterilization and safety. Several mechanisms were studied to determine its functionality and suitability for using it in the new slave arm. The parallelogram mechanism was chosen due to the fact that it guaranteed a RCM, the distance from the base can be adjusted by increasing the length of the links and its simple design.

The final concept of the arm was analyzed through software, the weights of each part of the system was checked for validating the weight requirement. There was FEA analysis carried out on critical parts to be sure that the parts would withstand the forces and stresses while in use.

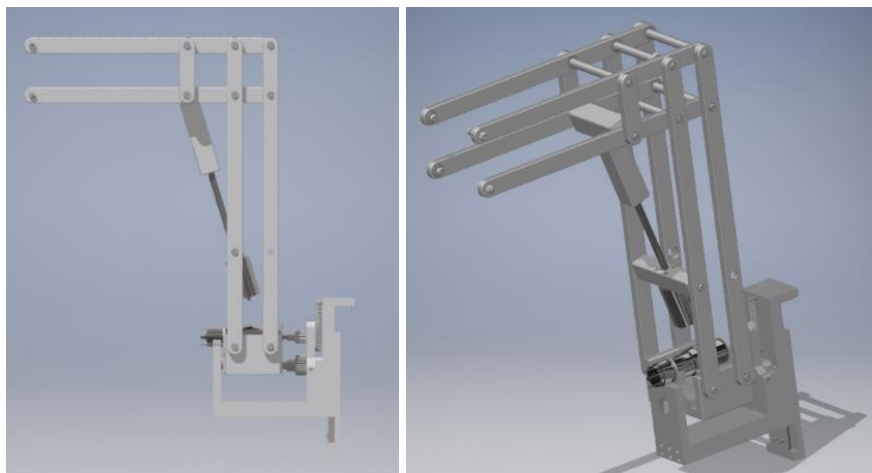


Figure 5: PoLaRS Slave Arm Design

1.4.2. Thesis Literature Study

The literature study was conducted with the goal of identifying the different mechanisms used in surgical systems and obtaining the top level requirements that will be used in the thesis project.

Laparoscopic surgical procedure was reviewed in the literature study to gain an insight into the needs of the surgeon, supporting staff and the surgical procedure itself. This helped to learn of the critical items that will need to be taken into account for the design of the Control Box and ZTM.

Summary

MIS procedures have become quite common in the recent years and the market for these procedures are growing rapidly given the advantages such as shorter hospital stay, better cosmetics, less pain, faster recovery etc. The disadvantages of the MIS are eliminated by using robotic systems which help the surgeons perform the surgeries with increased ease.

The focus of the literature study was on laparoscopic surgeries which are performed by making a small incision in the abdominal wall. Robotic laparoscopy is classified depending on how the robotic surgical system is controlled. Robotic surgical systems are classified as Supervisory, Tele-surgical and Shared control. In Supervisory system, the surgical system performs the surgery as programmed by the surgeon before the surgery and need no input from the surgeon during the surgery. Tele-surgical systems are controlled by the surgeon remotely to perform the surgery through a master-slave device. In Shared control system, the surgical system augments the movements of the surgeon during surgery. Robotic laparoscopy can also be classified as Intraluminal, Transluminal, Extraluminal and Hybrid Intervention. These differ in the manner in which the surgical site is accessed. Intraluminal intervention is through natural orifices which are exposed to the environment at one of their extremities. Transluminal Intervention is through natural orifices, a controlled break is made in the luminal barrier to gain access to perform the surgery. In Extraluminal Intervention an incision on the skin is made to gain access to the surgical site. Hybrid Intervention is a combination of 2 or more of the earlier interventions.

Preoperative planning is carried out before robotic surgery is performed to determine the best access points, patient position, surgical system placement etc. A veress needle is used during the surgery to insufflate the abdomen and achieve pneumoperitoneum. After full pneumoperitoneum is achieved a trocar is introduced in the abdomen and a camera is used to view the surroundings. The remaining trocars and instruments are introduced under direct vision.

The robotic surgical systems have several safety features to prevent an accident during the surgery. This includes Backdrivability, Counterbalancing, RCM etc. These systems are not present in every surgical system but each system has some of these safety features apart from safety design in software or control system. The surgical systems available in the market and in development helped to identify the features and requirements that will be needed for the PoLaRS. The requirements found were divided into 3 categories to provide a clear overview. The 3 categories are Design Requirements, which include compact design, weight limitation of 2kg, ease of attachment and detachment of the instrument etc. Performance Requirement provides requirements like max velocities, forces, rotational and translational resolution etc. The Safety Requirements include safety features like backdrivability and sterilizability.

At the end of the literature study, we were able to determine the requirements for the PoLaRS system, gain an understanding of the surgical procedure and study the existing surgical systems in development and market.

1.5. SATA Instrument

The Shaft-Actuated Tip Articulation (SATA) instrument which is going to be used for the PoLaRS was developed at Surge-On Medical B.V. The instrument consists of 3 hollow cylinders, rotations of these cylinders with respect to each other cause the movement of the instrument tip/gripper. There are helical slots in these cylinders which use pins on the adjacent concentric cylinder to rotate with respect to each other. The rotation and opening and closing of the instrument is achieved by using linear movement of the middle cylinder.



Figure 6: Steerable Punch Cutter



Figure 7: Steerable Punch

The SATA mechanism was first used in the steerable punch used for arthroscopy (Fig.7) (Surge-on Medical, 2018), this instrument provides 110 degrees of tip steering, which helps to access difficult to reach locations. This reduces the number of surgical cutting tools needed on the table and reduces the force exerted on the portals during surgery. The cutter (Fig.6) (Surge-on Medical, 2018) is used to cut meniscal edges and the cuts obtained are smooth and clean. The instrument is rigid, easy to clean and has adjustable bending radius.

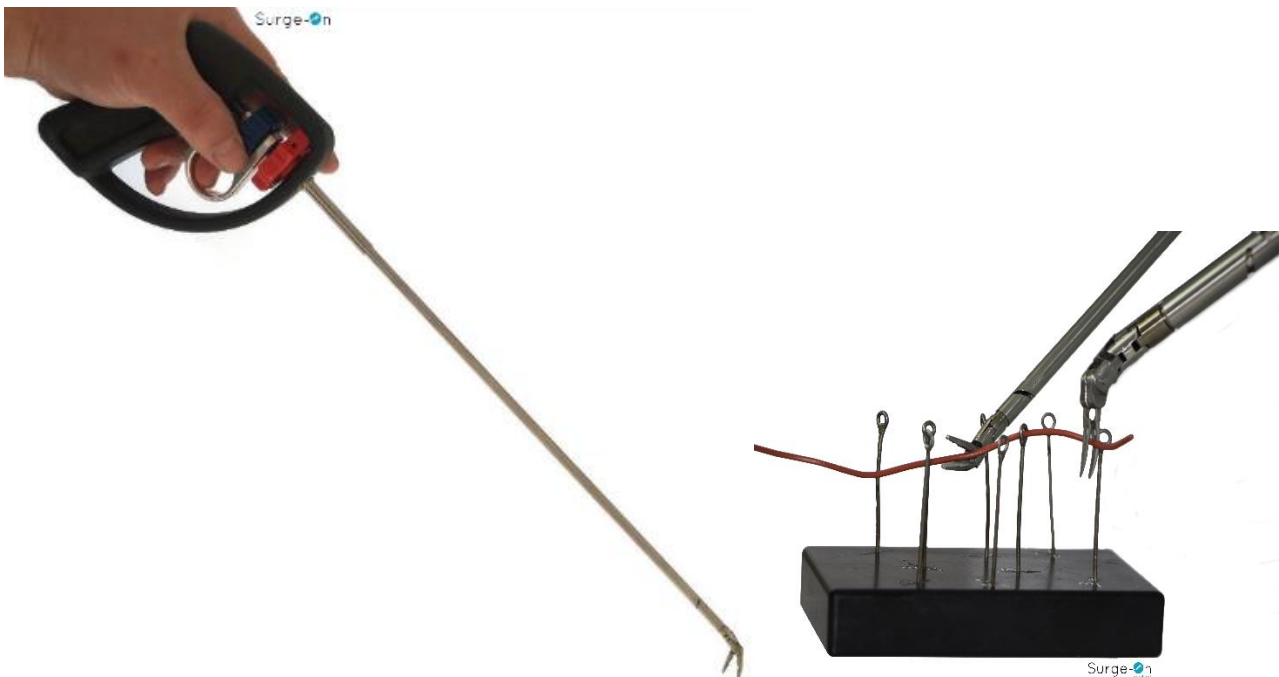


Figure 8: SATA Instrument Laparoscopic Handheld

Another instrument based on the SATA mechanism is the steerable laparoscopic handhelds (Fig.8) (Surge-on Medical, 2018). These are modular, easy to detach, clean and rinse. The operation is carried out by 2 wheels which can be rotated to move the tip in different directions (Fig.9). The rotation of the blue wheel causes the instrument gripper to pitch and rotation of the red wheel causes the instrument to yaw. Pulling on the finger hole causes the gripper to close. In the default setting the gripper is open due to a spring pushing on the finger handle.

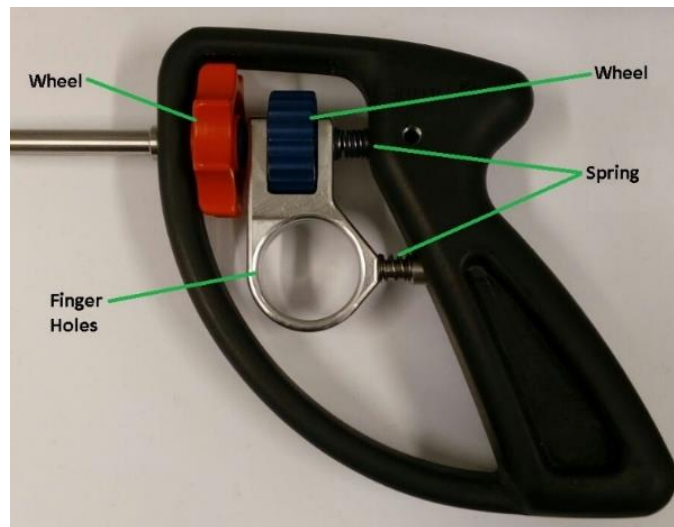


Figure 9: SATA Instrument Laparoscopic Handheld

An important consideration in this instrument is the detachment of the instrument from the handheld and the gripper. The instrument can be detached along the length of the shaft for cleaning and sterilization needs. There is a mechanism which allows for easy removal of the instrument is shown in Fig 10. This mechanism consists of a groove which fits in with another part of the instrument with the opposite groove. This makes a complete connection between the instrument tip and the shaft.



Figure 10: Instrument Attachment/Removal Coupling

Range of movement of the SATA instrument is are shown in the (Fig.11, Fig.12, Fig.13) The gripper opens and closes by ≈ 40 degrees, when the handle finger hole opens and closes by ≈ 4 mm. The neutral position for the gripper is in the open position with the jaws open (Fig.11)

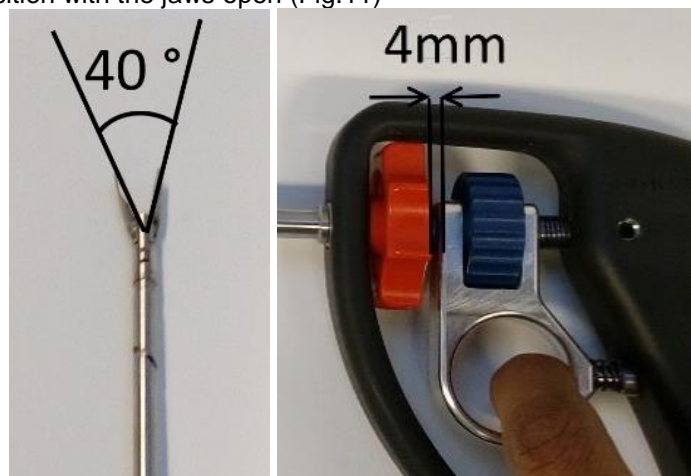


Figure 11: Gripper Opening/Closing

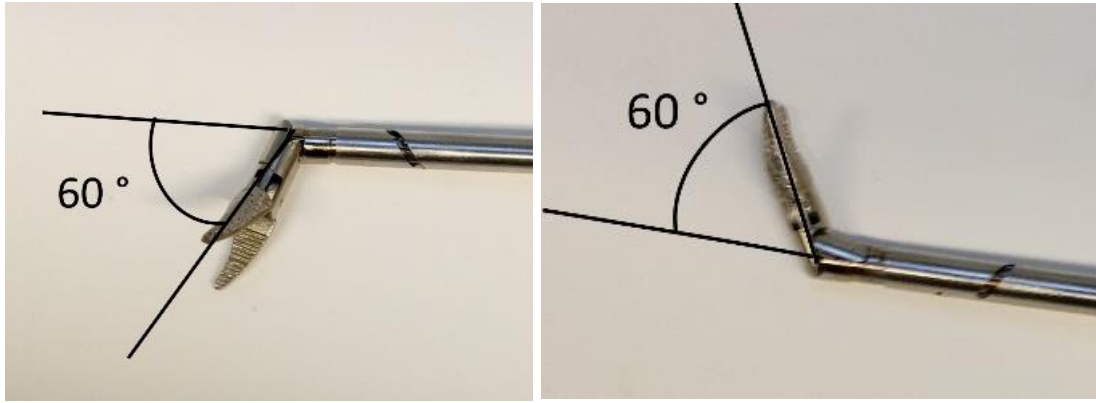


Figure 12: SATA Instrument Yaw

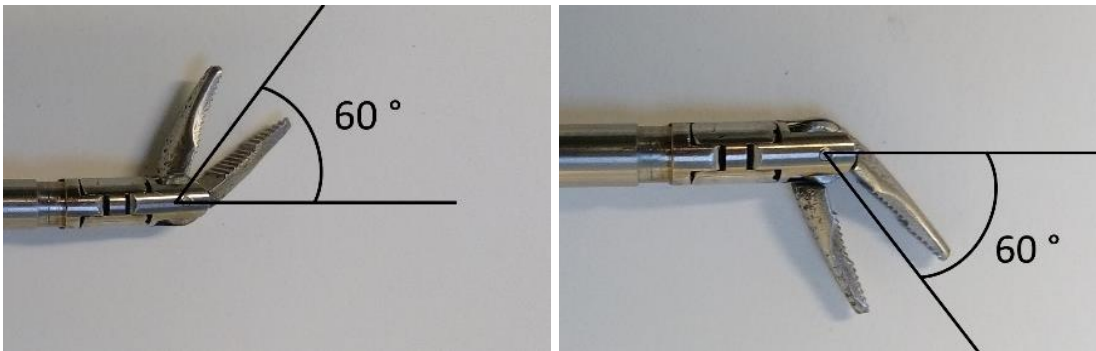


Figure 13: SATA Instrument Pitch

The yaw and pitch movements are ± 60 degrees from the neutral position (when the instrument is in a straight line with its shaft) (Fig.12, Fig.13). For achieving these pitch and yaw movements of the SATA Instrument the cylinders of the SATA Instrument should rotate by ± 90 degrees in either direction from the neutral position.

1.6. Coupling Mechanism for SATA Instrument and Control Box

The coupling mechanism was developed in parallel by Jasmijn, while the design of the Control Box and ZTM was being developed by me. The mechanism is used to couple the SATA instrument with the Control Box. It acts as an additional interface between the SATA instrument and the Control Box. It functions to allow easy decoupling and coupling of the SATA instrument from the Control Box. The coupling between the instrument and the Control Box is done by the coupling piece (Fig.14).

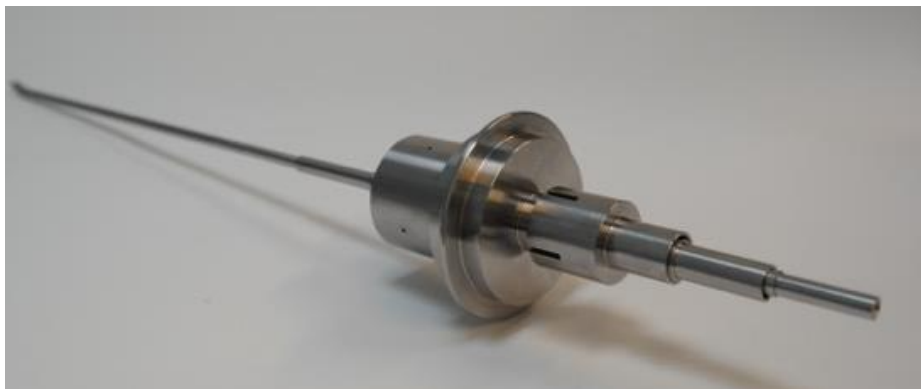


Figure 14: Coupling Piece

There are 2 rods to the coupling mechanism. The Control Box Coupling piece (CBC) which is held in the Control Box and the instrument coupling piece (IC) on which the SATA instrument is coupled (Fig.15).



Figure 15: CBC (Left) and IC (Right)



Figure 16: Groove Design for Connections

The CBC is inserted inside the Control Box and the IC is connected to the SATA instrument. Each of these couplings has three rods inside it. These rods are used to control the three cylinders of the SATA instrument. The CBC rods which are controlled by the Control Box, move the IC rods. The rotation of the innermost, middle and outer rods of the CBC rods, rotate the innermost, middle and outer rods of the IC. The SATA instrument also has the function of opening and closing the gripper, this is achieved by moving the middle rod translationally. The middle rod can move inside the outer rod of the CBC and IC which helps to achieve the opening and closing of the gripper.

The innermost rods of the CBC and IC have a particular groove design which helps to connect the other coupling innermost rod (Fig.16). The middle rods of the CBC and IC are connected to each other by use of magnets. The outer rods of the CBC and IC are held in place by means of a ball groove and pre-tension of a spring. This coupling mechanism helps to transfer the movements inside the control rod to the SATA instrument (Berendsen, 2018)

1.7. Goal

Most robotic systems have 7-DOF, where 3-DOF are from the robotic arm and the remaining DOF are achieved by using actuators to control the instrument movements inside the patient body. Robotic systems like the Da Vinci surgical robot have the actuators to control the instrument tip, outside the Control Box on the arm and the Control Box only consists of the mechanism to control the instrument tip.

The design of the PoLaRS slave Control Box and ZTM was done in this thesis. As seen in Fig.17 we focused on 5 of the 7 DOF's, needed to control a single instrument. The SATA instrument can be controlled in 4-DOF and the entire Control Box can be moved in 1 DOF. Each of these DOF controls one function of the instrument movement. The rotation of the outer cylinder controls the tip/gripper yaw, the rotation of the middle cylinder controls the tip pitch and the rotation of the innermost cylinder controls the rotation of the instrument tip. The translational movement of the middle cylinder with respect to the other cylinders causes the gripper to open and close. The translation of the instrument toward and away from the abdomen is achieved by moving the entire Control Box translationally. The system developed in this thesis project will be used in the PoLaRS slave device.

5-DOF with SATA Instrument

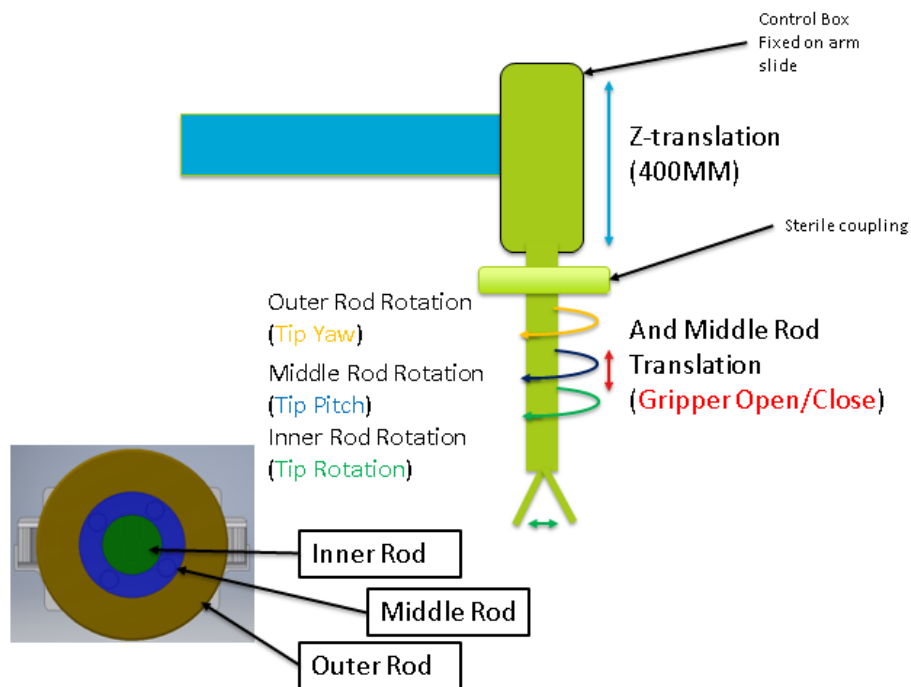


Figure 17: Instrument DOF and Actuation

The goal of the thesis project was “Design and Manufacture of a Compact, Ergonomic, Low Cost, Portable System/Mechanism to control A Multi DOF SATA instrument on the PoLaRS slave arm”. Each of the 5-DOF should be controlled independent of each other (decoupled) and comply with other requirements like speeds, torques, resolution of the instrument movement etc.

2. Analysis of Requirements

The requirements in the literature study are obtained from the analysis of surgeon's capabilities during surgery, relevant papers, studying robotic surgical systems and input from my supervisor (Hadavand et al., 2013) (Bedem, L., 2010) (Rutala and Weber, 2013) (van Aaken, R.J.T., 2006). These requirements were made clearer and developed further into more concrete requirements. The SMART approach was used to further define the requirements. The requirements are specified for the ZTM and the Control Box separately.

Some of the requirements from the literature study were broad and not well defined. To have clear and defined requirements the SMART approach was used. The acronym SMART stands for Specific, Measurable, Achievable, Realistic and Time bound (Lawlor, K.B., 2012). These provides a base to setup goals in a meaningful manner with the requirements clearly specified. The SMART approach can be followed by using the following guidelines (Swanson, M., 2016) (Lawlor, K.B., 2012):

- (a) Specific: This means to be to the point and clear in mentioning of the requirement. The specificity of the requirement will enable the proper measurement of the requirement.
- (b) Measureable: The requirement has to be measurable. This will help to determine if the requirement has been achieved or not. The measurability of the requirement provides a tangible evidence that the requirement has been achieved or not.
- (c) Achievable: The requirements can be set up in a manner that helps the person feel challenged but also ensure that the requirements are attainable.
- (d) Realistic: The requirement needed should be realistically possible and doable.
- (e) Time bound: The time bound nature of the smart approach deals with the time constraint while achieving a requirement.

This approach provides a guideline to refine the top level requirements further.

2.1. Requirements for ZTM

The requirements for ZTM are divided into 3 categories depending on the type of requirement and to provide a well-defined list of requirements.

Design Requirements

1. Attachment and Removal of the Control Box

The Control Box should be able to be attached to the ZTM and be removed when needed for cleaning or replacement purpose.

2. Providing Smooth Movement of the ZTM

The smooth translation of the ZTM can be interpreted as having a constant or linear movement of the SATA instrument, when the Control Box moves inwards or away from the abdomen. This movement should not have jerky movement and abrupt uncontrolled increase or decrease in speed. This would mean that the system has to be supported by mechanisms that do not allow such behavior and the actuators should be strong enough to move the instrument as desired without abrupt uncontrolled movements.

The factors for this requirement are:

- (a) No abrupt movements when the instrument moves in or out the body of the patient.
- (b) No random increase or decrease in speed of instrument.

3. Backlash

In gear systems, there is some backlash in the system. Backlash is caused by the gap in the teeth between the gears in mesh, this makes a dead-zone. In the dead-zone, there is no movement of the driven gear when there movement from the driving gear as first it needs to travel the dead-zone. When it is moving in the dead zone it does not transmit motion to the driven gear. After this dead-zone is crossed the driving gear moves the driven gear. Backlash can cause problems in motion control of the gear systems and should be minimized (Imasaki et al., 1995).

The factors for this requirement are:

- (c) Backlash if present should not cause any problem with the movement of the instrument.

4. ZTM Weight

The weight of the system is determined by the materials used and the number of the parts used. The weight of PoLaRS is fixed due to the weight of the other mechanisms on the slave device (the base and the arm).

The weight restrictions on the surgical arm and the mechanisms are obtained from by considering the weight of the already manufactured base of the system and considering the important requirement of the system being portable. The weight of the complete slave assembly should be below 50kg, this includes the weight of the 2 arms, Control Box, base, suitcases needed to pack and transport the system. After subtracting the weights of the arms, base and suitcases a weight of 2kg is left for the ZTM mechanism.

For this requirement the factor would be:

- (d) Weight less than 2 kg.

5. Compact Design

The PoLaRS slave device should be able to fit in a suitcase of size 200mmx200mmx400mm. The compact design will determine the size of the actuation mechanisms for the ZTM. Therefore the mechanism design should be under these dimensions so as to fit in the compact design criteria.

For this requirement the factor would be:

- (e) The mechanism should fit in 200mmx200mmx400mm box.

6. No Interference with the Drape

The PoLaRS slave device should will be covered in a drape on the arm. The ZTM should be able to accommodate this drape and ensure that it doesn't interfere or get stuck during the ZTMo.

For this requirement the factor would be:

- (f) Easy movement with drape with no parts interfering or getting stuck during the ZTMo.

Performance requirements

7. Translational Speed and Distance

The instrument should be able to translate between 0-350 mm in z-direction (toward and away from the abdomen) (van Aaken, R.J.T., 2006) with a velocity range of 0-60mm/s (Bedem, L., 2010).

In another paper (Hadavand et al., 2013) a velocity of 200mm/s was the maximum velocity for lateral and insertion movements with an insertion depth of 200mm.

For this requirement the factors are:

- (g) Maximum linear velocity between 60mm/s to 200mm/s.
- (h) Maximum linear movement between 200mm-350mm.

8. Translational Resolution

The ZTMo of the instrument should have a resolution of 50µm ideally, but a resolution of 0.1mm is sufficient for suturing blood vessels (Bedem, L., 2010).

For this requirement the factors are:

- (i) A linear resolution of at least 0.1mm.

9. Pull-Push Force

The ZTMo of the instrument should be able to pull on the tissue/ tear off tissue held in the gripper by a force of 26N (Yamanaka et al., 2015)

For this requirement the factors are:

- (j) A pull/push force of at least 26N.

Safety requirements

10. Backdrivable

Backdrivability can be incorporated in the system by means of a backdrivable actuator or in the design of the mechanism. Backdrivability is the ease of moving the system from the output to the input by an externally applied force (Fumagalli, M., 2014). This requirement can be broken down into selection of backdrivable actuators or creating mechanisms that allow backdrivability.

The question of the system being backdrivable or not, is dependent on the type of actuation and the weight of the system. In some systems a backdrivable design makes the system safer while in other systems a non-backdrivable system makes it safer. In cases where the instrument is heavy and there is a chance of it moving after the power is turned off to the actuators due to the inertia of the parts, a non-backdrivable system is better. In cases where the instrument removal can cause problems with the tissue surrounding the instrument, it is better to have backdrivable system.

In the case of the PoLaRS, a backdrivable system is favored as the weight of its parts is small and it is better to move the arms manually in case of an error during operation.

For this requirement the factors are:

- (k) Backdrivable mechanism for the ZTM.

2.2. Requirements for Control Box

The requirements for the Control Box are divided into 3 categories to provide a clearer list of requirements similar to the ZTM.

Design Requirements

1. Providing Smooth Movement of the SATA Instrument

Smooth translation can be interpreted as having a linear movement of the SATA instrument when the master device controls the SATA instrument tip to move in rotation, pitch and yaw. This movement should not have jerky movement and cause abrupt increase or decrease in speed. This would mean that the system has to be supported by mechanisms that do not allow such behavior and the actuators should be strong enough to move the instrument as desired without abrupt movements.

The factors for this requirement are:

- (a) No abrupt movements when the instrument moves in or out the body of the patient.
- (b) No random increase or decrease in speed of instrument.

2. Backlash

It is better to have systems with small or no backlash. Backlash can cause problems in the finer movements of the instrument tip.

The factors for this requirement are:

- (c) Backlash if present should not cause any problem with the movements of the instrument.

3. Control Box Weight

The weight requirement of this mechanism is obtained similar to the ZTM, where the entire system of the arm should weigh around 5kg out of which 4 kg is allocated to the ZTM and the arm. The remaining 1 kg is allocated for the Control Box.

For this requirement the factor would be:

- (d) Weight less than 1 kg.

4. Compact Design

The space available between the 2 parallelogram linkages of the PoLaRS arm which will hold the Control Box and the ZTM is around 84mmx290mmx150mm, this means that the Control Box cannot exceed 84mm in width otherwise it will hit the linkages of the PoLaRS slave arm. Therefore the mechanism design should be under these dimensions so as to fit in the compact design criteria.

For this requirement the factor would be:

- (e) The width of the Control Box should be below 89mm.
- (f) The length of the Control Box should be below 150mm.

5. Cable Routing

In order for the Control Box containing the mechanisms to rotate and move the rods, the motors need to be actuated. This data and power for the motors is done by use of cables, several cables in the Control Box can either be routed directly to the main electrical location or can be first connected at some place inside the box and then moved through other connections outside the box along the slide and then to the main connector. It is necessary that there is enough space for the cables in the Control Box to safely route it out of the Control Box, without excessive cramping or stress on the cables.

The factors for this requirement is:

- (g) Enough space for the cables to pass out from the Control Box.

Performance requirements

6. Translational Speed and Distance

From the SATA instrument we see that the middle rod needs to be translated 4mm at a speed of around 4mm/s. This requirement is obtained by moving the instrument manually it can be opened and closed in one second. Therefore the middle rod needs to cover a distance of 4mm to open and 4mm to close in 1 second, giving 4mm/s.

For this requirement the factors are:

- (h) Middle rod translation speed 4mm/s.
- (i) Middle rod translation 4mm.

7. Rotation of Instrument

A rotation with angular velocity of 0.5 rad/s for moving the tip in pitch and yaw is needed and an angular velocity of 4 rad/s (Bedem, L., 2010) or 30rpm (approx. 3 rad/s) (Hadavand et al., 2013) for rotation of the instrument tip.

For this requirement the factors are:

- (j) Movement of the instrument tip in pitch and yaw with a maximum 0.5 rad/s.
- (k) Rotation of the instrument tip with a maximum velocity of 3 rad/s or 4rad/s.

8. Rotational Resolution

The instrument tip in pitch, yaw and rotation should ideally have a resolution of 50µm however a resolution of 0.5 deg. is sufficient for suturing blood vessels (Bedem, L., 2010).

For this requirement the factors are:

- (l) A rotational resolution of at least 0.5 deg.

9. Actuation of the SATA Instrument

There are 4 actuations needed for the movement of the instrument tip, which uses the rotation of the 3 cylinders in the SATA instrument and the linear movement of the middle cylinder. Hence the actuator should be able to provide these 4 actuations of the cylinders. The mechanisms should be simple as to prevent unintended problems or complexities in the design.

The actuations of the instrument are ± 90 deg. in both the pitch and yaw (Bedem, L., 2010) and it has a rotation of ± 90 deg. about its longest axis (Cavusoglu et al., 1999). The opening and closing of the instrument tip is ± 45 deg. (Bedem, L., 2010). These angles are with respect to the instrument in its neutral position, where the instrument jaws are closed and the tip is straight in line with its shaft. A similar workspace requirement is mentioned in (Hadavand et al., 2013), where the instrument pitch is ± 90 deg. and the instrument yaw is ± 60 deg. The instrument should be able to rotate to 150 deg. The maximum range of the SATA instrument is around ± 60 deg. in pitch and yaw.

A nominal gripper force of 10 N (Bedem, L., 2010) (Hadavand et al., 2013) and a maximum force of 20 N (Bedem, L., 2010) is needed by the gripper to grip on the tissue. For torque interactions, a maximum torque of 0.5 Nm (Hadavand et al., 2013) can be considered.

For this requirement the factors are:

- (m) Instrument pitch between ± 60 deg. to ± 90 deg.
- (n) Instrument yaw between ± 60 deg. to ± 90 deg.
- (o) Instrument rotation between 150 deg. to 180 deg.
- (p) The gripper should be able to hold a load of 10N.

10. Torques for Rotation of SATA Cylinders

The torques of the SATA Instrument cylinders were obtained from DEMO lab, which had carried out experiments to check the torque of the SATA instrument. The torque was found to be 20Nmm at most, hence using the FOS of 2. The torque considered was 40Nmm. However, these torques are for the SATA Instrument tubes, there are coupling rods (CBC and IC) connecting the SATA Instrument to the Control Box. Hence increasing the FOS to 4, to account for these coupling rods, we have 80Nmm. The torques can be measured at the CBC without attaching the SATA Instrument to prevent damage to the SATA Instrument.

For this requirement the factors are:

- (q) CBC torques should be above 80Nmm.

11. Attachment and Removal of SATA Instrument Normal Operation

During the normal operation, Attaching of the instrument to the Control Box is done by pulling back the middle rod by the motor by 2.5mm from the Neutral Axis (N.A.), which exposes the inner cylinder of the CBC (attached to the Control Box) (Fig.18). Once the inner CBC is exposed by the motor, the inner rod of the CBC can be connected to the inner cylinder of the IC (attached to the SATA instrument), to complete the connection between the inner rods. The middle rods of the CBC and IC connect to each other by rotating the motor until the magnets connect. The outer rods of the CBC and IC couplings connect by rotating the motor until the grooves fall in place.

During normal operation of removing the instrument from the Control Box, the middle rod of the CBC is pulled back by the motor beyond its 4mm operational range by an additional 2.5mm, this pushes back the middle rod and the outer rod of the CBC, which exposes the inner rods of the CBC and IC, which can then be detached.

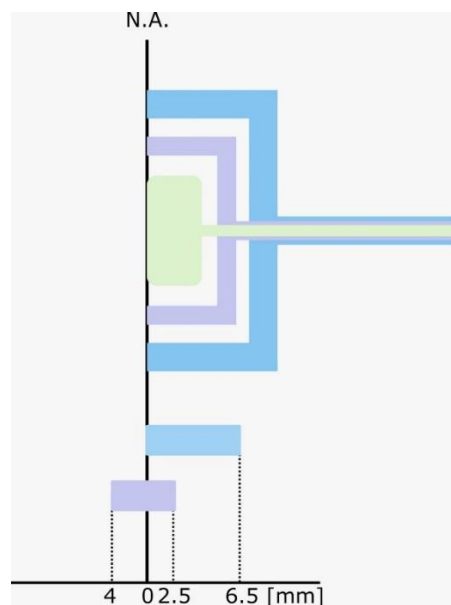


Figure 18: Operational Region of the CBC rods

For this requirement the factors are:

- (r) The middle cylinder should be completely pulled in by the motor by 2.5mm from its N.A.

12. Attachment and Removal of SATA Instrument Emergency Operation

Removal of the instrument in emergency case, the outer rod of the CBC is pushed back by hand, this pushes back the middle rod of the CBC, which exposes the inner rods of the CBC and IC, which can then be detached.

For the removal of the instrument during an emergency, the middle cylinder of the instrument should be able to be pushed back during any point of its translational motion (functional region) (Fig.18). At the extreme ends, i.e. when the middle cylinder is either completely pushed out (at 4mm from N.A.) or completely pulled in (2.5mm from N.A.) the mechanism should be able to push back the middle cylinder by 2.5mm, when completely pulled in and 6.5mm (2.5mm+4mm), when completely pushed out. This push should be able to be performed manually by the assistant during surgery.

For this requirement the factors are:

- (s) The middle cylinder when completely pulled in by the motor should be able to be pushed in manually by 2.5mm.
- (t) The middle cylinder when completely pushed out by the motor should be able to be pushed in manually by 6.5mm.

Safety requirements

These requirements play a role in increasing the safety of the system and make the surgical safe by designing the safety in the surgical system.

13. Backdrivable

The Control Box needs to allow the instrument to be moved by hand. This requirement is necessary so that in case of emergencies when the instrument is retracted from the body, the tip will easily shift to allow the instrument to be retrieved.

For this requirement the factors are:

- (u) Backdrivable mechanism for the Control Box design.

14. Sterilizable

The sterilizability of a system depends on how easily the system can be disassembled into the components like critical, semi-critical and non-critical items. Once the separation has been made, each component in these categories will have to be cleaned in a different manner. The component should be able to undergo the cleaning procedures in its respective categories.

The 3 categories are Critical, Semi-Critical and Non-critical (Rutala and Weber, 2013).

Critical items- These include items that are in direct contact with any tissue or vascular system.

Semi-Critical Items- These include items that come in contact with mucous membranes or non-intact skin.

Non-Critical Items- These include items that come in contact with intact skin.

The instrument will be in direct contact with the patient and hence belongs to the critical category. The slave arm will be covered by a sterile drape, so that it does not have direct contact to the patient and can be placed in the non-critical category. The slave arms require then only low level sterilization and cleaning. But in the design of these components it is necessary that the system does not have deep grooves or other intricate shapes that can harbor bacteria or microorganisms and make cleaning difficult.

For this requirement the factors are:

- (v) No deep grooves or other locations that can harbor micro-organisms.
- (w) Possibility to attach a cover/drape for the surgical system.

3. Methods

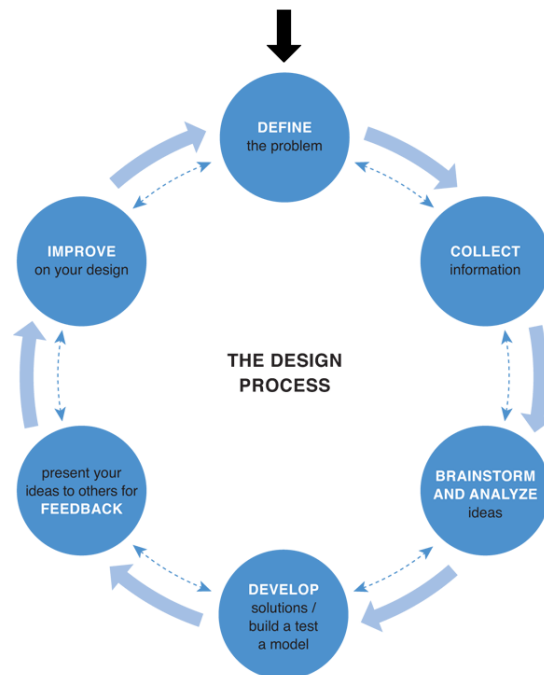


Figure 19: The Design Process

The design and manufacture of the mechanisms for the PoLaRS SATA instrument control was the aim of the thesis project. The scope of the project was from developing a concept to building a functional prototype. Hence, there was a need for a methodology to develop ideas, select best concepts, create iterations etc.

The design process used was a combination of different design processes (Fig.19) (CAC.C Studio V, 2018) and methods that I came across during my studies and by literature searches.

The design process involved the following steps (Fig.20):

1. Define the goal
2. Gather information about the goal
3. Sub-divide the goal
4. Brainstorm multiple solutions for each sub-goal
5. Select solutions and define further for each sub-goal
6. Combine the selected solutions to obtain the main goal
7. Test the feasibility of the solution
8. Manufacture the solution
9. Test the solution
10. Iterate on the solution by comparing with the goal
11. Finalized solution

Steps 6 and 7 are interchangeable as we can test the sub- solutions first and then combine them to provide the main goal or we can first combine the solutions and then test the complete goal. In this design process the combinations was made first and then the concepts were tested.

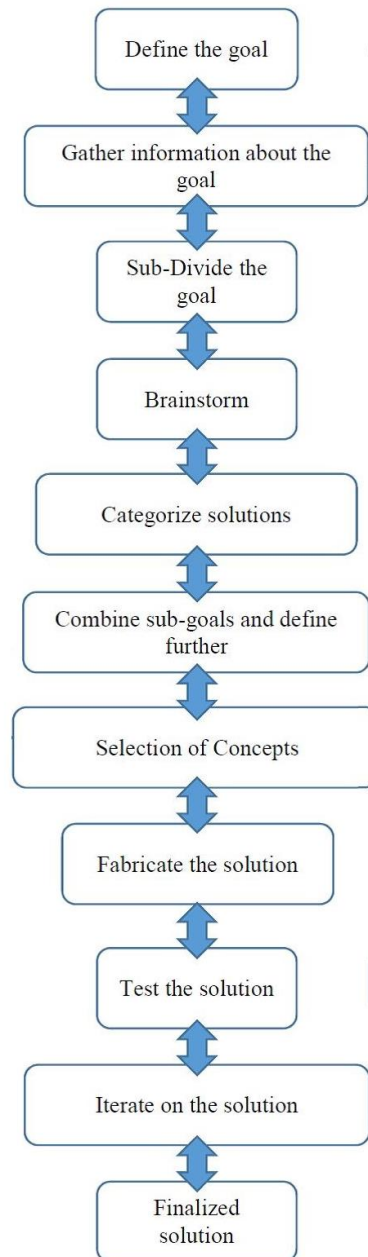


Figure 20: Design Process

3.1. Design Approach

The design process began, when the design requirements and the thesis goals were specified. The large goal of building the mechanism for the control of the SATA instrument, was broken down into its constituent sub-goals. The solutions to each of these sub-goals were found separately by a series of brainstorming sessions and several design solutions were listed. These solutions were then categorized into different mechanisms that were used for the control of the SATA instrument movements.

Morphological chart was used to check for other missed solutions and categorize the concepts more efficiently in a table form. This also provided an overview of all the solutions that were thought of during the brainstorming session.

Selection of concepts was done by using the Pugh Matrix Analysis (PMA). There were several criteria listed and a weighted point system was used to select the most promising solution from the different solutions listed. Once the solution was found. It was further developed and improved, the FEA of the critical parts was carried out to check for the structural strength of the components in the mechanism.

After the FEA analysis, calculations were performed for the speeds, torques and forces to obtain the requirements for the selection of actuators. The actuators, springs, belts, pulleys etc. were brought and the other parts were manufactured in the workshop at 3me or the DEMO lab.

Once all the parts were assembled and the first prototype was build. After performing tests on the first prototype, the problems arising were noted and corrections were listed. Another design iteration was carried out where the solutions to these problems were implemented in the new design and another test was done before the second prototype was build.

3.1.1. Define the Goal

A study of the existing system parts like the base, arm of the PoLaRS slave device and the SATA instrument was carried out. The goal of the project was clearly defined, with no ambiguity. The goal also took into account the coupling rods (CBC and IC), which were in development phase that would be used in the design of the Control Box.

3.1.2. Subdivide

The main goal of controlling the movement of the instrument was divided into sub-categories to facilitate brainstorming for ideas.

The DOF needed to be controlled were:

- (a) *Control of the instrument yaw* – controlled by the **rotation** of the outer cylinder of the SATA Instrument.
- (b) *Control of the instrument pitch* – controlled by the **rotation** of the middle cylinder of the SATA Instrument.
- (c) *Control of the instrument rotation* – controlled by the **rotation** of the innermost cylinder of the SATA Instrument.
- (d) *Control of the gripper (open/close)* – controlled by the **linear translation** of middle rod of the SATA Instrument.
- (e) *Control of the linear movement of the instrument* – controlled by the translational movement toward and away from the abdomen (**z translation**) of the entire SATA Instrument.

The goal was subdivided into 3 sub-categories, these categories were obtained from combining similar functions (**rotation, linear translation and z translation**) that needed to be achieved. The 3 sub-categories were:

- (a) Rotation of the 3 cylinders of the SATA Instrument
- (b) Translation of the middle cylinder of the SATA Instrument
- (c) Translation of the entire SATA Instrument

This made it easier to focus on obtaining solutions to the sub-goals as it would create a simpler design if the same mechanism was used for the same function in the entire system. In each of the sub-goals the focus was on the sub-goal and only at the end of the brainstorming sessions and creation of the morphological chart, that the sub-goals were combined into a complete goal. The combination of the sub-goals with each other was done by checking for the fit (in terms of space available, interference of mechanisms, force interaction and ease of combining one mechanism with the other), these were checked by using 2-D drawings and 3-D modelling was used when they would fit well with each other in 2-D drawings.

3.1.3. Brainstorm

A brainstorming session was carried out to generate ideas for the sub-goals. There were several concepts obtained during the brainstorming session. For each of the idea there was a drawing associated with it to make it easier to understand. Each of the solutions obtained for the sub-goals had their own advantages and disadvantages which were analyzed (Appendix A).

3.1.4. Categorize Solutions: Morphological Chart

Morphological Chart consists of all the solutions that were thought of during the brainstorming session. A morphological chart with the 3 sub-goals was created. The first row is for the ZTM, the second row is for rotation of rods and the third row is for linear movement of middle rod (Fig.21). The ideas generated were used to find solutions to these individual sub-goals in each row. The concepts generated were listed in the row of each sub-

goal. Further reflection on the ideas generated and possibilities for other types of mechanism were also checked.

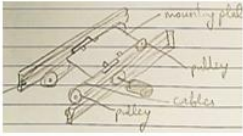



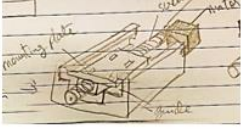




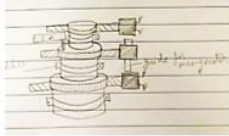



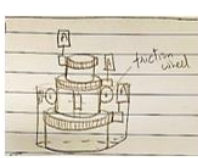

Solutions						
Sub-functions	Mechanism	Concept 1	Concept 2	Concept 3	Concept 4	Concept 5
		Cable Drive	Rack and Pinion Drive	Magnetic Drive	Belt Drive	Nut/Screw Drive
	Z-translation					
Rotation of Rods		Belt System	Cable System	Gear System	Rack and Pinion System	Worm Gear System
						
Middle Rod Translation		Screw Mechanism	Linear Actuator Mechanism	Rack and Pinion Mechanism	Friction Wheel Mechanism	Pulley System
						

Figure 21: Morphological Chart

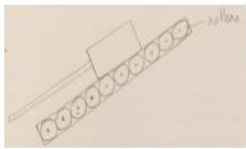
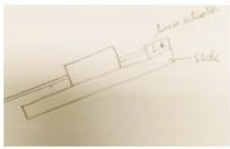
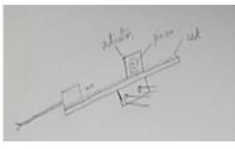
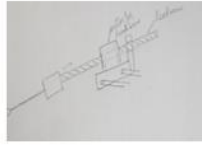
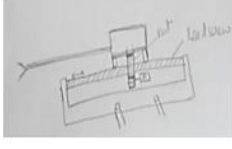
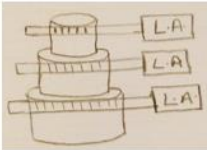
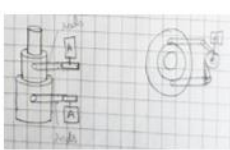

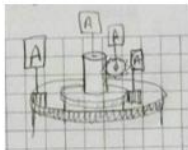

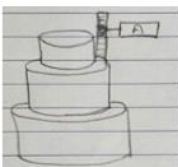
Solutions						
Sub-functions	Mechanism	Concept 6	Concept 7	Concept 8	Concept 9	Concept 10
		Roller	Linear Actuator	Reversed Rack and Pinion	Leadscrew Motor	Reversed Nut/Screw
	Z-translation					
Rotation of Rods		Linear Actuator	Rods and Links	Bevel Gears	Internal Gear	Offset
						
Middle Rod Translation		Rack and Pinion 2				
						

Figure 21: Morphological Chart (Continued)

3.1.5. Combine Sub-goals and Define further

The solutions of the sub-goals obtained from the previous steps were combined to obtain complete solutions for the main design goal. The combination of these individual solutions into a larger solution was done by checking which of the sub-solutions fit well (in terms of space available, interference of mechanisms, force interaction and ease of combining one mechanism with the other) with the other sub-solutions. A total of 12 suitable solutions were obtained from the combinations created in this manner. The combination of the solutions are shown in Appendix B

3.1.6. Pugh Matrix Analysis

The Pugh Matrix Analysis (PMA) is used to compare and make decisions on different ideas, approaches, projects etc. and helps to determine the best possible option/solution from a set of possible options/solutions. This approach is commonly used in organization teams to select the best possible solution from a set of solutions. It helps to eliminate unfeasible solutions based on an objective matrix. This is similar to the Harris Profile or the Weighted Decision Matrix approach.

The process of PMA is composed of the following steps (Cervone, 2009):

1. Selection of criteria for comparison.
The criteria are the ideas or models or concepts that need to be compared. The different criteria are formed through brainstorming sessions and by further developing the ideas obtained. The criteria can also be a highly developed criteria for example, a model or a prototype. In this design process, the 12 solutions obtained from the combination of the sub-goals were the criteria for the PMA.
2. Selection of factors to be compared.
The factors that need to be compared are the different items which are considered across the criteria. The factors can be selected based on the design requirements or can be determined by considering factors that will affect the selection of the criteria. The factors such as cost, robustness, complexity, controllability etc. were the factors that were compared for this design process.
3. Drawing of the matrix
Once the criteria and the factors are selected the matrix can be drawn. It consists of a table with the list of criteria on one axis and the list of factors on the other axis. Commonly the criteria are mentioned on the x-axis and the factors on the y-axis. Additional rows are created at the bottom of the factor list, to calculate the total of the scores.
4. Assignment of weights to factors
The factors for the selection of the criteria may not be of the same importance. Some of the factors may have higher importance than the rest. This can be taken into account by assigning weights to the factors. Factors with a higher importance are assigned higher weights and the lower importance factors are assigned lower weights.
5. Define a baseline
Normally a baseline is defined by comparing the criteria to a similar idea, concept or a current product. The scale can be either better(+1), the same (0) or worse (-1). This scale can be made finer by using a finer rating scale such as 3,2,1,0,-1,-2,-3. In cases where it is difficult to find the baseline, the scale can also be altered by using only positive values for comparison and each of the criteria can be compared with the rest of the criteria.
6. Generating scores for factors
Normally each individual of a design team would assign scores for each of the factors and then these scores would be averaged and a set of scores for the factors would be determined. In the case of single person performing this PMA, the scores are determined individually and assigned to the factors.
7. Computing scores for criteria
The scores against each of the criteria are added up and the ranks are generated for each criteria. There are generally four scores generated: The number of plus scores, the number of minus scores, the overall total score and the weighted total score. The overall total score is obtained by subtracting the number of minus scores from the number of plus scores. The weighted total score is obtained by multiplying the scores with the respective weighted factors.

It is important to realize that the PMA provides a list of criteria with their scores. It is possible that the solution with the highest score in PMA may not be the most suitable for the application, the task may not have the highest priority or be the most important. PMA does not guarantee that the criteria with the highest score is the best but it provides a useful tool to see the relative scores of each of the criteria to make the selection process easier.

3.1.7. Selection of Concept using PMA

There were 12 concepts selected from the combination of sub-goals. The best concept from these concepts had to be selected. PMA was used to identify the best solutions based on certain factors as listed:

1. **Cost:** This refers to the cost of the components and the mechanisms needed for the system. A system with low cost components is preferred.
2. **Robustness:** The ability of the system to function under different conditions and still have the same performance. Higher robustness is preferred.
3. **Complexity of system:** The complexity of the construction can be broken down into the individual systems and the interaction that the systems have with the other sub-systems. It also encompasses the inherent complexity of the system. For example, complex alignment of certain cables or gears. A simpler system is preferred.
4. **Ease of use:** A system use should be intuitive. The ease of use can be broken down in to the number of steps needed to perform a procedure or action on the system and the time it takes to activate the system. It is important to have a system that is simple and easy to use.
5. **Structural stiffness/Mechanical strength of the system:** The system should be stiff and have enough strength to support the forces that are generated in the system. The mechanisms and the arrangement of the different mechanisms determine the structural strength/stiffness of the system. A more stable system is preferred.
6. **Controllability/Accuracy:** The system need to be highly accurate. The accuracy of the system depends on the accuracy of the actuators used and the accuracy of parts of the mechanism connecting them. The accuracy of the system also depends on the materials used in the mechanisms. A high accuracy system is preferred.
7. **Compactness of design/ Volume of system:** The overall dimensions and the placement of the mechanisms/parts in the system determine the space that will be taken by the system. There is a limited amount of space available for the design of the system and hence a system with a smaller volume or a compact design is preferred.
8. **Weight of the system:** The density of the materials and the number of parts used in the design determine the mass of the system. The system with a smaller mass is preferred since the system needs to be within a certain weight constrain.
9. **Safety:** The safety is difficult to determine at this stage as the concepts are not fully developed. Nevertheless, it is highly important to consider this criteria. The designs with no protruding sharp parts, use of safe materials, protection from high speed/fast moving parts etc. are preferred for safety.
10. **Reliability:** The system should be able to perform at the same level even after a certain amount of time has passed. There should be no decrease in the level of performance of the system due to repeated use or with time. This is also difficult to determine at this stage, however some signs like the use of elastic materials, use of thin wires, use of friction systems etc. can cause a decrease in performance with time/use. A system with a higher reliability is preferred.
11. **Ease of assembly/disassembly:** The system should be easy to assemble and disassemble.
12. **Range of Motion:** The system should be able to access the entire range of motion mentioned in the requirements.

Some of the factors were removed as they were either too vague or could not be determined at this initial stage of design .For example, the ease of assembly or disassembly and ease of use was difficult to comprehend since the criteria were in a very early stages of development, factors like the range of motion was also not considered as this had to be achieved by every concept and hence was an inclusive criteria.

The Pugh Matrix was built (Appendix C) and initially 3 concepts with the highest scores were chosen. Concept 8, Concept 9 and Concept 12 were selected from PMA (Fig.22, Fig.23, Fig.24).

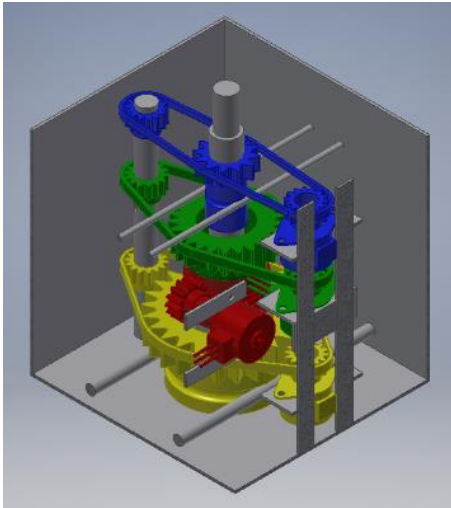


Figure 22: Concept 8

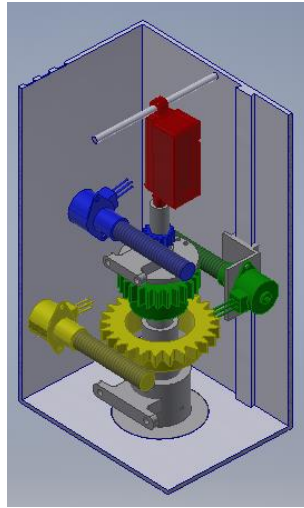


Figure 23: Concept 9

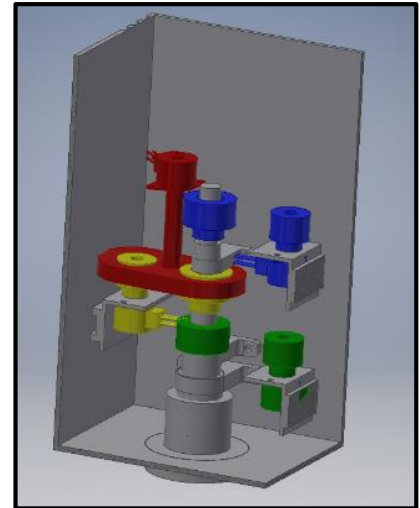


Figure 24: Concept 12

After further analysis, the 12th concept was chosen for further development and refining of the concept idea.

The chosen concept was further detailed and the calculations were performed for the actuators and other components like belts and springs needed. Size of these components were chosen so as to make sure that the complete Control Box would be under the size requirements.

3.1.8. Manufacture the Solutions

Concept 12 was detailed further and the locations of the motors and the sizes of the actuators needed were determined. The calculations for the actuators, belt and spring were performed in this step.

Once the design detailing was complete, a FEA analysis was conducted on some critical parts to check for the stability of the parts (Section 3.2.3). The analysis was able to point to some changes that needed to be done. These parts were changed before they could be manufactured. Further details of the manufacture and detailing are presented in Section 3.2 and Section 4.1.

3.1.9. Test the Solutions

The validation of the solution was carried out after building the prototype. Tests were carried out to check for the conformity to the requirements. There were additional experiments carried out to check for the functioning of the sub-systems for example the cable pulley system, timing belt- pulley system, bead forces, spring forces and the fit of all the parts in the box. These tests were done to ensure that the prototype was built as smoothly as possible..(Section 3.3)

3.1.10. Iterate on the Solution

There were several iterations carried out in the design of the Control Box and the ZTM. The design iterations were performed on individual parts as well as complete assemblies. There were several modifications done on parts for reducing the weight of the system and to improve the aesthetics.

While some iterations were done during the design phase, other iterations were carried out in the prototype phase, after the parts had been manufactured. These iterations were done to adjust the actual dimensions of the actuators, deal with tolerance issues, adjust to the belt sizes etc. All these solution iterations were used to obtain a final design solutions.

3.1.11. Final Solution obtained

The final solution was obtained after several iterations and (re-)runs through the design process. Elimination of errors and problems in the design allowed for the development of the latest prototype model. The problems arising in phase 1 of the testing were noted and solutions to these problems were implemented in the design before phase 2 testing, Creating the final prototype of this thesis project.

However, it is important to note that the design built in this thesis is the 1st prototype. This solution is not the final solution for the goal of the PoLaRS system but it is a starting step for improving on this system. Further improvements in the design and control of the system can make the system even better.

3.2. Concept Design

The PoLaRS Control Box and its ZTM was designed through iterative design process. This section includes the final design concept and its working principles. This section also contains the calculations for the torques and speeds of the motors, belt lengths, springs and leadscrews.

3.2.2. Complete Assembly of the Slave Arm

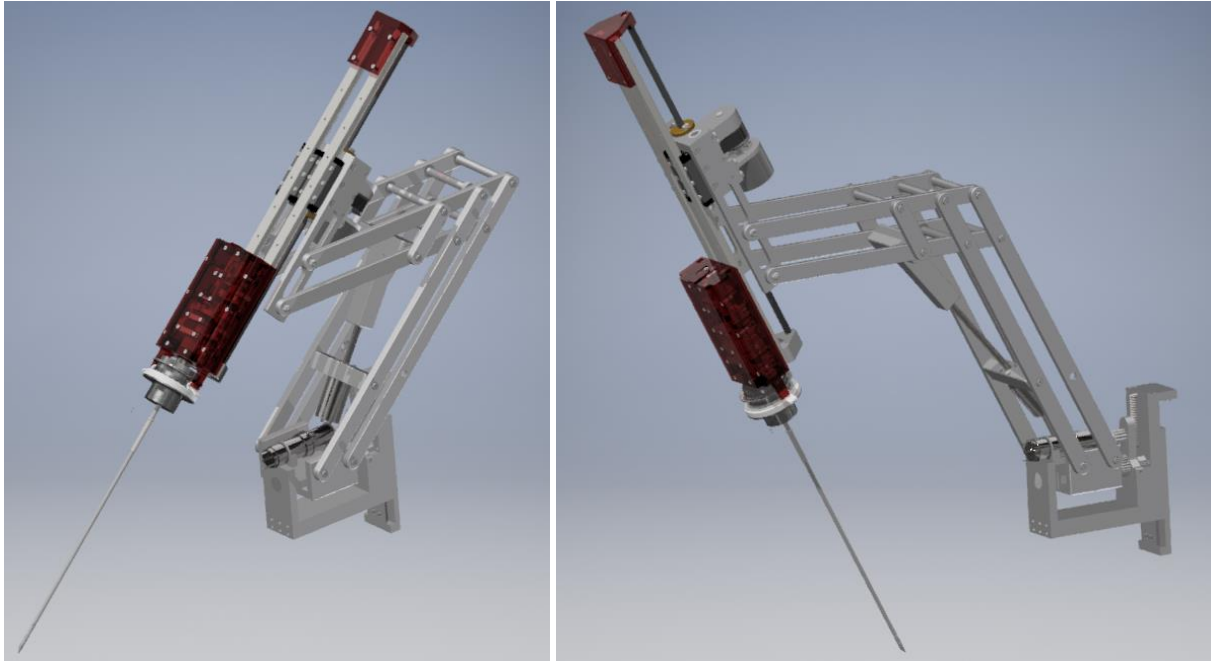


Figure 25: Complete Assembly on PoLaRS Arm

Complete assembly of the ZTM and the Control Box on the slave arm is shown in Fig 25. The connection of the ZTM to the PoLaRS arm is done by using a screw and bolt with bearings between them through the connecting bars. The connection is made on the two side rectangular parts (2, 14) called connecting bars (Fig.29). These hold the system in place on the PoLaRS slave arm and support the ZTM. The slave arm can move in the forward-backward and left-right directions. The ZTM follows the movements of one of the linkages of the slave arm, due to the use of parallelogram mechanism for the slave arm. These movements allow the surgeon to gain additional 2 DOF to maneuver the SATA instrument.

This completed assembly of the slave arm will then be mounted on the base of the slave device to complete the assembly of the slave cart. There are 2 completed slave arm assemblies mounted on one base of the slave device. The total DOF available from the completed assembly of the PoLaRS slave is 7 DOF, which includes the 4 DOF from the Control Box, 1 DOF from the ZTM and 2 DOF from the slave arm.

3.2.1. ZTM

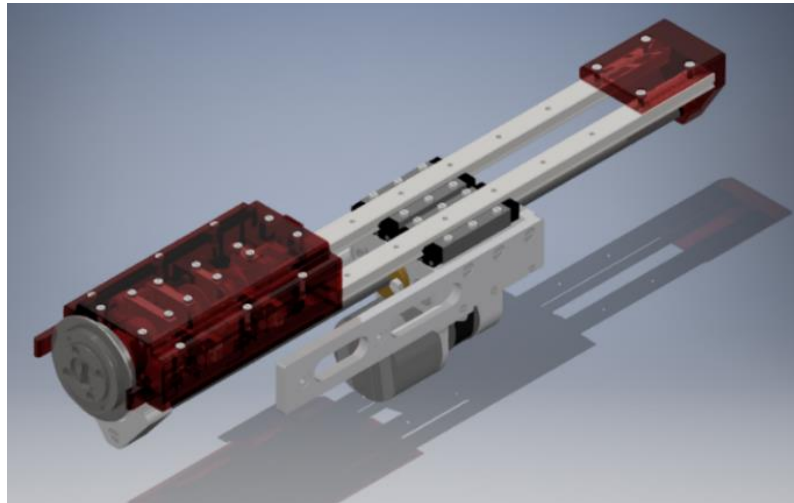


Figure 26: PoLaRS ZTM

The ZTM is shown in Fig.26. This system will be mounted on the PoLaRS slave arm as shown in Fig.25. The Control Box along with the slides and the leadscrew (red colored) is moved over a slide to achieve the ZTMo i.e. to move the instrument towards and away from the abdomen (Fig.27). The ZTMo of the instrument provides a movement range of around 406mm. This is achieved by means of a leadscrew mechanism.

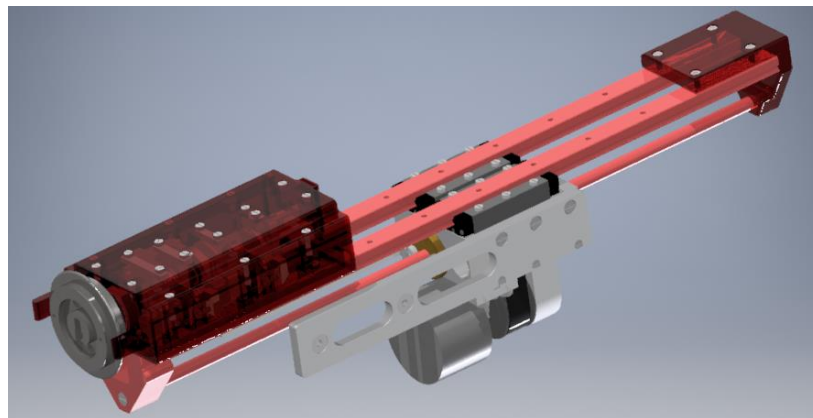


Figure 27: ZTM Functioning

The numbered components in Fig.28 and Fig.29 make it easier to understand the text that follows.

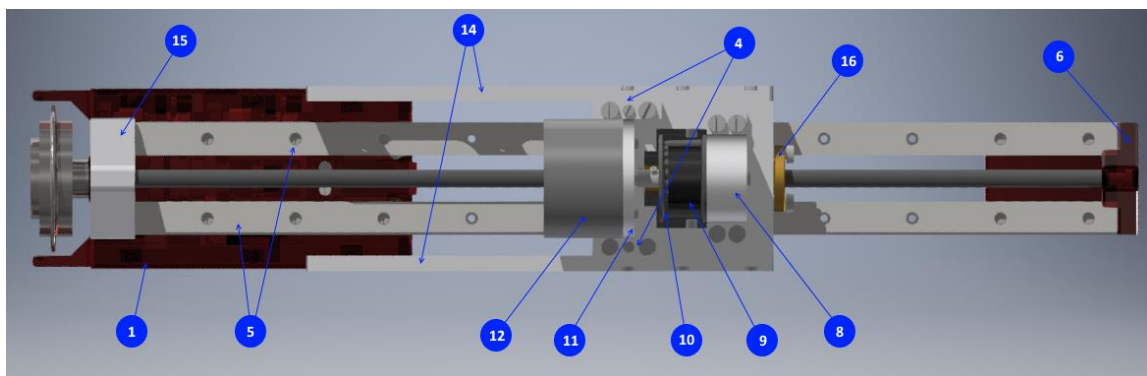


Figure 28: ZTM Back View

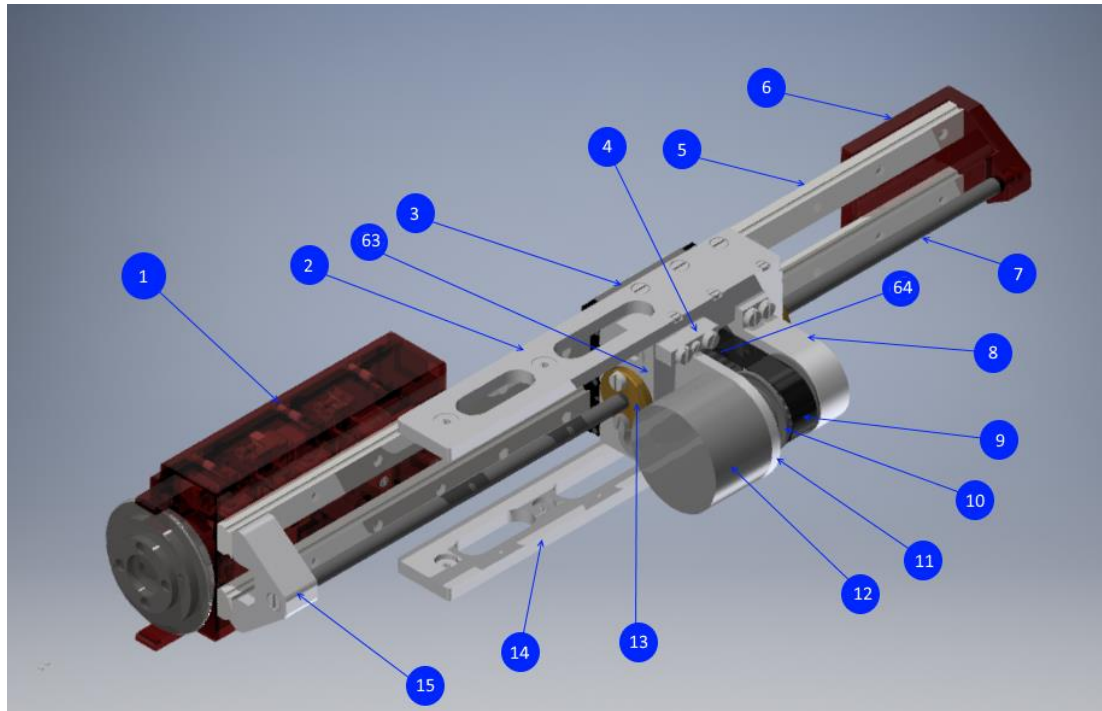


Figure 29: ZTM Orthogonal View

The ZTM has a single motor (12), which rotates a pulley (10) by using a belt (9). Another pulley (64) closer to the leadscrew (7) is also connected to the other end of the belt (9). The pulley (64) has trapezoidal threads internally through its center. These threads mate with the threads of the leadscrew (7). When the pulleys (64, 10) rotate, the leadscrew (7) moves translationally along its axis through the center of the pulley (64). The pulley is fixed in a small gap by using 2 end parts (13, 16). These ensure that the pulley (64) does not travel with the leadscrew and only rotates. There are 2 slides (3, 5) in the system to guide the Control Box (1). The slides are attached inverted with the travelling part (3) fixed on the main body (63) and the slides (5) allowed to move translationally only. The leadscrew pulls/pushes the end parts (6, 15), which moves the Control Box on the slides with it. The slides are kept in position by using a 3-D printed end (6) and the Control Box. This ensures that the slides are not misaligned and are parallel to each other. The motor is attached to an aluminum plate (11) by using the holes provided in the motor. The aluminum plate (11) is fixed on the main body (63) by means of 2 tiny holders (4). The shaft of the motor is extended to hold the pulley (10) and to support the other end in a bearing on a motor shaft support part (8). This ensures that the motor shaft does not bend due to the bending forces arising from the belt.

3.2.1. Control Box

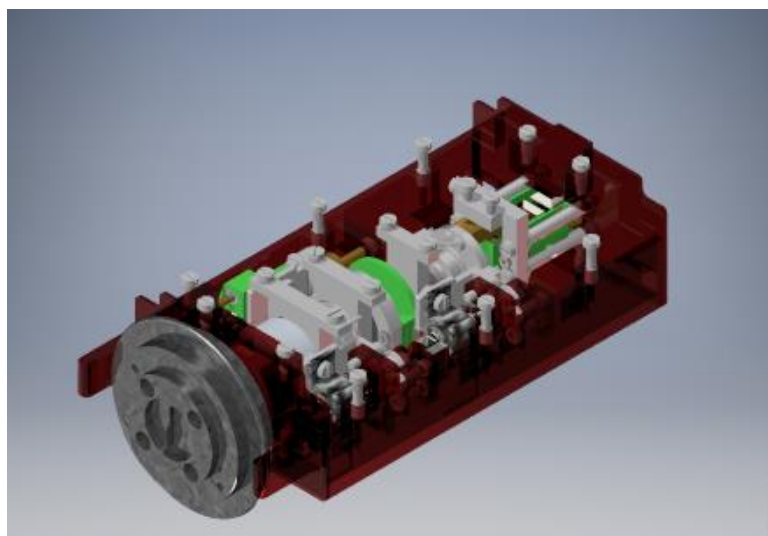


Figure 30: PoLaRS Control Box

The Control Box controls the yaw, pitch, rotation and opening/closing of the gripper (Fig.30). In order to achieve this, the Control Box uses a cable-pulley driven system (Appendix H) where the pulleys rotate the 3 cylinders of the SATA instrument through the CBC and IC coupling by 180 degrees, which drive the SATA instrument tip (Fig.31.Fig.32). The green colored motor-pulley system rotates the pulley on the innermost rod, the yellow colored motor-pulley rotates the pulley on the outermost rod and the red colored motor-pulley rotates the middle rod pulley. The middle rod along with the red colored parts are moved translationally 4mm during normal operation and 2.5mm more for removal and attachment of the CBC to the IC. The actuators are installed inside the Control Box for these movements, there is space available for routing actuator wires inside the Control Box.

The numbered components in Fig.33, Fig.34 and Fig.35 make it easier to understand the text that follows.

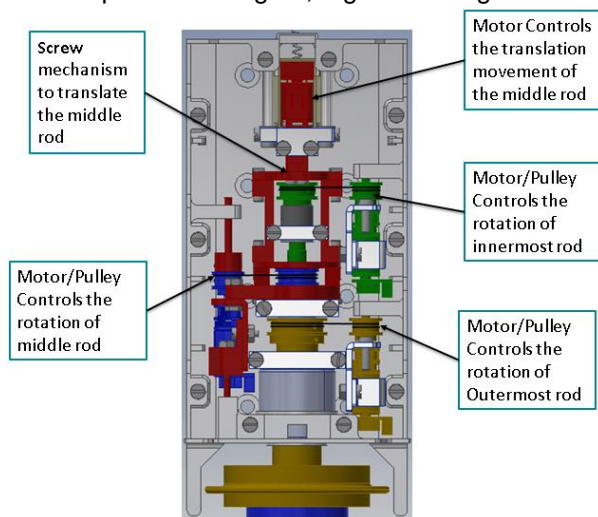


Figure 31: Mechanisms in the Control Box

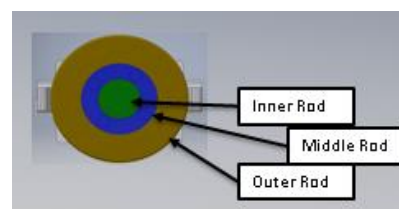


Figure 32: Instrument Control Box with CBC rods

The Control Box is made of 4 cover parts (17, 18, 19, 20), which forms the box in which the other components are fitted. There are 4 motors (59,33,41,49) in the Control Box, 3 motors (33,49,41) are connected to the pulleys (51,31,39) which have a cable running through it and passing on to other pulleys (32,37,40) attached to one of the cylinders (inner, middle or outer). The motors (33, 41) are fixed by means of a motor bracket (42, 34), plastic support (35,43) and bushing parts (30,38). The other motor (49) is held by the motor bracket (50), plastic support (47) and longer bushing part (54).

When the pulleys rotate due to the motors, it pulls on one side of the cable, which causes the pulleys on the cylinder to rotate, which in turn rotates the CBC rods (21,22,23). When the direction of the motor is reversed, the pull is on the other side of the cable and the cylinder rotates in the other direction. The CBC rods are held in place by means of 3 holders (44,38,55). There is a bushing (45) between the box part (20) and the outer CBC piece to allow smooth rotation. The inner CBC piece is prevented from falling out of the Control Box by means of a shaft collar (56), which touches the holder (55).

The other motor is connected to a tiny threaded leadscrew (61). This leadscrew connects to the thread inside a nut part (29). This arrangement is similar to a screw nut mechanism, when the screw is rotated the nut will move forward or backward. The nut part is held in place by means of 2 rectangular supports (57) Thus when the leadscrew is rotated the entire mechanism (red colored) for the translation also moves translationally (Fig.31).The mechanism is guided by means of 2 rods (46), that move in holes in the box part (20) and the guide bar (58) which mates with the 2 L- blocks (28). The middle pulley (37) also moves along with the middle CBC rod (22). This movement of the middle pulley (37) is obtained by sandwiching the middle pulley (37) between the support arm (52) and a circular disk (36). There are 2 spacers (53) which prevent the crushing of the middle pulley (37).

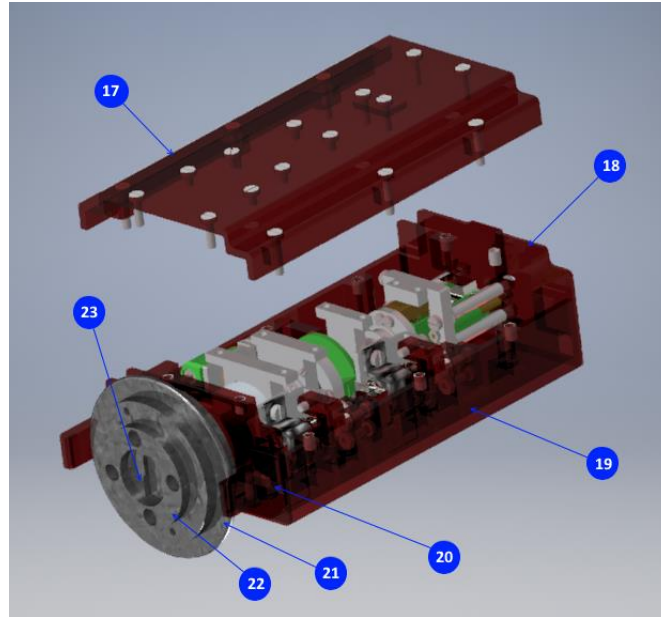


Figure 33: Control Box Orthogonal View

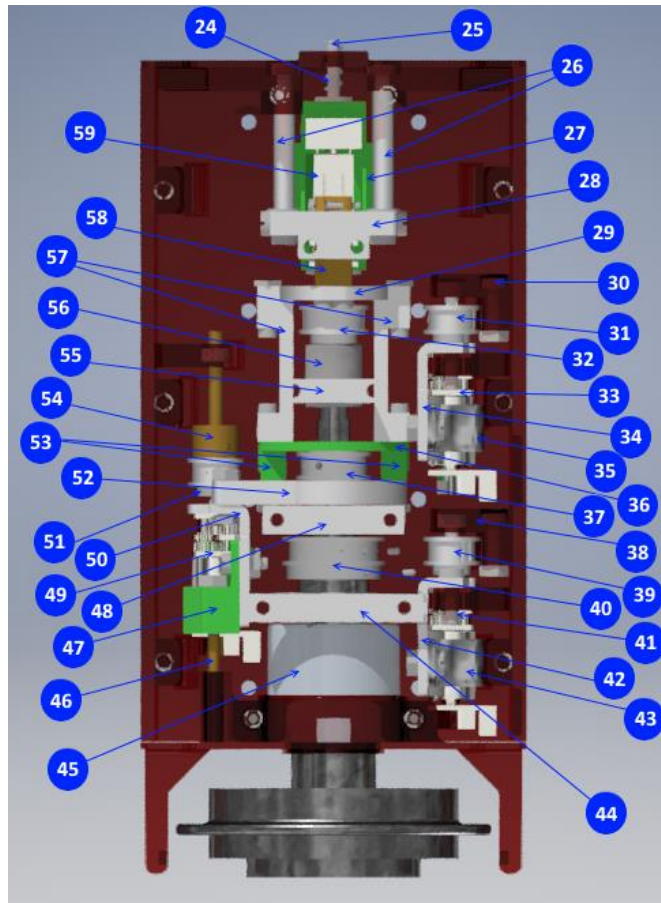


Figure 34: Control Box Front View

Another important mechanism inside the Control Box is for the detachment of the SATA Instrument in case of emergency i.e. emergency decoupling to remove the IC and SATA instrument from the CBC. The need was that the middle cylinder (22) should be able to be pushed back by at least 2.5mm, when the middle cylinder is completely pulled in by the motor (59) in the motor box (27) and 6.5mm, when the middle cylinder is completely pushed out by the motor (59). The motor (59) is guided by rods (26) and guides (60), which ensure the motor only translates.

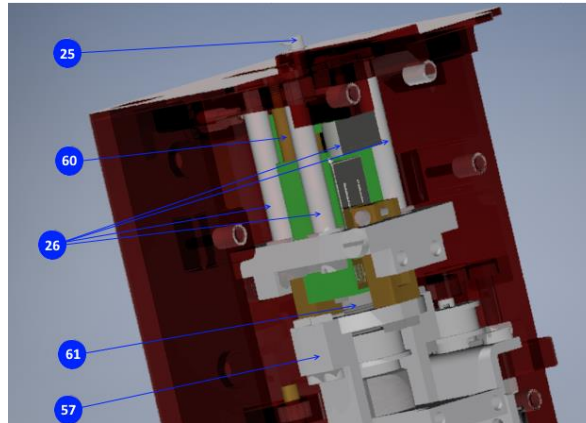


Figure 35: Control Box Angled View

For this mechanism, a spring (24) and a spring support (25) was used to provide constant pressure to the motor connected to the tiny leadscrew (61) so that the screw nut mechanism can have contact at all times. This constant spring pressure is held by 2 L-blocks (28). In case of emergencies the middle cylinder along with the motor and the entire middle cylinder translation mechanism (red colored) will be pushed back by pushing on the outer CBC rod (21), which compresses the spring (Fig.35) and once released the spring will set back the middle cylinder translation mechanism back to its normal position.

The assembly instructions of all the parts of the Control Box and the ZTM are mentioned in Appendix I.

3.2.3. Mechanical/Strength Analysis

The Finite Element Analysis (FEA) was carried out in Inventor. The critical parts that were under loads or stress were tested by using FEA stress analysis in Inventor. There were 2 components in the Control Box (motor box and linear movement middle pulley holder) that were under load and 2 components from the ZTM (threaded leadscrew and connecting bars) which were loaded by external forces or weights. A FOS above 2 is considered good and sufficient for use.

Motor Box

The Motor Box (Fig.36, Fig.37, Fig.38) is connected to the spring which pushes on the top face of the motor box. There is constant force on the top face, which is at the maximum (30.29N) when the middle rod is pushed back. The push back causes the entire middle rod translation mechanism to be pushed back and the spring to be compressed, which provides the force on the top face of the motor box.

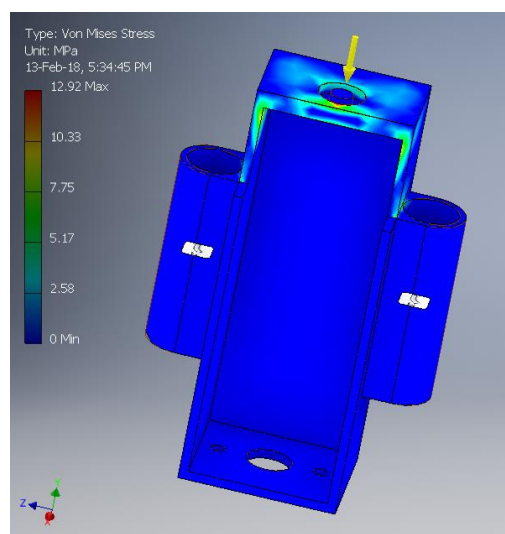


Figure 36: Motor Box Von Mises Stress

Force used for this analysis was 31N.

The results show that the maximum Von Mises Stress on the part is 12.92MPa.

The material used for this case is R05 which has a maximum yield strength 31-39MPa (EnvisionTEC, 2018) and hence the part has a factor of safety (FOS) as follows:

$$FOS = \frac{\sigma_{limit}}{\sigma_v}$$

Where, σ_{limit} = maximum yield strength of material

σ_v = maximum stress obtained from FEA

$$FOS = \frac{39}{12.92} = 3.01$$

The FOS≈3, which is sufficient.

The force acting on the opposite side of the motor box.

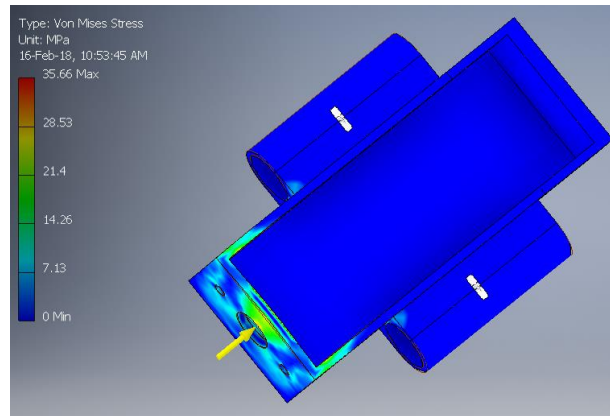


Figure 37: Motor Box Push Side

Force used for this analysis was 50N.

The results show that the maximum Von Mises Stress on the part is 35.66MPa.

The material used for this case is R05 which has a maximum yield strength 31-39MPa (EnvisionTEC, 2018) and hence the part has a factor of safety (FOS) as follows:

$$FOS = \frac{39}{35.66} = 0.869$$

The FOS≈0.8, which is NOT sufficient. Therefore the thickness of the part needs to be increased so that the FOS reaches above 2.

After increasing the thickness from 0.8mm to 1.3mm.

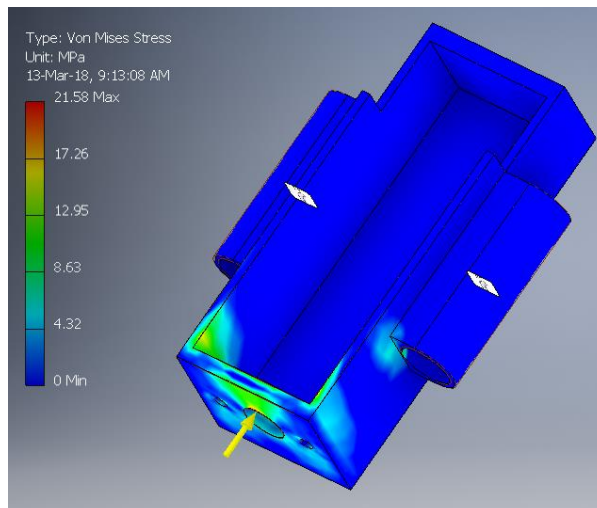


Figure 38: Motor Box Push Side Increased Thickness

The results show that the maximum Von Mises Stress on the part is 21.58MPa.

The material used for this case is R05 which has a maximum yield strength 31-39MPa (EnvisionTEC, 2018) and hence the part has a factor of safety (FOS) as follows:

$$FOS = \frac{39}{21.58} = 1.8$$

The FOS≈2, which is sufficient for use.

LMMPH

The LMMPH (Fig.39), connects and holds the driven and the driving pulley of the middle rod together. It moves the pulleys translationally, when the middle rod is moving translationally. It also allows the driving middle rod pulley to rotate the middle rod through the driven middle rod pulley on the middle rod. When the middle rod is pushed or pulled, the LMMPH needs to handle the force generated by the leadscrew mechanism.

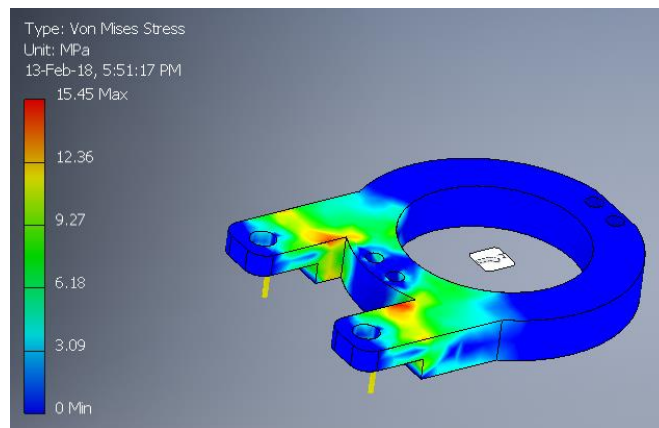


Figure 39: Middle Pulley Holder Von Mises Stress

Force used in this analysis was 65N, this was obtained by considering that the force from the leadscrew which is 130 N will be distributed between the 2 extended arms of the LMMPH (Section 4.2.2).

The results show that the maximum Von Mises Stress on the part is 15.45MPa

The material used for this case is Aluminium 6061 which has a maximum yield strength of 55 MPa and hence the part has a factor of safety (FOS) as follows:

$$FOS = \frac{55}{15.45} = 3.55$$

The FOS≈3.5, which is sufficient for use.

Threaded Leadscrew of ZTM

The leadscrew of the ZTM (Fig.40), is connected at its 2 end points and also between the pulleys by 2 guide rings. The driving pulley uses a belt to turn the driven pulley, hence the tension of the belts is transferred to the leadscrew. The tension in the belt will try to pull the driven and driving pulleys together while the leadscrew should not bend due to the tension in the belt.

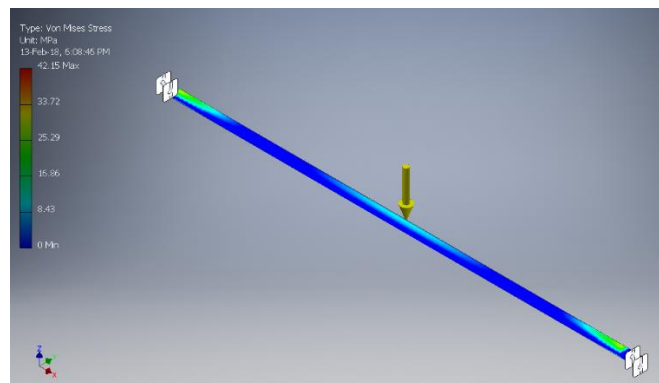


Figure 40: Leadscrew Von Mises Stress

Force used in this analysis is 50N, this is obtained by considering the torque of the motor and finding out the tension in the belt. We obtain 25 N as the tension force in the belt by using the torque equation,

$$Torque = Force * Distance$$

$$150 = Force * 6$$

$$Force = 25N$$

Since there are 2 sides of the belt, we obtain 50N of force acting on the leadscrew.

The results show that the maximum Von Mises Stress on the part is 42.15MPa, The material used for this case is Stainless Steel which has a maximum yield strength of 215 MPa and hence the part has a factor of safety (FOS) as follows:

$$FOS = \frac{215}{42.15} = 5.1$$

The FOS≈ 5.1, which is sufficient for use.

ZTM Connecting Bars

The entire ZTM is attached to the arm by means of 2 translation holders called connecting bars. These connect the ZTM to the slave arm. These connecting bars need to be able to hold the entire weight of the system (Fig.41).

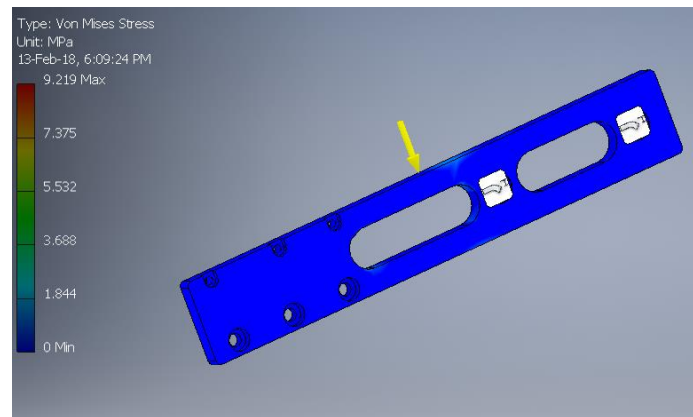


Figure 41: ZTM Holder Von Mises Stress

Force used for this analysis is 40 N, which is obtained by considering the weight of the system held by these connecting bars, which is around 3.2 kg. Increasing the force to account for additional weights of the coupling rods and the SATA Instrument we arrive at a weight of around 4 kg≈40N.

The results show that the maximum Von Mises Stress on the part is 9.219 MPa, The material used for this case is Aluminium 6061 which has a maximum yield strength of 55 MPa and hence the part has a factor of safety (FOS) as follows:

$$FOS = \frac{55}{9.219} = 5.9$$

The FOS≈ 5.9, which is sufficient for use.

3.2.4. Calculations for the Design

Calculations were performed for the selection of the actuators, spring force needed and the size of the belt that is needed for the design. There are several assumptions made as some data was not available or difficult to find or verify, these are listed before each calculations. A safety factor (FOS) of at least 2 was used in most of the design calculation.

Torque and Speed for Linear Translation of the Middle Rod

Assumptions:

1. The weight to be lifted by the leadscrew mechanism of the Control Box is 3 kg. This includes the weight of the middle cylinder and the coupling mechanism that attaches the SATA instrument to the middle cylinder.
2. The coefficient of friction is assumed as 0.15, for steel surfaces.
3. The speed of translation for the middle cylinder should be around 4mm/s, to have the gripper open and close at the same speed by the robot as done by hand.

Torque T needed to lift a weight w is given by (Vahid-Araghi et al., 2010)

$$T \geq r * \left(\frac{\mu + \tan \gamma}{1 - \mu * \tan \gamma} \right) * w$$

Where,

r is the radius of the leadscrew.

μ is the coefficient of friction.

γ is the lead angle.

We can further define,

$$\tan \gamma = \frac{l}{\pi * d_m}$$

$$\begin{aligned} l &= n_s * p \\ d_m &= d + \frac{p}{2} \end{aligned}$$

Where,

l is the lead.

n_s is the number of starts.

p is the screw pitch.

d_m is the pitch diameter.

d is the diameter of the leadscrew.

In this design,

$$\begin{aligned} d &= 6mm \\ p &= 0.5mm \\ \mu &= 0.15 \\ n_s &= 1 \\ w &= 30N \end{aligned}$$

Hence,

$$l = n_s * p = 1 * 0.5 = 0.5mm$$

$$d_m = d + \frac{p}{2} = 6 + \frac{0.5}{2} = 6.25mm$$

$$\tan \gamma = \frac{l}{\pi * d_m} = \frac{0.5}{\pi * 6.25} = 0.025$$

Therefore the Torque T ,

$$T \geq r * \left(\frac{\mu + \tan \gamma}{1 - \mu * \tan \gamma} \right) * w = 3 * \left(\frac{0.15 + 0.025}{1 - 0.15 * 0.025} \right) * 30 = 15.8Nmm$$

Hence Torque T should be higher than approx.16Nmm.

For the speed N needed,

$$N = rps * p$$

Where,

rps is revolutions per second of the leadscrew.

$$rps = \frac{N}{p} = \frac{4}{0.5} = 8$$

Hence,

$$rps \text{ in revolutions per minute} = 60 * rps = 60 * 8 = 480 \text{ rpm}$$

We need to select a motor for lifting the middle cylinder that will have,

$$T \geq 16 \text{ Nmm and } N \geq 480 \text{ rpm}$$

Motor for ZTM

Assumptions:

1. The weight to be lifted by the leadscrew mechanism is 5 kg. This includes the weight of the Control Box and a part of the slide weight.
2. The coefficient of friction is assumed as 0.15, for steel surfaces.
3. A linear speed of 60mm/s is assumed to be needed.

In this design,

$$\begin{aligned} d &= 8 \text{ mm} \\ p &= 1.5 \text{ mm} \\ \mu &= 0.15 \\ n_s &= 1 \\ w &= 50 \text{ N} \end{aligned}$$

Hence,

$$l = n_s * p = 1 * 1.5 = 1.5 \text{ mm}$$

$$d_m = d + \frac{p}{2} = 8 + \frac{1.5}{2} = 8.75 \text{ mm}$$

$$\tan \gamma = \frac{l}{\pi * d_m} = \frac{1.5}{\pi * 8.75} = 0.054$$

Torque T

$$T \geq r * \left(\frac{\mu + \tan \gamma}{1 - \mu * \tan \gamma} \right) * w = 4 * \left(\frac{0.15 + 0.054}{1 - 0.15 * 0.054} \right) * 50 = 41.13 \text{ Nmm}$$

Speed N ,

$$N = rps * p$$

$$60 = rps * 1.5$$

$$rps = 40 \text{ revolutions per second} = 2400 \text{ rpm}$$

We need to select a motor for ZTM that will have,

$$T \geq 41.13 \text{ Nmm and } N \geq 2400 \text{ rpm}$$

Belt Length Calculations

Assumptions: No expansion or shrinkage of the cable. The belt is thin and has negligible thickness.

The length of the cable needed is given by the following equation (Kovacevic, n.d.),

$$L = \frac{\pi}{2} * (D + d) + 2 * C + \frac{(D - d)^2}{4 * C}$$

Where,

L is the length of the belt .

D is the radius of the driven timing pulley.

d is the radius of the driven timing pulley.

C is the center distance between the two timing pulleys.

Since, $D=d$ in our case the equation reduces to,

$$L = \pi * (D) + 2 * C$$

$D=35.01\text{mm}$
 $d=35.01\text{mm}$
 $C =50\text{mm}$

$$L = \pi * (35.01) + 2 * 50 = 209.98\text{mm}$$

Hence a belt length of $\approx 210\text{mm}$ is needed.

Spring Calculations

Assumptions:

1. Force to push back spring is 30N.

The spring needs to have the following features from the design restrictions of the Control Box in order to fit inside the Control Box.

1. Maximum length of the undeformed spring $\approx 18\text{mm}$.
2. Minimum length of deformed spring $\approx 6\text{mm}$.
3. Diameter should be $\approx 4\text{mm}$
4. Thickness of the spring 0.5 or 1 mm.

Using,

$$F = k * \Delta x$$

$$\Delta x = x_{ud} - x_d$$

Where,

F is the spring force.

k is the spring constant.

x_{ud} is the undeformed length.

x_d is the deformed length.

Therefore,

$$\Delta x = x_{ud} - x_d = 18 - 6 = 12\text{mm}$$

$$k = \frac{F}{\Delta x} = \frac{30}{12} = 2.5 \text{ N/mm}$$

Hence, the spring should have a spring constant $k \approx 2.5 \text{ N/mm}$

3.3. Test Setup

The built prototype has to be tested for meeting the requirements, this section lists the tests needed to be carried out.

There are 2 phases to the tests, in the 1st phase of the tests, the experiments are conducted on the CBC rods. This is done to ensure that during the first phase of testing, the errors encountered can be eliminated. A redesign or reworking of components can be carried out to eliminate these issues.

The second phase of tests will involve the SATA instrument along with the IC rods, only if the tests show improved results and the instrument can be used for the testing without damaging it or else tests similar to the phase 1 will be performed with the CBC piece.

The tests were carried out at MISIT lab, TU Delft. The equipment used to perform the measurements were:

1. Two pull-push gauges- Model ANF-50 (capacity 50N, min unit-0.5N) for the control box and Model ANF-100 (capacity 100N, min 1N) for ZTM.
2. Power supply unit (digimess® DCPOWERSUPPLY, HY3003, 0-30V, 0-3A)
3. Markers- (3-D printed from PLA to measure torques, range of motion and speed of CBC.
4. Video capturing device, vernier caliper, clamps and holders.

Each of the tests had 3 measurements taken, the values of these measurements were then averaged to obtain the final value.

3.3.1. Tests for Requirements Phase 1 and Phase 2

There are 9 tests in total for each of Phase 1 and Phase 2, with 6 tests for the Control Box and 3 tests for the ZTM to test the functioning and the requirements. The results of the test for Phase 1 and Phase 2 are also listed in this section in order to improve readability.

Tests for Control Box

Test 1: The Range of Motion of CBC

The requirement from the literature are:

- (a) Instrument pitch between ± 60 deg. to ± 90 deg.
- (b) Instrument yaw between ± 60 deg. to ± 90 deg.
- (c) Instrument rotation between 150 deg. to 180 deg.

Introduction: The Control Box consisting of 4 dc motors is used to drive the CBC rods, which in turn drive the IC coupling rods and the SATA instrument. The rotations of the CBC rods are transferred to the SATA instrument and converted to the instrument tip movements.

It is observed that a rotation of 180 degrees on the 2 knobs (Red and Blue) of the SATA Instrument handle (Fig.9) causes the tip to Yaw and Pitch respectively. The rotation of the entire instrument is done by hand by rotating the wrist and hence a maximum range of 180 degrees can be assumed for the rotation.

The coupling rods should be able to rotate the instrument tips in the range mentioned in the requirements. The range of the SATA Instruments is ± 60 deg in Pitch and Yaw. The rotation of the handheld instrument is done by hand and a range of ± 90 degrees can be assumed.

The range of the SATA instrument tips corresponds to the turning of the SATA instrument cylinders by ± 90 degrees, hence when the SATA instrument tip is at the extreme end of its range, i.e. either -60 deg or + 60 deg for pitch and yaw, and -90 deg or +90 deg for rotation, the cylinders are at -90 deg or +90 deg respectively. Hence we should test if the coupling rods are able to rotate at least ± 90 degrees.

Methods and Materials: The Control Box is held vertically in a clamp (Fig.43). A piece of cloth was used to protect the Control Box cover from being damaged due to the force at the teeth of the clamp.

The test can be carried out by using a camera, where the start of the motion is recorded and the end point is recorded. Rotate the dc motor until the rod stops, reaching the maximum range it can travel. Repeat the steps for each of the rods. Measurement can be done by measuring the number of rotations and measuring the angles digitally in pictures. It is noted how many rotations the coupling rods make. The angle between the start and the end point can be measured and we can obtain the range of the coupling rods.

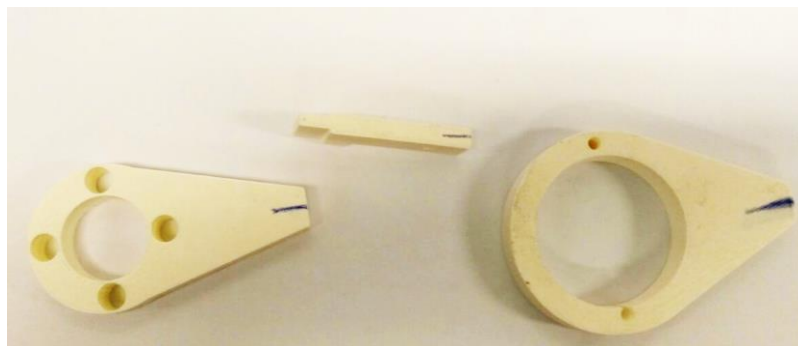


Figure 42: Markers for CBC rods

A marker is used to mark the start and the end of the rotations. Each of the 3 rods had their own marker (Fig.42). For the digital measurement, pictures were clicked of the CBC rods from the start position, at the start of the rotation and at the stop position when the rotation was stopped. These pictures were then superimposed on each other in Paint.net software. Since the pictures were taken from the same position, the superimposition was easy to create, as the marker edges matched. The angles were measured by using ImageJ software, used for measuring distances or angles in images.

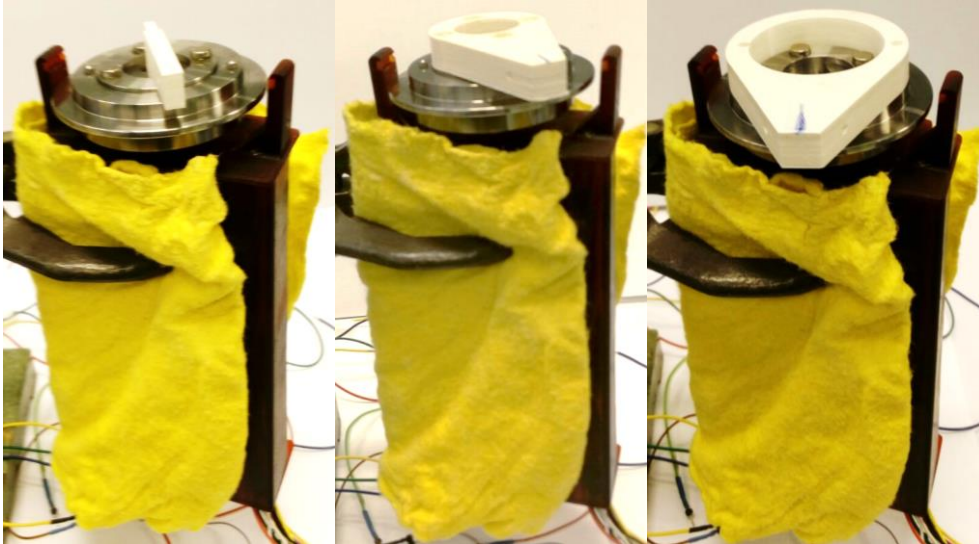


Figure 43: Control Box with Markers for Inner, Middle and Outer CBC piece (left to right)

Results: The measurements of the angles were taken both manually and digitally and the results are presented in the Table 1. The Fig.44 shows the superimposed pictures and direction in which the measurements were taken.

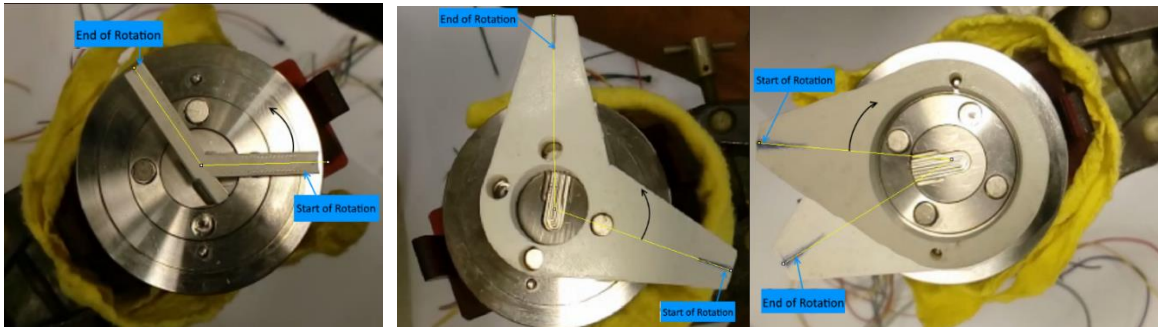


Figure 44: Range of Rotations of Inner, Middle and Outer CBC rods (left to right)

Phase 1

	Rotation Amount 1 (deg.)	Rotation Amount 2 (deg.)	Rotation Amount 3 (deg.)	Rotation Amount avg. (deg.)
Outer	324	325	322	323.6
Middle	469 (360+109)	468(360+108)	466 (360+106)	467 (360+107.6)
Inner	483 (360+123)	480(360+120)	479(360+119)	480.6(360+ 120.6)

Table 1: Values of Range of Motion Phase 1

The range of motion for the inner rod, middle rod and the outer rod are sufficient to achieve the range of movement needed by the SATA instrument (above 180 deg). It was found that there is significant slippage when the dc motor tries to move the outer rod and the middle rod. This is because of the decrease in the tension of the cable in the opposite side of the pull, which causes the cable to loosen and develop slack.

Phase 2

The use of the timing belt meant that the dc motors can rotate the CBC rods as many times as needed, beyond the required 180 degrees. Hence the 3 CBC rods can be rotated in both directions many times as required.

Test 2: The Speed of Pitch, Yaw and Rotation of CBC

The requirements mentioned in literature are:

- Movement of the instrument gripper in pitch and yaw with a maximum velocity of 0.5 rad/s.
- Rotation of the instrument tip with a maximum velocity of 4 rad/s or 3rad/s.

Introduction: The motor used for the rotation of the SATA cylinders move the cylinders by means of a cable and pulley system. The pulley rotates the CBC and IC rods, which in turn rotate the SATA instrument cylinders. The speed of the CBC rod will be transferred to the IC and further to the SATA instrument cylinders. Hence the

speed of the CBC cylinders can be compared with the speeds of the SATA cylinders needed. This can determine if the speed requirements of pitch, yaw and rotations of the gripper have been met. We have already converted the movement range of the SATA instrument to the rotation of the SATA cylinders (Appendix G- Experiment 4) in order to determine the range. Hence, if the SATA instrument has to pitch and yaw with a maximum speed of 0.5 rad/s, which means it has to cover the range of 120 degrees of the SATA instrument tip (pitch and yaw) in a certain amount of time. If in the same time, it is able to cover the 180 degree rotation then we can say that the requirement of the speed is achieved, the speed for the rotation of the SATA cylinders is 0.76 rad/s. Similarly for the rotation of the SATA instrument tip, the time it takes to rotate the instrument tip should be the time it takes to rotate the cylinder by 180 degrees.

Methods and Materials: Create a video of the rotation of each of the CBC rods. Rotate each of the rods for a certain amount of time and repeat in the opposite direction (to check if there is a difference). We have the number of rotations of each of the rods and the time it takes to complete these rotations. Hence the speed of the CBC rods can be determined. The setup is the same as in Test 1 (Fig.43).

Results: The results of the speeds obtained from the test are presented in Table 2 for Phase 1 and Table 3 for Phase 2.

Phase 1

	Number of rotations (deg)	Time taken (sec)	Speed obtained (deg/s)	Speed obtained (rad/s)	Required speed (rad/s)
Outer	324	3	108	1.88	0.76
Middle	469	4	156	2.04	0.76
Inner	483	3	161	2.8	3

Table 2: Values of Speed: Pitch, Yaw and Rotation Phase 1

The speed of the outer cylinder and middle cylinder is sufficient for the movement of the yaw and pitch as the obtained speed is more than the required speed. The speed of the inner cylinder is a bit less than the maximum needed speed from the requirements, this means that the rotation of the SATA instrument tip will be slower than required.

Phase 2

CBC piece	Number of Rotations (deg)	Time taken (sec)	Speed obtained (deg/s)	Speed obtained (rad/s)	Required Speed (rad/s)
Outer	360	2.71	132.7	2.3	0.76
Middle	360	1.88	191	3.3	0.76
Inner	360	2.03	177.3	3.1	3

Table 3: Values of Speed: Pitch, Yaw and Rotation Phase 2

The speeds of the cylinders are sufficient for the movement of the pitch, yaw and rotation of the cylinders.

Test 3: The Manual Pushback of CBC Middle Rod (Emergency Removal)

The requirements for the emergency removal are:

- The middle cylinder when completely pulled in should be able to be pushed back manually by 2.5mm.
- The middle cylinder when completely pushed out should be able to be pushed back manually by 6.5mm.

Introduction: In cases of emergency the instrument should be able to be removed from the surgical site. This means that the instrument should be able to disconnect from the mechanism holding it with ease. The emergency removal of the instrument is done by separating the CBC and IC coupling.

In case of the PoLaRS surgical system, the coupling rods (CBC and IC) need to disconnect in case of emergency. This disconnection mechanism is activated by means of pushing back the middle rod along with the outer rod of the CBC part, this disengages the coupling of CBC and IC middle and outer parts. Then the innermost coupling piece can be detached by pulling out inner IC rod through the groove on the CBC rod.

Methods and Materials: Push back the middle CBC rod through the CBC coupling from its Neutral position by hand and measure the distance it moved back (Fig.45). Repeat the same when the middle CBC rod is at its extreme ends i.e. when it is completely pulled in by the motor and when it is completely pushed out by the motor. Note the distances in each case.

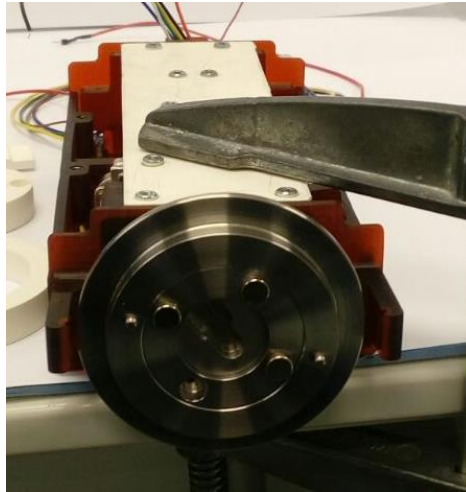


Figure 45: Horizontal Fixation for Middle Rod

Results: The results of the distances obtained from the test are presented in Table 4 for Phase 1 and in Table 5 for Phase 2.

Phase 1

<i>Position of middle rod</i>	Actual distance moved	Required distance to move
Pulled in completely	2.5mm	2.5mm
Pushed out completely	6.15mm	6.5mm

Table 4: Distance Values Phase 1

The manual push back of the middle rod seems hard sometimes when trying to push back the middle rod, however, if a slight turn is given to the middle rod during the push back, it is pushed back easily. This can be due to the magnetising effect of the magnets used in the middle rod coupling.

It is seen from the results that the middle rod can be pushed back by 2.5 mm when it is pulled in completely by the motor (at one of the extreme ends). But when the middle rod is pushed out completely by the motor, it also causes the spring to be pushed back by some amount. Hence, at the completely pushed out position of the middle rod, the manual push back is 6.15mm, which is less than the needed 6.5mm. Leaving a deficit of 0.35mm.

Phase 2

<i>Position of Middle rod</i>	Actual distance moved	Required distance to move
Pulled in completely	2.51mm	2.5mm
Pushed out completely	4.77mm	6.5mm

Table 5: Distance Values Phase 2

The push back of the middle CBC rod is easy but the range is lesser than the needed value by 1.73mm.

Test 4: The Range and Speed of Middle Rod Movement

The requirements for the middle rod movement are:

- (a) Middle rod speed of 4mm/s.
- (b) Middle rod translation 4mm.

For moving the middle rod translationally.

Introduction: The middle rod of the CBC coupling is used to close and open the gripper. The speed of 4mm/s was determined by opening and closing the gripper by hand.

Methods and Materials: The Control Box is placed in a horizontal position, with a clamp (Fig.45), as in Test 3. We use a camera to record a video of the movement of the middle rod. We can physically measure the distance the middle rod has moved when the motor was turned on. From the video recording we can obtain the time it takes to cover the distance moved by the middle rod. By using the equation of speed = time * distance, we can obtain the speed of the middle rod translation and the range of the middle rod is the distance it has travelled from end to end.

Results:

Phase 1

The range of middle rod translation is 3.6mm (with 1mm pulled inwards and 2.5mm pushed out)

The speed of middle rod translation is 1.55 mm/s. (since time taken to cover 2.8 mm is 1.8 seconds)

The distance travelled by the middle rod is 0.4mm less than the requirement amount, this will cause the instrument gripper to not close completely. The speed of the middle rod translation is much lower than expected, which means that with a speed of 1.55mm/s it will cover the range of 4mm needed in around 2.5 seconds.

Phase 2

The range of middle rod translation is 3.71mm (with 1.38mm pulled inwards and 2.33mm pushed out)

The speed of middle rod translation is 0.99 mm/s. (since time taken to cover 1.18mm is 1.19 seconds)

The speed of 0.99mm/s means that the gripper will take around 4s to cover the range of 4mm needed. The range of motion is also less than required and hence the gripper will not be able to close completely.

Test 5: CBC Middle Rod Push/Pull Forces

Introduction: The middle rod is moved by a motor translationally to push it in and out, which closes and opens the gripper. The middle rod has to push out the middle coupling rod to close the gripper and pull in the middle coupling rod while pushing out the motor. The force by which the middle rod pushes is important as it will determine the force that the gripper will grip with.

Methods and Materials: The Control Box is placed in a horizontal position, as in Test 3 (Fig.45). The middle rod motor is activated which causes the middle rod translation mechanism to activate and move the middle CBC rod in and out. A pull push gauge is used to measure the forces exerted when the middle rod is pushed out and pulled in by the motor. This will cause the middle rod to either push or pull on the pull-push gauge tip, which will generate a force reading on the gauge.

Results: The results of the forces obtained from the test are presented in Table 6 for Phase 1 and in Table 7 for Phase 2

Phase 1

	F1(N)	F2(N)	F3(N)	F4(N)	F(N)
Pull	6	5	5	5	5.25
Push	5	5	4	5	4.75

Table 6: Pull/Push Force Values Control Box Phase 1

Phase 2

	F1(N)	F2(N)	F3(N)	F4(N)	F(N)
Pull	7	8	8	8	7.75
Push	12	12	10.2	12	11.55

Table 7: Pull/Push Force Values Control Box Phase 2

Lower values for the pull force are due to the magnet used to attach the pull-push gauge disconnecting at 8N.

Test 6: Torques at CBC Rods

Introduction: The torques from the motors are transferred to the pulleys on the CBC rods by means of pulleys and cables. The torques are needed to be measured at the CBC rods to check if the motors are able to provide enough torque to move these coupling rods and further move the SATA instrument. It would be important to note if there are any large decrease in torques and determine the cause of the decrease in torques. The torques at the driven pulleys are determined theoretically, however as in every system we expect some losses to the torques and it is need to check the amount of torque lost in the mechanisms. The torques at the pulleys of the rods are obtained theoretically by using the torque and speed equations as mentioned in Section 4.2.1. However, it is possible that there is a decrease in the torque due to friction or other effects.

Methods and Materials: The torques at the CBC and the IC rods are determined by physically checking the forces at a certain distance away from the centre of the coupling rods.



Figure 46: Torque Test Setup

The test for torques of the CBC and IC rods can be done by using a pull push gauge and an marker component that can be used as an arm (Fig.46) to measure forces at a certain point from the coupling rods. This marker component used needs to have a point at which the pull push gauge tip can be touched at a known distance. The rods can then be turned, which will cause the marker component to push on the tip of the pull push gauge. This will give a force reading on the pull push gauge. We can find out the torque by using the equation

$$\text{Torque} = \text{Force} * \text{Distance}$$

Results: The results of the forces obtained from the test are presented in Table 8 for Phase 1 and Table 9 for Phase 2. Fcc refers to the movement of the rods in counter clockwise direction and Fc refers to movement of the rods in clockwise direction.

Phase 1

	Distance(m)	Fcc1(N)	Fc1(N)	Fcc2(N)	Fc2(N)	Fcc3(N)	Fc3(N)	F(N)	Torque(Nm)
Outer	0.04	2	1.25	1.5	1.25	1.75	1	1.45	0.058
Middle	0.04	2.5	2	3	2.5	3	2	2.5	0.1
Inner	0.03	2	2	2.5	2	2	2	2.08	0.0625

Table 8: Torque Values at CBC Phase 1

The torques needed by the SATA instrument to rotate is 0.04Nm, this means that the torques at the CBC couplings should be at least 0.08Nm to maintain the FOS of 2. Therefore we see that only the middle rod is able to achieve the torque needed.

Phase 2

	Distance(m)	Fcc1(N)	Fc1(N)	Fcc2(N)	Fc2(N)	Fcc3(N)	Fc3(N)	F(N)	Torque(Nm)
Outer	0.04	2.2	1.8	1.4	1.2	1.6	1	1.53	0.06
Middle	0.04	1.2	1	1	1.2	0.8	0.8	1	0.04
Inner	0.03	2	2	2.2	2	2	2	2.03	0.06

Table 9: Torque Values at CBC

The torques are equal or higher than 0.04Nm, however since the FOS of 2 is used, all the torques are lesser than 0.08Nm needed for the rotation of the SATA instrument.

Tests for ZTM

Test 1: The Range and Speed of ZTMO

The literature suggests:

- (a) speed between 60-200mm/s
- (b) range of 200-350mm

For moving the instrument toward and away from the abdomen i.e. ZTMO

Introduction: For the ZTM, the mechanism used is a leadscrew mechanism, in which an internal threaded pulley causes the leadscrew to move translationally. The speed of this movement is dependent on the pitch of the leadscrew and the speed of the motor used. The literature suggests a speed between 60-200mm/s and a range of 200-350mm. These requirements are tested with the prototype to check if the requirements are achieved.

Methods and Materials: The completed prototype of the ZTM is fixed on supports (Fig.47). The dc motor (12v) driving the threaded pulley is activated. The Control Box on the ZTM is allowed to move until it reaches one of its ends. Once the Control Box is at one end the dc motor is reversed to move the Control Box to the other side. The distance between these 2 ends is measured by using a scale.

For measuring the speed the dc motor and a stopwatch is turned on at the same time. After the Control Box has moved a certain distance, the timer and dc motor are stopped. From the time it has taken the Control Box to move from point A to point B, the speed of the ZTMo can be determined.

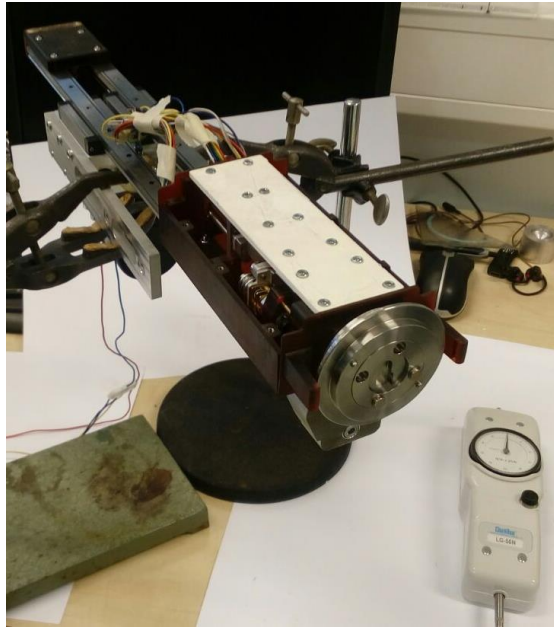


Figure 47: Horizontal Fixation for ZTM

An easier method to determine the speed of ZTMo would be by multiplying the speed of the dc motor with the pitch of the leadscrew. This provides the linear speed of the ZTMo. However, this is theoretical and hence the earlier method is better at giving a more realistic estimate of the speed.

Results:

Phase 1

The range of motion of the ZTMo is 403mm.

The speed of movement of the ZTMo -mm.

The ZTM was not able to move smoothly, the pulley was needed to be given a start by hand. The motor does not have enough torque to move the Control Box, hence the speed calculation cannot be done.

Phase 2

The distance between the two markers is 227mm and the time taken to cover this distance is 0.75s. Hence the speed is,

$$speed = \frac{distance}{time} = \frac{227}{0.75} = 302.6 \text{ mm/s}$$

The range of motion of the z translation is 403mm.

The speed of movement of the z translation ~ 302mm/s.

Test 2: ZTM Push/Pull Forces

Introduction: The ZTM needs to move the Control Box along with the SATA instrument towards and away from the abdomen. The SATA instrument moving with the Control Box will be pushed/pulled by the ZTM. The forces that are output by the ZTM for these movements are recorded in this test. These forces can be compared to the forces expected from the calculations in Section 4.2.3.

Methods and Materials: The ZTM is held in horizontal position by means of 2 holders. The pull-push gauge measuring tip can be attached to one of the ends of the moving slides to measure the forces generated by the ZTM when it is made to move forward and backwards by activating the motor. The pull push gauge will generate a reading, when the motor is activated and the slides start to move. The setup is shown in Fig.48.



Figure 48: ZTM Force Setup

Results: The results of the forces obtained from the test are presented in Table 10 for Phase 1 and in Table 11 for Phase 2

Phase 1

	F1(N)	F2(N)	F3(N)	F4(N)	F(N)
Pull	-	-	-	-	-
Push	9.5N	-	-	-	-

Table 10: Pull Push Force Values ZTM Phase 1

Phase 2

	F1(N)	F2(N)	F3(N)	F4(N)	F(N)
Pull	98	100	110	98	96
Push	98	110	110	100	98

Table 11: Pull Push Force Values ZTM Phase 2

The forces obtained are much higher than the needed 26N from literature, hence the ZTM has sufficient force.

Test 3: ZTMo for Critical Angle

Introduction: The ZTM will be mounted on the PoLaRS slave arm, this arm has a range of ± 60 degrees, from the vertical axis. Hence the most important or extreme angle will be when the arm is at 0 degrees with the vertical axis. This would mean that the Control Box with ZTM is also vertical with the SATA instrument pointed downwards. This would provide the most load on the ZTM to lift up the Control Box.

Methods and Materials: Mount the Control Box on the ZTM, hold the ZTM such that is vertically aligned and the coupling rods of the Control Box face downward (Fig.49). The motor of the ZTM can be turned on to check if the ZTM moves the Control Box upwards and downwards.



Figure 49: Vertical Alignment of the ZTM

Results:

Phase 1

The ZTM was not able to move the Control Box upward or downward, without pushing the pulley by hand. The torque of the motor used in the ZTM is not sufficient to move the Control Box when placed in a vertical direction. The motor will need to be changed with a higher torque motor to allow this movement.

Phase 2

The ZTM was able to move the Control Box upward or downward. The speed was 283.75mm/s. Hence the ZTM can be used in other orientations too without noticeable loss in speed.

4. Results

4.1. Prototype

The prototype was built in the 3ME workshop and DEMO lab of the Mechanical, Maritime and Materials Engineering faculty at TU Delft. Actuators, belts, springs, bearings and bushings were purchased from online sites. The parts were made on the milling machine, lathe, water-cutting and 3-D printing at the 3ME workshop. Pictures and lists of the parts with the methods used to manufacture these parts for the Control Box and the ZTM is shown in Appendix E.

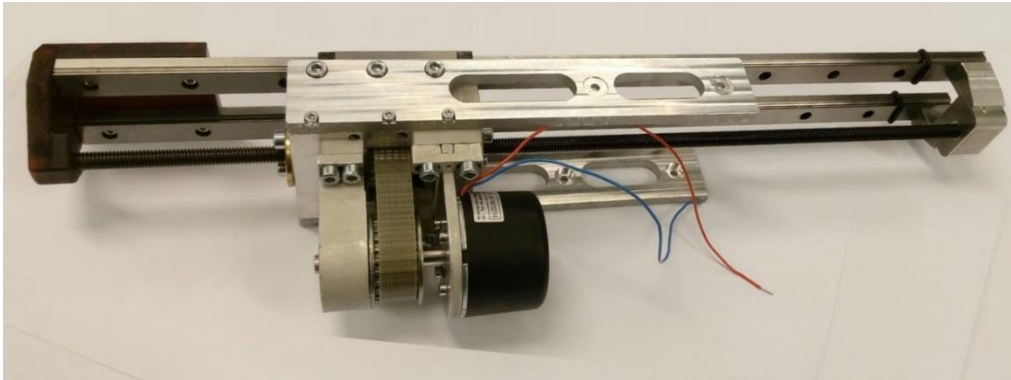


Figure 50: ZTM without the Control Box Attached

The ZTM (Fig.50) controls the movement of the instrument toward and away from the abdomen. This control is achieved by a leadscrew controlled by a dc motor.

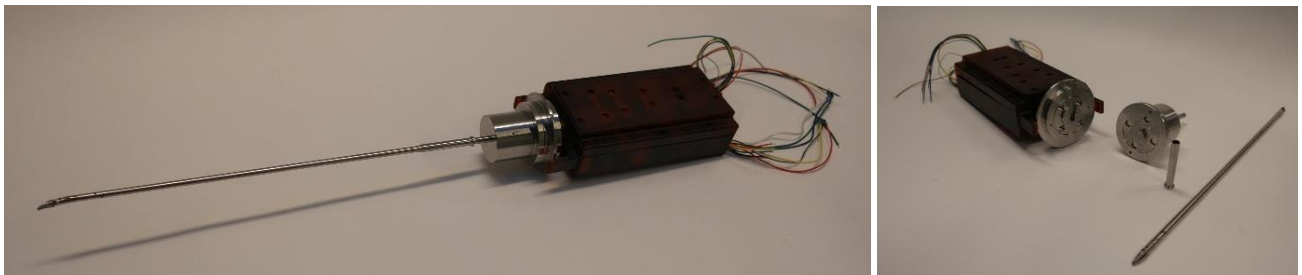


Figure 51: Prototype Complete Assembly of Control Box with CBC and IC rods

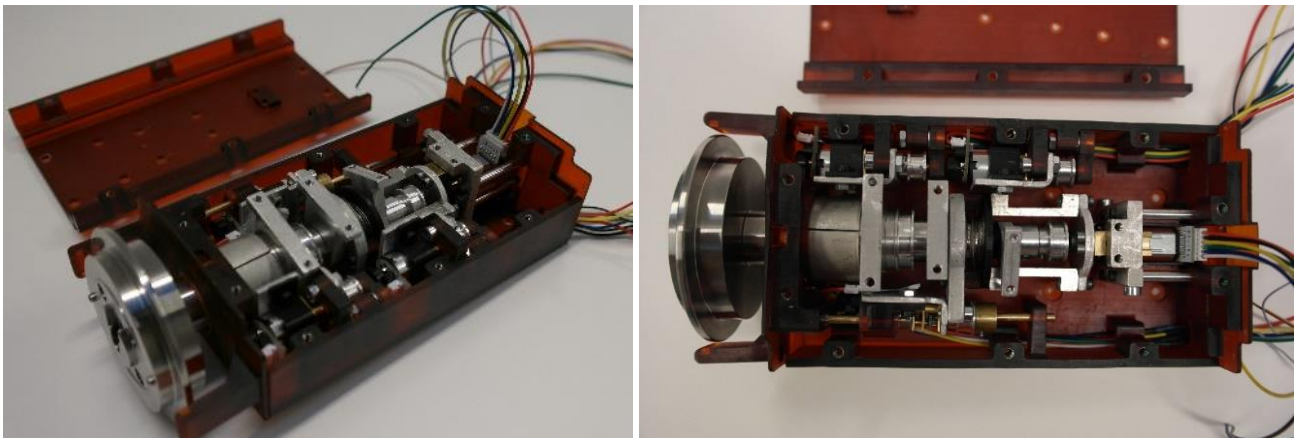


Figure 52: Control Box Internal Mechanisms

The prototype Control Box has mechanisms to control the movement of the SATA instrument (Fig.51, Fig.52). The 3 dc motors control the rotation of the SATA instrument cylinders which provide the tip yaw, pitch and rotation of the SATA instrument. Another dc motor controls the linear movement of the middle rod, which allows the gripper to open and close.

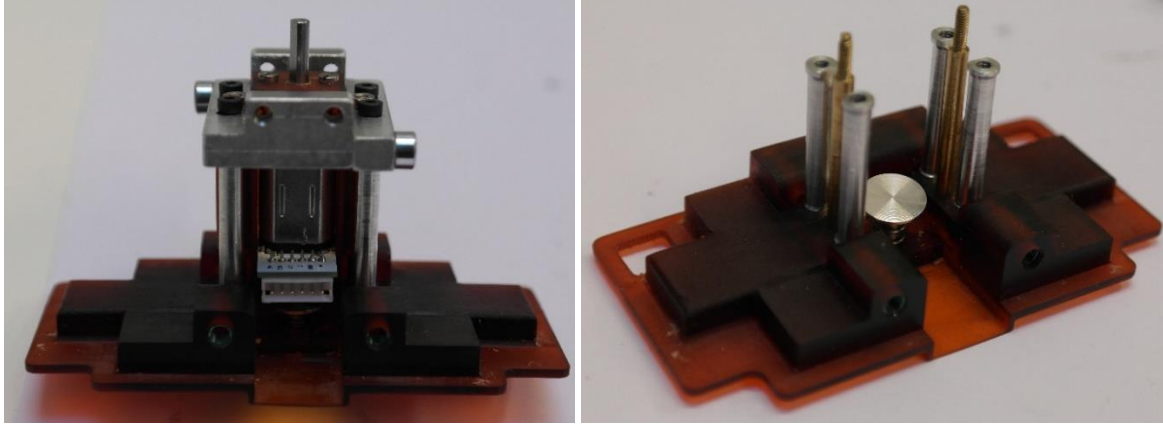


Figure 53: Emergency Removal Spring Mechanism

An additional mechanism to detach the instrument in case of emergency is also designed (Fig.53). This mechanism allows the middle rod to be pushed back to allow the 2 coupling rods to detach. The prototype consists of 5 dc motors in total, 4 dc motors use 6v power supply and are in the Control Box and the dc motor to run the ZTM used 12v and was replaced by a brushless dc motor using 5,000 mAh battery in phase 2 testing.

The Control Box and the ZTM weighs (435g + 2782g) = 3217 g in the prototype (without the coupling rods).

4.2. Component Selection

There were 3 types of dc motors selected based on the calculations from the earlier section. When the needed dc motors could not be found then adjustments were made by negotiating on the speed or increasing size of the dc motors. The list of dc motors and other components purchased is provided in Appendix D.

4.2.1. Motors for Rotation of the Rods

Assumptions: No slip for the pulleys as the cable is held in position by the cable holes.

The motors chosen for this are geared dc motors with a torque of 0.196Nm and 52 rpm and geared dc motors with 41 rpm and 0.245 Nm torque.

The torques and speeds of the pulleys connected to the outer, inner and middle cylinders of the SATA instrument are calculated below:

Mechanical Advantage (Armstrong, 2016)

$$MA = \frac{\tau_{out}}{\tau_{in}}$$

Where,

τ_{out} is the torque output.

τ_{in} is the torque input.

As,

$$Torque = Force * Distance$$

$$\tau_{out} = F_{out} * r_{out}$$

$$\tau_{in} = F_{in} * r_{in}$$

Since the 2 pulleys are connected by a common belt/cable the Force in = Force out,

Hence,

$$MA = \frac{\tau_{out}}{\tau_{in}} = \frac{r_{out}}{r_{in}} = \frac{d_{out}}{d_{in}}$$

And for two closed pulleys connected by a cable or belt (Armstrong, 2016)

$$\frac{d_{out}}{d_{in}} = \frac{\omega_{in}}{\omega_{out}}$$

Where,

d_{out} is the diameter of the driven pulley.

d_{in} is the diameter of the driving pulley.

ω_{in} is the rotational velocity of the driving pulley.

ω_{out} is the rotational velocity of the driven pulley.

Therefore we can say that,

$$\frac{\omega_{in}}{\omega_{out}} = \frac{r_{out}}{r_{in}}$$

Known values are:

$$\begin{aligned} r_{in} &= 5mm \\ \omega_{in} &= 52 \text{ rpm} \\ \tau_{in} &= 0.196Nm \end{aligned}$$

Outer Rod:

$$r_{out} = 9.5 \text{ mm}$$

Torque calculation,

$$\frac{\tau_{out}}{\tau_{in}} = \frac{r_{out}}{r_{in}}$$

$$\frac{\tau_{out}}{0.196} = \frac{9.5}{5}$$

$$\tau_{out} = 0.372Nm$$

Speed calculation,

$$\frac{\omega_{in}}{\omega_{out}} = \frac{r_{out}}{r_{in}}$$

$$\frac{52}{\omega_{out}} = \frac{9.5}{5}$$

$$\omega_{out} = 27.36 \text{ rpm}$$

Middle Rod:

$$r_{out} = 7 \text{ mm}$$

Torque calculation,

$$\frac{\tau_{out}}{0.196} = \frac{7}{5}$$

$$\tau_{out} = 0.274Nm$$

Speed calculation,

$$\frac{52}{\omega_{out}} = \frac{7}{5}$$

$$\omega_{out} = 37.14 \text{ rpm}$$

Inner Rod:

$$r_{out} = 6.5 \text{ mm}$$

Torque calculation,

$$\frac{\tau_{out}}{0.196} = \frac{6.5}{5}$$

$$\tau_{out} = 0.254Nm$$

Speed calculation,

$$\frac{52}{\omega_{out}} = \frac{6.5}{5}$$

$$\omega_{out} = 40 \text{ rpm}$$

A similar calculation for the motors of 41 rpm with 0.245 Nm torque gives the following result,

Outer Rod:

$$\begin{aligned}\tau_{out} &= 0.465Nm \\ \omega_{out} &= 21.5 \text{ rpm}\end{aligned}$$

Middle Rod:

$$\begin{aligned}\tau_{out} &= 0.343Nm \\ \omega_{out} &= 29.2 \text{ rpm}\end{aligned}$$

Inner Rod:

$$\begin{aligned}\tau_{out} &= 0.318Nm \\ \omega_{out} &= 31.5 \text{ rpm}\end{aligned}$$

4.2.2. Motors for Translation of Middle CBC piece

The middle cylinder translation needed to have torque and speed as
 $T \geq 16Nmm$ and $N \geq 480 \text{ rpm}$

The dc motor with 530rpm and torque 19.6Nmm did not possess sufficient torque to move the middle CBC piece. Therefore a dc geared motor with the second lower speed of 155 rpm and torque 68.6 Nmm was used.

Therefore, the weight the mechanism can lift,

$$\begin{aligned}T &\geq r * \left(\frac{\mu + \tan\gamma}{1 - \mu * \tan\gamma} \right) * w \\ 68.6 &\geq 3 * \left(\frac{0.15 + 0.025}{1 - 0.15 * 0.025} \right) * w\end{aligned}$$

$$w = 130.4N \sim 13kg$$

At maximum speed of,

$$\begin{aligned}N &= rps * p \\ N &= \frac{155}{60} * 0.5 = 1.29mm/s\end{aligned}$$

Hence the middle rod will now translate at 1.29mm/s (max) and move a load of 13kg (max).

4.2.3. Motors for ZTMo

The z translation needed to have

$$T \geq 41.13 \text{ Nmm and } N \geq 2400 \text{ rpm}$$

Therefore a dc motor with torque 30 Nmm and speed of 4550 rpm was selected.

Therefore, the weight the mechanism can lift,

$$T \geq r * \left(\frac{\mu + \tan\gamma}{1 - \mu * \tan\gamma} \right) * w$$

$$30 \geq 4 * \left(\frac{0.15 + 0.054}{1 - 0.15 * 0.054} \right) * w$$

$$w = 36.49N \sim 3.6kg$$

At maximum speed of,

$$N = rps * p$$

$$N = \frac{4550}{60} * 1.5 = 113.75 \text{ mm/s}$$

Hence the z translation will have a speed of 113.75 mm/s (max) and move a load of 3.6 kg (max).

4.2.4. Belt for ZTM

The belt chosen is a T5 type with a width of 15mm, as this fits with the pulleys selected for the z translation. It had 45 teeth and trapezoidal thread profile.

The closest belt length that was available was 225mm, but we needed 210 mm. Therefore, there is 15mm more belt length, this can be divided on either side of the belt and hence an increase in the center distance of 7.5mm would be needed to use this belt. After increasing the center distance by 7.5mm, the belt would fit the timing pulley.

4.2.5. Belt for Control Box

When the driving motor with 52rpm and 0.196Nm is used and the radius of the timing motor pulley is 5mm. The force in the belt can be calculated as,

$$T = F * r$$

$$0.196 = F * 0.005$$

$$F = 39.2N$$

When the driving motor with 41rpm and 0.245Nm is used,

$$0.245 = F * 0.005$$

$$F = 49N$$

These are the effective tensions in the belt and the transmitted force from the belt to the driven pulley for 2 different types of dc motors.

The pretension forces due to the stretching of the belt for the outer rod are calculated using the following equation (Physics.bu.edu, 2018),

$$F = \frac{EA\Delta l}{L}$$

Where,

E is the Young's modulus

A is the cross sectional area

Δl is the change in the length

L is the initial length

Calculate the change in the length

The circumference of the belt used is 96mm. Since both the sides of the belt are the same we have half the circumference to 48mm and consider only half of the belt for ease of calculation (Fig.54).

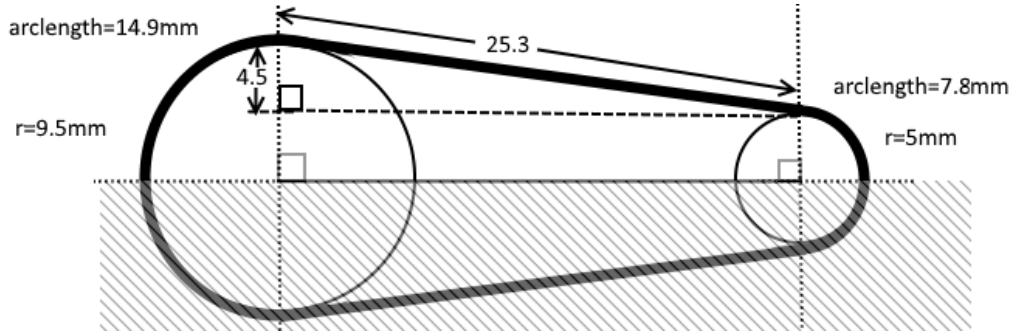


Figure 54: Belt Geometry

The arc lengths $arcl1$ and $arcl2$ of the belts over the pulleys are calculated as follows,

$$arcl1 = \frac{2\pi * r * \theta}{360}$$

$$arcl1 = \frac{2\pi * 9.5 * 90}{360} = 14.9mm$$

$$arcl2 = \frac{2\pi * 5 * 90}{360} = 7.8mm$$

Therefore we have the remaining half circumference length as

$$48 - 14.9 - 7.8 = 25.3mm$$

For the right angles geometry, using Pythagoras theorem,

$$25.3^2 = 4.5^2 + x^2$$

$$x = 24.89mm$$

Hence,

$$\Delta l = 25 - 24.89 = 0.103mm$$

The cross sectional area of the belt with 4mm width and 0.6mm thickness is,

$$A = 4 * 0.6 = 2.4mm^2$$

The Young's Modulus E is 9.4N/mm² (PolyFlexTM Technical Data Sheet, 2018)

Therefore,

$$F = \frac{EA\Delta l}{L}$$

$$F = \frac{9.4 * 2.4 * 0.103}{25} = 0.092N$$

As seen these forces are negligible as compared to the belt tension.

Therefore the force in the belts can be assumed to be $F = 39.2N$ and $F = 49N$, for motors of 51 rpm and 42 rpm respectively.

4.2.6. Spring

The spring was selected from a number of springs obtained from the workshop (Appendix G-Experiment 3).

The spring selected has free length of 17.6mm and deformed length of 7.8 .The inner diameter and outer diameter of 2.8mm and 4mm respectively. The wire diameter is 0.5mm. The spring constant is 2.91N/mm. Hence the force can be calculated ,

$$\Delta x = x_{ud} - x_d = 17.6 - 7.8 = 9.8 mm$$

$$F = k * \Delta x = 2.91 * 9.8 = 28.5N$$

Hence a force of 28.5 N would be needed to push back the middle cylinder by hand to the complete end position.

However in reality, the maximum deformation of the spring will be ≈ 6.5 mm (emergency removal requirement). Hence checking the force for a deformation of 6.5mm,

$$F = k * \Delta x = 2.91 * 6.5 = 18.9N$$

The force of $\approx 19N$ is closer to the force that will be needed to be exerted on the middle rod to compress the spring.

4.3. Actuator Control

The actuators are controlled by Arduino Uno Board and L298N Motor Driver. The dc motors used in the prototype have their own encoder which can be used to obtain inputs for the programming. The resistors for the buttons are in the range of 20k Ω . The motors used are one motor of 41 rpm, two motors of 52 rpm and a motor of 155 rpm for the middle rod translation.

The speed of the motors was controlled by using a potentiometer and the reversal of the motor rotation direction was controlled in time. The control of direction with time resulted in a motor that will rotate in one direction for a certain amount of time and then switch directions. The speed of the motor was controlled by a potentiometer, however this reduction in speed also caused a reduction in the torque output of the motor and hence the speed could not be reduced by a large amount.

The circuit diagram is shown in (Fig.55). Arduino is able to read the state of each of the buttons and send PWM signals to the enable pins i.e. ena and enb pins of the L298N motor controller. The Arduino code (Appendix F) controls the direction of the motors by setting pins In1, In2, In3, In4 to HIGH or LOW for each of the motor controller. Pins In1, In2 control Motor 1 and pins In3, In4 control Motor 2. Similarly for the other L298N motor controller pins In1, In2 control Motor 3 and pins In3, In4 control Motor 4. When either In1 or In2 are set to HIGH and the other pin to LOW, the dc motor will rotate in one direction. When the pins are set in reverse with either In1 or In2 set to LOW and the other set to HIGH, the dc motor will rotate in the other direction. When both the pins are set to either HIGH or LOW, the dc motor will not rotate.

The speed control is achieved by changing the PWM signals sent to the enable pins of the microcontroller. This is done by mapping the range of the potentiometer to the range of the PWM signal that can be used, with a range from 0 to 255. With 0 being when the speed is 0 and 255 being the maximum speed of the dc motor.

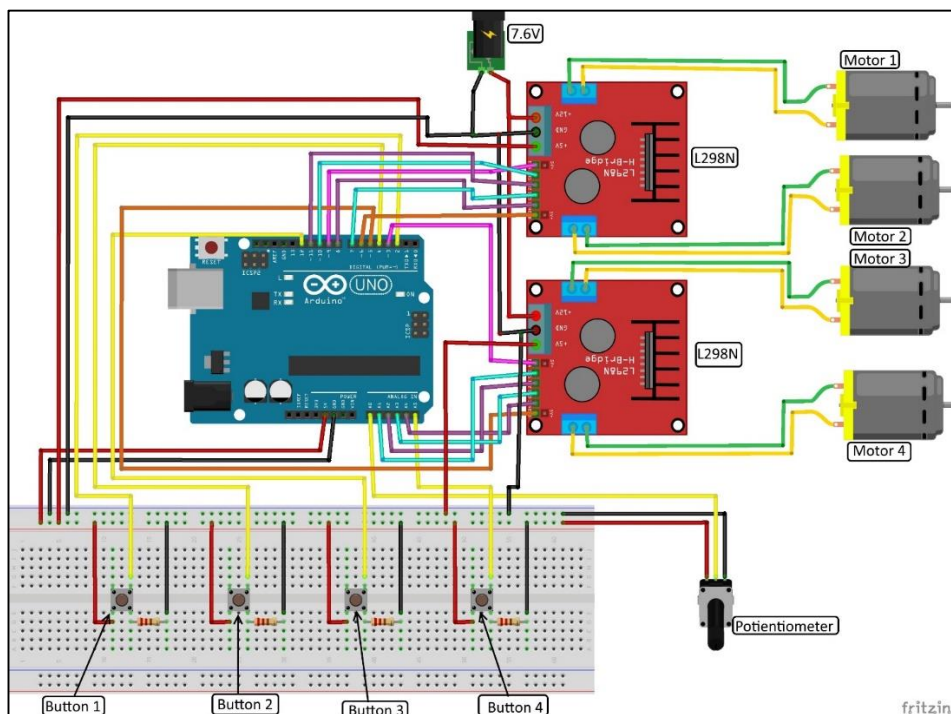


Figure 55: Circuit Diagram

4.4. Requirement Check after Phase 1

The requirements that were listed in Section 2 were compared with the results obtained from phase 1 tests (Table 13, Table 14). A color scheme was used to mark requirements that were met, met with certain conditions or not met (Table 12). In the case when the requirements are met with certain conditions, the conditions are mentioned in the comments section. In the case when the requirements are not met or cannot be measured, the possible solutions are mentioned in the comments section.

Legend:

	Requirement met
	Requirement met with certain conditions
	Requirement not met
	Not measured

Table 12: Legend for Requirement Check

On inspecting the Control Box and the ZTM and performing validation tests the following results were obtained for the requirements:

Control Box Requirements Check:

Requirement	Measured value	Comments
1. Providing Smooth Movement of the SATA Instrument		
a) No abrupt movements when the SATA instrument moves in pitch, yaw or rotation.	X The movements were not accurate and it caused abrupt starts	Change the cable pulley system to a timing belt and pulley system.
b) No random increase or decrease in speed of SATA instrument..	X There was some increase or decrease in speed due to slip.	Change the cable pulley system to a timing belt and pulley system.
2. Backlash		
c) Backlash if present should not cause any problem with the movement of the instrument.	✓ Met	
3. Control box weight		
d) Weight below 1 kg.	✓ Weight is 0.435kg	This does not include the weight of the coupling rods, which is an additional: CBC coupling-323.34g and IC-249.69g.
4. Compact design		
e) The width of the Control Box should be below 89mm.	✓ The width of the Control Box is 82mm.	
f) The length of the Control Box should be below 150mm.	✓ The length of the Control Box is (147mm +26mm)	The length of the Control Box is increased due to the snapfinger holder whose length is 26mm.
5. Cable routing		
g) Enough space for the cables to exit from the Control Box.	✓ Met	
6. Translational speed and distance for middle rod of Control Box		
h) Middle rod translation speed 4mm/s.	X Middle rod translation speed 1.55mm/s.	Using a higher rpm motor for the leadscrew mechanism to increase translation speed.
i) Middle rod translation distance 4mm.	X Middle rod translation distance 3.6mm.	Using a higher torque motor for the leadscrew mechanism and spring with higher k value to increase the translation distance.

7. Rotation of instrument		
j) Rotational velocity of the instrument gripper in pitch and yaw with at maximum 0.5 rad/s.	✓ Rotational velocity of the CBC for instrument gripper movement in pitch and yaw is 2.7rad/s and 1.88rad/s respectively.	
k) Rotation of the instrument tip with a maximum velocity of 4 rad/s or 3 rad/s.	✗ Rotation of the instrument is 2.88 rad/s.	Reduce the friction between the inner rod holder bushing and the inner rod by increasing the bushing hole diameter.
8. Rotational resolution of Control Box rods		
l) A rotational resolution of at least 0.5 deg.	✓ The rotational resolution for the 155rpm, 52rpm and 41rpm dc motors are 0.5 deg/step, 0.14 deg/step and 0.17 deg/step respectively.	
9. Actuation of the SATA instrument		
m) Instrument pitch between ±60 deg to ±90 deg.	✓ Instrument pitch is ±60 deg.	
n) Instrument yaw between ±60 deg to ±90 deg.	✓ Instrument yaw is ±60 degrees.	
o) Instrument rotation between 150 deg to 180 deg.	✓ The instrument rotation is above 180 degrees.	
p) The gripper should be able to hold a load of 10N.	• The gripper force cannot be measured since the instrument cannot be attached to the coupling piece.	Software control to limit the coupling piece movement under 180 deg. and attach the SATA instrument.
10. Torques for Rotation of SATA Cylinders		
q) CBC torques should be above 80Nmm	✓ Torques obtained are 100Nmm for middle rod. ✓ Torques obtained are 58Nmm and 62.5Nmm at the outer and inner CBC rods.	Torque requirement is met only for the middle rod.
11. Attachment and Removal of SATA Instrument Normal operation		
r) The middle cylinder should be completely pulled in by the motor by 2.5mm from N.A.	✓ 1mm pulled back by motor from N.A.	Remove the rim of the control box to increase the distance of pull back.
12. Attachment and Removal of SATA Instrument Normal operation		
s) The middle cylinder when completely pulled in by the motor, should be able to be pushed in manually by 2.5mm.	✓ The middle cylinder when completely pulled in by the motor, can be pushed in manually by 2.5mm	
t) The middle cylinder when completely pushed out by the motor, should be able to be pushed in manually by 6.5mm.	✓ The middle cylinder when completely, pushed out by the motor, can be pushed in manually by 6.15mm.	Remove the rim of the control box to increase the distance of pull back.

13. Backdrivable		
u) Backdrivable mechanism for the Control Box design	✓ The mechanisms used for the rotation of the inner, outer and middle rod are backdrivable. The middle rod can be pushed in by hand.	The middle rod is backdrivable due to the push-back mechanism and not due to the leadscrew mechanism which is driven by the dc motor.
14. Sterilizable		
v) No deep grooves or other locations that can harbor micro-organisms.	✓ The outer side of the Control Box has no deep grooves on its surface, an effort is made to make the surface as smooth as possible. However, there are grooves for inserting screws.	There is still some grooves on the surface to insert screws, however using screw caps can close these gaps.
w) Possibility to attach a drape for the surgical system.	✓ There is a snapfinger holder for attaching a drape around the slave device.	

Table 13: Requirements for Control Box Check Phase 1

ZTM Requirements Check:

Requirement	Achieved (Actual Value)	Not Achieved (Actual Value)
1. Attachment and Removal of the Control Box		
a) Attachment/removal provision	✓ Met	
2. Providing smooth movement of the ZTM		
b) No abrupt movements when the instrument moves in or out the body of the patient.	✓ Smooth movement for ZTMo, no abrupt movements.	
c) No random increase or decrease in speed of instrument.	• The ZTMo speed not able to be checked as the ZTM motor torque was not sufficient to move the Control Box.	Use a higher torque and speed motor.
3. Backlash		
d) Backlash if present should not cause any problem with the movement of the instrument.	✓ Backlash is present, but it is too small and does not interfere with the movement of the instrument.	
4. Entire mechanism should weigh below 2 kg		
e) Weight below 2 kg.	✗ The ZTM weight is 2.782 kg	Remove material from the components. Use slides and pulleys made of aluminum instead of steel.
5. Compact design		
f) The mechanism should fit in a box of 200mmx200mmx400mm.	✗ The ZTM length is 475mm.	The ZTMo can be decreased to bring the length of the ZTM below 400 mm.
6. Translational speed and distance		
g) Maximum linear velocity between 60mm/s to 200mm/s.	• The linear velocity of ZTM could not be checked due to the motor torque being insufficient to move the Control Box.	Use a higher torque and speed motor.

h) Maximum linear movement between 200mm-350mm.	✓ Maximum linear movement range is 403mm.	
7. Translational resolution		
i) A linear resolution of at least 0.1mm.	<ul style="list-style-type: none"> The translational resolution was not able to be checked as the ZTM motor torque was not sufficient to move the Control Box. 	Use a higher torque and speed motor.
8. Pull-push force		
j) A pull/push force of at least 26N.	✓ The push/pull force exceeds 26N (value around 100N).	
9. Backdrivable		
k) Backdrivable mechanism for ZTM	✗ ZTM is not backdrivable due to the leadscrew mechanism used.	Change mechanism to another type or use backdrivable leadscrew

Table 14: Requirements for ZTM Check Phase 1

4.5. Testing Phase 1 Analysis of Problems

After the phase 1 testing, it was seen that there were requirements that were not met. These were analysed to find the problems and certain modifications were performed on the prototype to solve these problems.

Initially after the phase 1 testing, a new manner of winding the cable over the pulley was tried for the cable pulley system in hopes of reducing the slip, however this method was worse than the earlier cable winding and gave higher slip and lesser tension. Therefore the timing pulley-belt system was used for the phase 2 testing. Since the belt and pulley sizes were not readily available from online stores, the belts were 3-D printed and the timing pulleys were made at the workshop (Appendix H)

There were also other smaller changes done on the system, for example filing of parts that were interfering with each other or removal of a redundant part. These changes were needed due to the manufacture of the parts being imprecise.

4.6. Requirement Check after Phase 2

After the modification were carried out the tests were performed again to check for the requirements. The results are summarised in Table 15 and Table 16.

Control Box Requirements Check:

Requirement	Obtained value	Comments
15. Providing Smooth Movement of the SATA Instrument		
a) No abrupt movements when the SATA instrument moves in pitch, yaw or rotation.	✓ No abrupt movement with the inner and middle CBC piece.	The outer CBC piece skips some steps.
b) No random increase or decrease in speed of SATA instrument.	✓ Met	
16. Backlash		
c) Backlash if present should not cause any problem with the movement of the instrument.	✓ Met	
17. Control box weight		
d) Weight below 1 kg.	✓ Weight is 0.435kg	This does not include the weight of the coupling rods, which is an additional: CBC coupling-323.34g and IC-249.69g.

18. Compact design		
e) The width of the Control Box should be below 89mm.	✓ The width of the Control Box is 82mm.	
f) The length of the Control Box should be below 150mm.	✓ The length of the Control Box is (147mm +26mm)	The length of the Control Box is increased due to the snapfinger holder whose length is 26mm.
19. Cable routing		
g) Enough space for the cables to exit from the Control Box.	✓ Met	
20. Translational speed and distance for middle rod of Control Box		
h) Middle rod translation speed 4mm/s.	✗ Middle rod translation speed 0.99mm/s.	Using a higher rpm motor for the leadscrew mechanism to increase translation speed.
i) Middle rod translation distance 4mm.	✗ Middle rod translation distance 3.71mm.	Manufacture of components in the control box need to be of higher tolerance.
21. Rotation of instrument		
j) Rotational velocity of the instrument gripper in pitch and yaw with at maximum 0.5 rad/s.	✓ Rotational velocity of the CBC for instrument gripper movement in pitch and yaw is 2.3rad/s and 3.3rad/s respectively.	
k) Rotation of the instrument tip with a maximum velocity of 4 rad/s or 3 rad/s.	✓ Rotation of the instrument is 3.1 rad/s.	
22. Rotational resolution of Control Box rods		
l) A rotational resolution of at least 0.5 deg.	✓ The rotational resolution for the 155rpm, 52rpm and 41rpm motors are 0.5 deg/step, 0.14 deg/step and 0.17 deg/step respectively.	
23. Actuation of the SATA instrument		
m) Instrument pitch between ± 60 deg to ± 90 deg.	✓ Instrument pitch is ± 60 deg.	
n) Instrument yaw between ± 60 deg to ± 90 deg.	✓ Instrument yaw is ± 60 degrees.	
o) Instrument rotation between 150 deg to 180 deg.	✓ The instrument rotation is above 180 degrees.	
p) The gripper should be able to hold a load of 10N.	✓ The gripper force cannot be measured since the instrument cannot be attached to the coupling piece.	Software control to limit the coupling piece movement under 180 deg. And attach the SATA instrument.
24. Torques for Rotation of SATA Cylinders		
q) CBC torques should be above 80Nmm	✗ Torques obtained are 60Nmm, 40Nmm and 60Nmm at the outer, middle and inner CBC rods.	Use a flexible but non-stretchable timing belt.
25. Attachment and Removal of SATA Instrument Normal operation		
r) The middle cylinder should be completely pulled in by the motor by 2.5mm from N.A.	✗ 0.8 mm pulled back by motor from N.A.	Manufacture of components need to be of higher tolerance.

26. Attachment and Removal of SATA Instrument Normal operation		
s) The middle cylinder when completely pulled in by the motor, should be able to be pushed in manually by 2.5mm.	✓ The middle cylinder when completely pulled in by the motor, can be pushed in manually by 2.51mm	
t) The middle cylinder when completely pushed out by the motor, should be able to be pushed in manually by 6.5mm.	X The middle cylinder when completely, pushed out by the motor, can be pushed in manually by 4.77mm.	The IC piece can still be attached/removed with 4.77mm push back.
27. Backdrivable		
u) Backdrivable mechanism for the Control Box design	✓ The mechanisms used for the rotation of the inner, outer and middle rod are backdrivable. The middle rod can be pushed in by hand.	The middle rod is backdrivable due to the push-back mechanism and not the leadscrew mechanism which uses motor to control it.
28. Sterilizable		
v) No deep grooves or other locations that can harbor micro-organisms.	✓ The outer side of the Control Box has no deep grooves on its surface, an effort is made to make the surface as smooth as possible. However, there are grooves for inserting screws.	The grooves on the surface to insert screws can be closed by using screw caps.
w) Possibility to attach a drape for the surgical system.	✓ There is a snapfinger holder for attaching a drape around the slave device.	

Table 15: Requirements for Control Box Check Phase 1

ZTM Requirements Check:

Requirement	Achieved (Actual Value)	Not Achieved (Actual Value)
10. Attachment and Removal of the Control Box		
a) Attachment/removal provision	✓ Met	
11. Providing smooth movement of the ZTM		
b) No abrupt movements when the instrument moves in or out the body of the patient.	✓ Smooth movement for ZTMo, no abrupt movements.	
c) No random increase or decrease in speed of instrument.	✓ The motion of the system is smooth and does not have sudden increase or decrease in speed.	
12. Backlash		
d) Backlash if present should not cause any problem with the movement of the instrument.	✓ Backlash is present, but it is too small and does not interfere with the movement of the instrument.	
13. Entire mechanism should weigh below 2 kg		
e) Weight below 2 kg.	X The ZTM weight is 2.782 kg	Remove material from the components. Use slides and pulleys made of aluminum instead of steel

14. Compact design		
f) The mechanism should fit in a box of 200mmx200mmx400mm.	✗ The ZTM length is 475mm.	The ZTMo can be decreased to bring the length of the ZTM below 400 mm.
15. Translational speed and distance		
g) Maximum linear velocity between 60mm/s to 200mm/s.	✓ The measured velocity is 302mm/s.	
h) Maximum linear movement between 200mm-350mm.	✓ Maximum linear movement range is 403mm.	
16. Translational resolution		
i) A linear resolution of at least 0.1mm.	✓ The translational resolution was not able to be checked as the ZTM motor did not arrive in time.	Use a encoder on the ZTM motor to measure the resolution
17. Pull-push force		
j) A pull/push force of at least 26N.	✓ The push/pull force exceeds 26N (value around 100N).	
18. Backdrivable		
k) Backdrivable mechanism for ZTM	✗ ZTM is not backdrivable due to the leadscrew mechanism used.	Change mechanism to another type or use backdrivable leadscrew

Table 16: Requirements for ZTM Check Phase 1

5. Discussion

The existing surgical systems in market are complex, expensive and use specialised components. The PoLaRS slave ZTM and the Control Box, which controls the 5-DOF of the SATA instrument developed in this thesis are simpler, cheaper and do not use specialised components. During the design and development phase of these systems, several iterations of the concept design were carried out. Followed by the prototyping phase, where the design was built as a prototype. This prototype functioning was tested in Phase 1 followed by a problem analysis and redesign of the prototype. After analysing and eliminating some design issues, the Phase 2 testing of the prototype was carried out leading to the final design/prototype of this thesis project.

In the design phase, the first step was the idea generation session where an effort was made to keep the solutions as simple as possible. Grouping together of the different functionalities into 3 groups - rotations of rods, linear movements of the rod and linear movement of the Control Box helped to simplify the main goal. After an initial inspection of the different solutions obtained through brainstorming sessions, first 2-D drawings were created to make it easier to understand, followed by 3-D models using Inventor. The 3-D models of the concepts provided a better insight into how the system would look like and the fitting of the different components of the system. The 3-D models provided an easier to understand solution for the PMA (Pugh Matrix Analysis). The PMA yielded 3 solutions which were then further developed and one of these solutions were selected for developing into the prototype.

In the prototype phase the production of the parts, buying of new parts and the redesign of some components was carried out. The materials used in the design of the system were varied, the parts that were in contact with each other had to be made of compatible materials. In case of bronze or brass bushings where there is movement of parts against each other steel parts had to be used. Aluminium was used for other parts with no moving contact which decreased the weight of the system. The Control Box itself was made from 3-D printing using R05 material. The other smaller 3-D printed parts were made using PLA and ABS, in the MISIT lab at the 3ME faculty, TU Delft.

The structure of the Control Box had to ensure that it holds the CBC coupling rods concentrically and the motors for the movements of the CBC rods. The use of a snapfit piece to hold on the drape which will cover the PoLaRS slave arm, had to be connected to the Control Box. The Control Box had limitations on its size set by the PoLaRS arm designed during my internship. The design of components in the Control Box had to be small so as to fit in the limited space. This limited the size of the motors that could be selected, which meant that motors with small sizes and higher torques were difficult to obtain. The cable pulley system was used in the first prototype and for the phase 1 testing. The cable was wound over the pulley in different manners of windings. Each was checked for the amount of slack and the number of rotations of the SATA cylinder.

For the ZTM, it required that the drape should not be in the way of the ZTMo. This resulted in reversal of the ZTMo mechanism in which the Control Box was attached to the rails of the slide instead of the guides of the slides. This allowed the entire rail to move over the guide with the Control Box and hence prevent the crushing of the drape between the rail and the guide. The brushless dc motor used for the ZTM has an encoder in it which will count the rotations of the motor. The zero position of the system can be found out by using a magnet and a hall sensor, which can detect the presence of the magnet and provide a signal which can act as a zero point for the motors. The magnet can be attached to one end of the leadscrew so that it does not interfere with the movement of the Control Box and provide a zero point.

There were several challenges faced during the design and prototyping of the ZTM and Control Box. In the initial design the spring was fitted to the Control Box by means of a small groove in the Control Box and motor box for the middle rod translation. When the motor box was pushed back, from the entire mechanism of the middle rod movement being pushed back, the spring pushed back harder on the groove on the Control Box. This caused the Control Box and the motor box, which are 3-D printed plastic parts to bend. In order to resolve this, a guide pin and housing for the spring was created. The housing encased the spring ends and the guide pin made sure the spring would not bend or buckle under load. The housing and the guide pin had large surface touching the Control Box and the motor box which spread the forces out and did not cause bending of these parts.

The winding pattern for the cable system that was used for the testing in phase 1 was the one that had the least amount of slip. However, the slip increased with use. Apart from that the use of a bead to hold the ends of the

cable meant that the force carrying capacity of the cable pulley system was decreased as the cable would slip through the bead. The torques obtained from the cable pulley system was not sufficient for the SATA instrument and it also had the problem of slip which increased with use.

Initially, the main reason for using the cable and pulley system instead of timing belts and pulleys was the unavailability of the small sizes of the belts and pulleys needed and the ones that could be brought were expensive as they were specially made. But since the cable-pulley system functioning was not sufficient, it was decided that timing belts and pulleys would be used. The timing pulleys were created by 3-D printing with polyflex material. Aluminium was lasercut to obtain the tooth profiles for the timing pulleys. These were then fixed using araldite glue to turned shafts at the 3ME workshop. A cover was made to ensure that the timing belt does not come off the top of the pulley. The problems with this type of timing belt and pulley system was that the belt was stretchable due to polyflex material and the tooth profile was not accurate due to 3-D printing precision limits. Apart from that, when the belt is kept stretched it retains its stretched shaped for a while after the tension is removed. When the forces on the belt were high, the tooth of the belt deformed to slide over the tooth of the timing pulley. The sliding of the belt over the pulley also caused wear in the tooth profile of the timing pulleys. Since the tooth profile of the belt were not accurate and it was needed to increase the tooth height, the tooth profiles in the CAD file were exaggerated to obtain higher tooth profiles after 3-D printing. However, the problem of cleaning the belts from the excess printing material could not be done well, resulting in imprecise timing belt.

The Control Box design used readily available, cheap dc motors from online stores. However, the CAD models of these parts were different from the actual components and hence it caused interference with other components in the Control Box, which then had to be modified. The slides brought online were made of hardened steel, which meant that holes could not be drilled through the slides to hold it to the main block of ZTM. In order to mount the slides the holes had to be made in a different manner by drilling holes in the main block so that the slide holes can be accessed in the opposite direction.

When the IC was then attached to the CBC, it was seen that the connection between the 2 parts was not perfect. There was a gap between the IC and CBC coupling rods, this caused the IC part to be slightly angled to the CBC. The slight angle between the coupling rods caused the IC rods to rub against the other concentric rods resulting in the rotation to stop at the IC end as the 2 concentric rods interfered with each other. The IC part was slightly angled due to the attachment of the magnets and the dust that is collected near the magnets.

The tests for the phase 1 and phase 2 were conducted after the prototype was built. The phase 1 of the tests were done with the cable system and the phase 2 of the tests were done with the timing belt and pulley system.

In Test 1: The range of motion of Control Box (Section 3.3), the cylinders of the SATA instrument needed to rotate a maximum of 180 degrees. It was seen that the CBC rods can rotate more than 180 degrees, hence it is necessary that the motors are able to be controlled and stopped at the end points or else the extra rotation beyond 180 degrees can damage the SATA Instrument. The dc motors used in this design consists of an incremental encoder, this can count the amount by which the motor has moved and determine its position. This can help to obtain precise movement of the dc motor. However since it is an incremental encoder, it is not able to determine the zero position for the start. This can be resolved by using an additional hall sensor on the timing pulley with a magnet. The hall sensor output can be read out and the zero position can be set when there is a sensor output i.e. when the magnet is interfering with the hall sensor.

In Test 4: The range and speed of middle rod movement (Section 3.3), it was seen that the ROM of the middle rod translation was 3.6mm for phase 1 testing and 3.71 mm for phase 2 testing, which is almost the same. The actual range of movement should have been 4mm. This means that the gripper is not able to open and close in its complete range. The speed of the middle rod translation was 1.55 mm/s and 0.99 mm/s for phase 1 and phase 2 respectively. The maximum speed determined was 4mm/s, hence the gripper is not able to close and open as quickly as needed. The speed of the middle rod translation can be increased by using a dc motor with higher rpm, the currently used dc motor has 155rpm. The linear movement was tried with a dc motor of 530 rpm, however the torque of this motor was not sufficient to move the middle rod. Hence a dc motor with speed above 480rpm should have sufficient torque and speed to provide a linear movement speed of 4mm/s to the middle rod.

In Test 6: Torques at CBC rods (Section 3.3), it is seen that the torques obtained are around 0.04Nm, which is just the amount of torque needed to move the SATA instrument cylinders. However, we need to have a FOS of 2 at least, hence these torques are lesser than the needed amount of 0.08Nm. The lower torque could be due

to insufficient torque supplied by the dc motors, interference between the components in the Control Box or the slipping of the timing belt when the forces in the belt are higher than 0.04Nm. Theoretically the dc motors should be able to provide a torque of 0.372Nm, 0.274Nm and 0.254Nm at the outer, middle and inner CBC rods. Hence the dc motors have sufficient power to provide the needed torque of 0.08Nm. Upon checking the system for interfering parts, there were a few modifications made to ease the movement of the CBC rods. The only problem that remained was the slipping of the timing belt over the timing pulleys, due to stretching.

To overcome this problem, using another method of making the timing belt could be advantageous. Manufacturing timing belts using different materials which are flexible but not stretchable can prevent the slipping of the tooth and prevent the stretching of the belt. Another production method would be to lasercut the flexible material in a lasercutter. This will give a superior tooth profile due to higher precision of the lasercutter. Another method of manufacturing timing belts would be by casting a flexible material in a mold. This method can also allow thin cables to be laid within the belt and increase the strength of the belt and make it non-stretchable.

In Test 1: The range and speed of ZTMo (Section 3.3), it was observed that the range of the system is 403 mm, the range of movement is limited to ensure that the end stoppers of the rails do not hit the main block of the ZTM. Therefore the ZTMo is stopped before the end stopper hit the main block. The length of the slides can be further reduced if needed but this will also cause the range of motion to be decreased. A greater length of the slide length can be used in the ZTMo by reducing the length of the end stoppers and making the socket screws on the main base flush with the surface.

The resolution of the dc motors used in the Control Box are measured in Appendix J, it is seen that the encoder resolution are different for different motors. The 3 dc motors from the Control Box gave the following resolutions, 0.507 degree per count for the 155rpm dc motor, 0.146 degree per count for the 52 rpm dc motor and 0.17 degree per count for the 41 rpm dc motor. In the experiment, the shaft of the motor was moved by hand to complete one revolution and the count of the encoder was recorded. Hence, it is important to note that there are bound to be errors while moving the shaft to complete 1 revolution. It can be that the shaft is moved to either 350 degrees or 370 degrees, due to human error. However, an effort was made to keep the rotation as accurate as possible. The error which was seen when stopping the dc motors, could be due to the inertia of the rotating parts. However, this inertia effects will be decreased when the dc motor is loaded, as the forces in the timing belt and timing pulley are much higher.

In terms of the cost prototype, the most expensive parts of the Control Box and ZTM are the 3-D printed parts, which cost around € 1920 (from 16 hours and cost of € 120 per hour). The labour costs of the ZTM and the Control Box without considering the costs material for machining is around € 2800 (assuming € 60 per hour), considering the machining of the parts takes 1 month time including lasercutting, watercutting, milling, turning and other operations. The approximate time of 1 month is obtained from considering it took the author (inexperienced user) around 3 months to manufacture these components. Apart from that the cost of the parts brought, which includes motors, bearings, springs, slides, belts, pulleys etc. is around € 600. The material cost (Steel, Aluminium, Bronze/Brass) to be around € 500, since the parts of the Control Box are small and the ZTM parts are larger but still uses little material. The total costs of the Control Box and the ZTM is then around € 5820, which includes the cost of labour, material, brought parts. Even assuming the cost of other parts to be around € 500,000 (very high approximate, since the other systems in the PoLaRS for example the base, arm and the master console are also made of non-specialised components).The cost of this system is still cheaper than the alternatives present in the market today with Da Vinci surgical system from Intuitive surgical costing over € 1 million and further maintenance cost of over € 150,000 per year. However, it must be noted that the cost of the complete PoLaRS system is difficult to predict accurately for now as the system is still in development and undergoing changes.

There are certain limitations with the current prototype:

- The system still needs to undergo replacement of all machined parts as the tolerances of the machined parts add up and cause problems such as increased friction between components or loose parts. Apart from that, the alignment of the parts also changed after phase 2 testing due to imprecise manufacture of the components and bending of the Control Box.
- There is no electronic control implemented in this thesis project, it was purely a mechanical system design with the inclusion of motors for the actuation. The control of the Control Box and ZTM has to be designed so that it can be controlled through the master console and be able to control the velocities, torques and positions of the SATA instrument.
- The prototype developed is not fully modular, while there are some parts that can be replaced with similar components like motors, bushings, bearings etc. However, it is still not possible to replace some

components, for example, larger motors for achieving higher torques cannot be put in place of the existing ones due to the Control Box size.

- The 3-D printing techniques resulted in slightly bent parts, which cause stress on other components, therefore the long term use of the prototype is uncertain. The belts and 3-D printed components deform. This deformation also contributes to the misalignment of the components in the Control Box.
- The system has not yet been connected to the SATA instrument though the coupling rods, this should be done after the programming of the system so that the SATA Instrument can be protected from damage. However, this means that the actual movements of the SATA Instrument gripper cannot be measured until then. The rotations of the CBC rods are used to extrapolate the movements of the SATA gripper. However, there can be other effects which are seen only when the SATA Instrument is connected to the coupling rods.
- The resolution of the brushless dc motors for the ZTM was not measured as the motor did not arrive in time. The resolution of the ZTM can be increased by changing the sizes of the timing pulleys to increase the accuracy.

The future goal of this thesis project:

- The Control Box and the ZTM created should be mounted on the PoLaRS slave arm and work as a part of the PoLaRS, with the control provided by the master console.
- The programming of the system in control and safety has to be carried out to make the system functional.
- The modularity of the system can be increased further to accommodate different shaped pulleys and motors.
- The weight of the system should be reduced as much as possible, by checking the components that are essential and those that can be removed/ replaced with lighter components. Another method of reducing the weight is by removing material from different components of the system. The use of a single slide would be sufficient for the movement of the system and to ensure that the Control Box is guided, while reducing the weight of the system.
- The assembly of the system is a difficult process for now, with a lot of components needed to be arranged precisely and in the correct sequence. This makes the disassembly and assembly of the Control Box difficult. Reducing the steps for assembly of the Control Box or making the assembly easier is an important goal.
- Replacing the 3-D printed parts made with R05 to a metal like steel or aluminium would ensure that the system does not have plastic deformations as with R05 material. It will also help to improve the aesthetics and strength of the system.
- Further addition of safety features for the system, both in terms of hardware and software needs to be done. Which can include haptic feedback, limitation of the ROM by software, backdrivability, collision detection etc.

6. Conclusion

A new control mechanism for SATA Multi-DOF Instrument is presented. A new method to manufacture timing belts and pulley is also presented in this thesis project. The rotations of the SATA Instrument cylinders are used to active the gripper in pitch, yaw and rotation. The translation movement of the middle cylinder of the SATA Instrument is used to activate the gripper open/close.

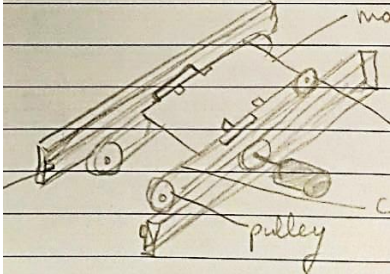
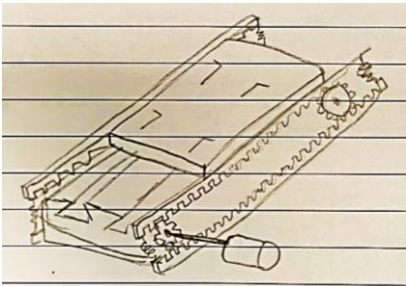
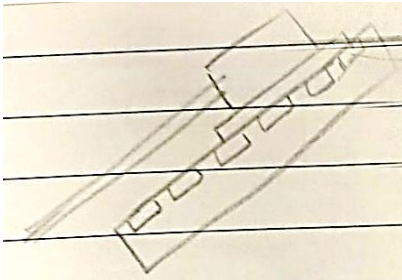
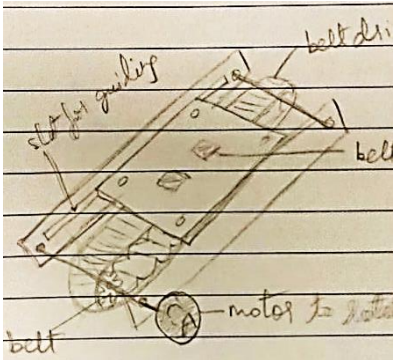
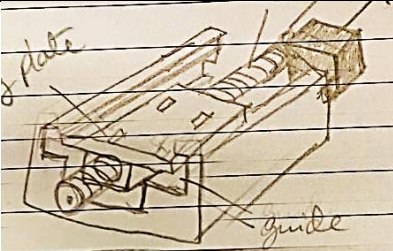
The aim of the thesis project was to design a mechanism to control 5-DOF i.e. 4 DOF of the SATA Instrument (pitch, yaw, rotation and opening/closing of the gripper) and 1 DOF for the ZTMo (insertion of the SATA Instrument to the surgical site and retraction away from it). The system needed to be compact, ergonomic, low cost and portable so that it can be used in low and middle income countries.

In this thesis the design and prototype of the system for the 5-DOF control of the SATA instrument was completed. The Control Box and the ZTM prototype was built which was lightweight, portable, and low cost. Since this is the first prototype there are several improvements that can be made to improve the system in the future.

Appendix A

Idea's from the brainstorming session:

For ZTM

Solution/Concept		Advantage	Disadvantage
Cable Drive		Small size	Unstable, shaky, needs additional supporting features
Rack and Pinion Drive		Easy actuation, smooth motion	Backlash in the system, weight might be an issue
Magnetic Drive		Quick, smooth motion.	Resolution of movement dependent on placement of magnets, stepping action, difficult to control.
Belt Drive		Absorbs vibrations, high efficiency,	Needs to adjust for tension, may slip
Nut/Screw Drive		Smooth motion, needs less power and smaller actuators.	Backlash due to gears, no backdrivability.

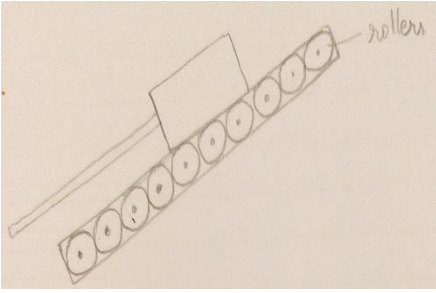
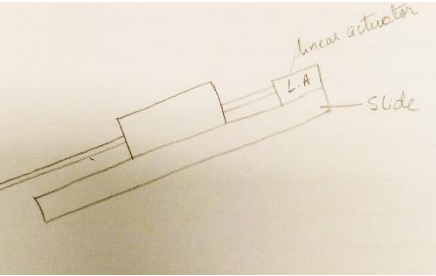
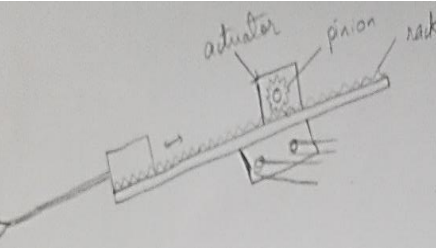
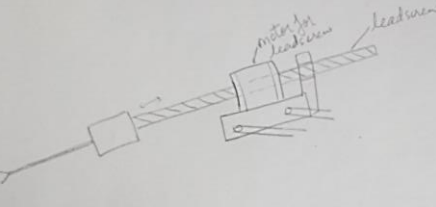
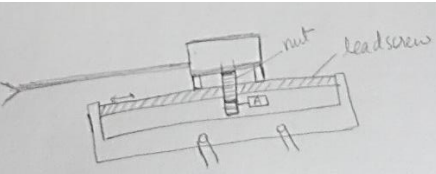
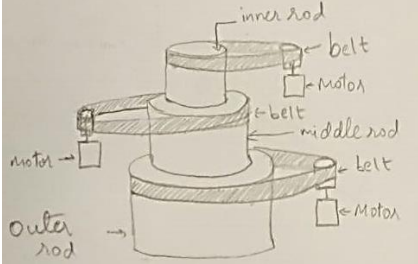
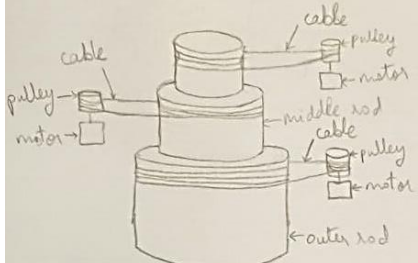
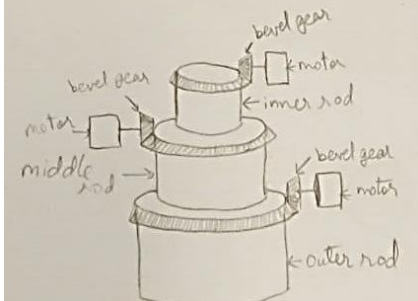
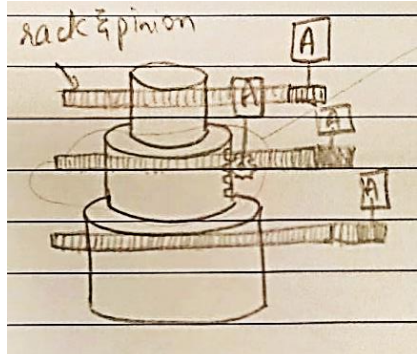
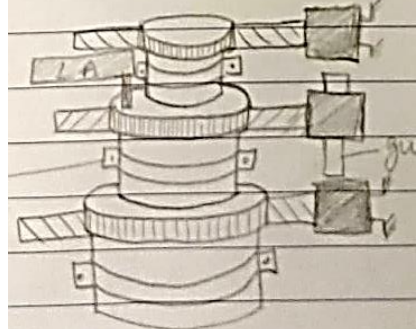
Roller		Each roller can be controlled independently	Difficult to control, shaky movement, complex design
Linear Actuator		Smooth motion, high resolution depending on the actuator.	Expensive, less power
Reversed Rack and Pinion		High control of the movement, precision can be controlled by using precise motors.	Backlash due to gears
Leadscrew Motor		Precise motion, smooth movement.	Expensive due to the actuator needed, large size
Reversed Nut/Screw		Low power actuators used, small size	Backlash due to gears used

Table 17: Concept Ideas ZTM

For Rotation of Cylinders:

Solution/Concept		Advantage	Disadvantage
Belt System		Precise motion transferred, can correct slight errors in alignment, small size	Any slack in the belt would cause the belt to come off, bending compensation system needed, slip possibility.
Cable System		Compensates for slight misalignments, small size, no slip if cable wrapped.	Low force transfers, cables can snap
Gear System		Easy design, small size	Problem with backlash due to gears
Rack and Pinion System		Easy design, simple construction	Backlash
Worm Gear System		Low power actuator	Large size, backlash

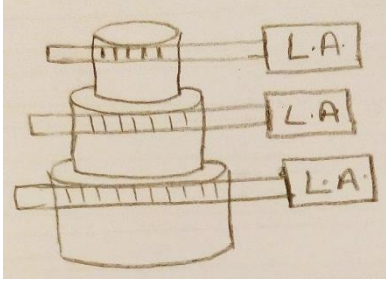
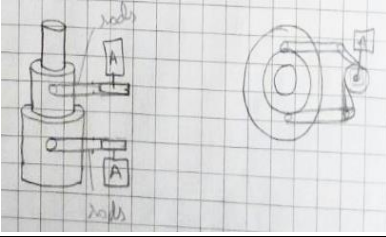
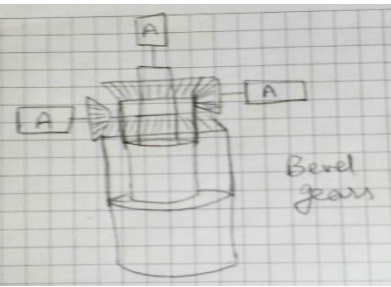
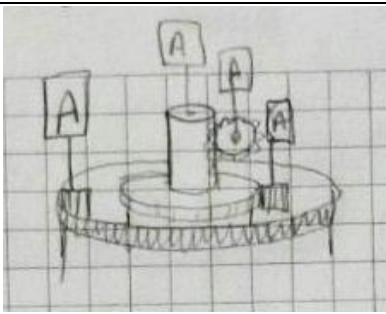
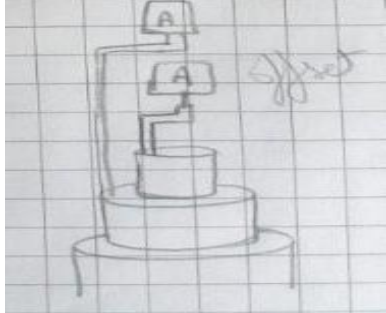
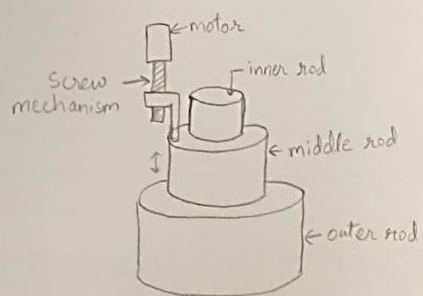
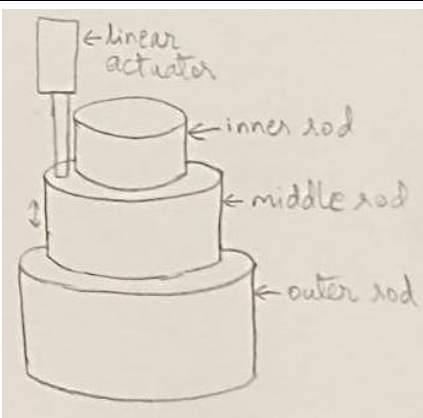
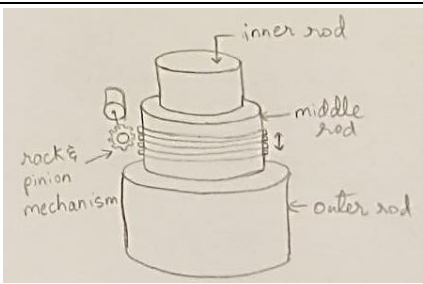
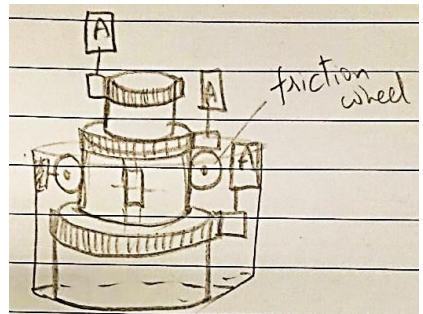
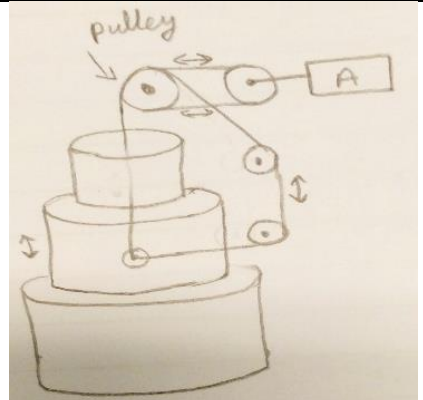
Linear Actuator		Good resolution, variable movement, easy actuation	Expensive, range of motion limited, power limited
Rods and Links		Can transmit large forces	Complex construction, limited movement
Bevel Gears		Compact size	Difficult construction, backlash
Internal Gear		Large range of motion	Large size, backlash, complex
Offset		Less power actuators due to moment arm	Difficult construction, large size.

Table 18: Concept Ideas Rotation of Cylinders

For Middle Cylinder Translation:

Solution/Concept		Advantage	Disadvantage
Screw Mechanism		Easy construction, low power actuators	Backlash, limited resolution
Linear Actuator Mechanism		Smooth motion, high resolution, small size	Size too large, small sizes too expensive, range issues, low power transmission.
Rack and Pinion Mechanism		Easy construction	backlash
Friction Wheel Mechanism		Smooth motion	Complex construction, large space needed, possibility of slip
Pulley System		Transmit power at angles of when misaligned	Large size, unstable operation

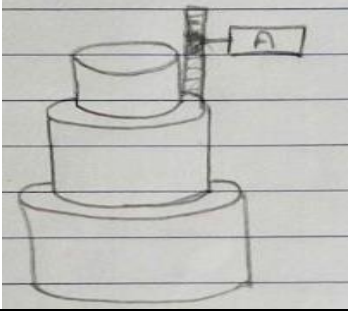
Rack and Pinion 2		Easy construction	backlash
-------------------	---	-------------------	----------

Table 19: Concept Ideas Middle Cylinder Translation

Appendix B

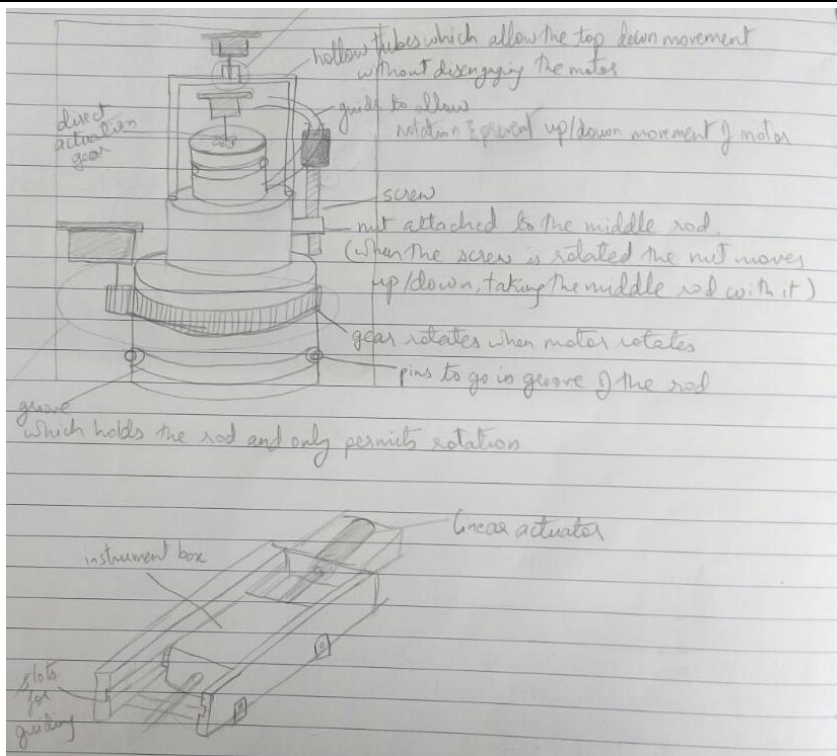
Concepts were created from the combination of ideas from brainstorming session. These concepts were used as criteria in the PMA.

There are 12 concepts/criteria listed below:

Concept Number	Drawings	Comments
1		<ul style="list-style-type: none"> • Use of Bevel gears to rotate the cylinders • A gear mechanism to translate the middle rod • Nut and Bolt (leadscrew) mechanism to move the ZTM
2		<ul style="list-style-type: none"> • Use of Timing Belt to rotate the cylinders • A Linear actuator to translate the middle rod • Cable pulley mechanism to move the ZTM
3		<ul style="list-style-type: none"> • Use of rack and pinion to rotate the cylinders • A gear mechanism to translate the middle rod • A belt drive mechanism to move the ZTM

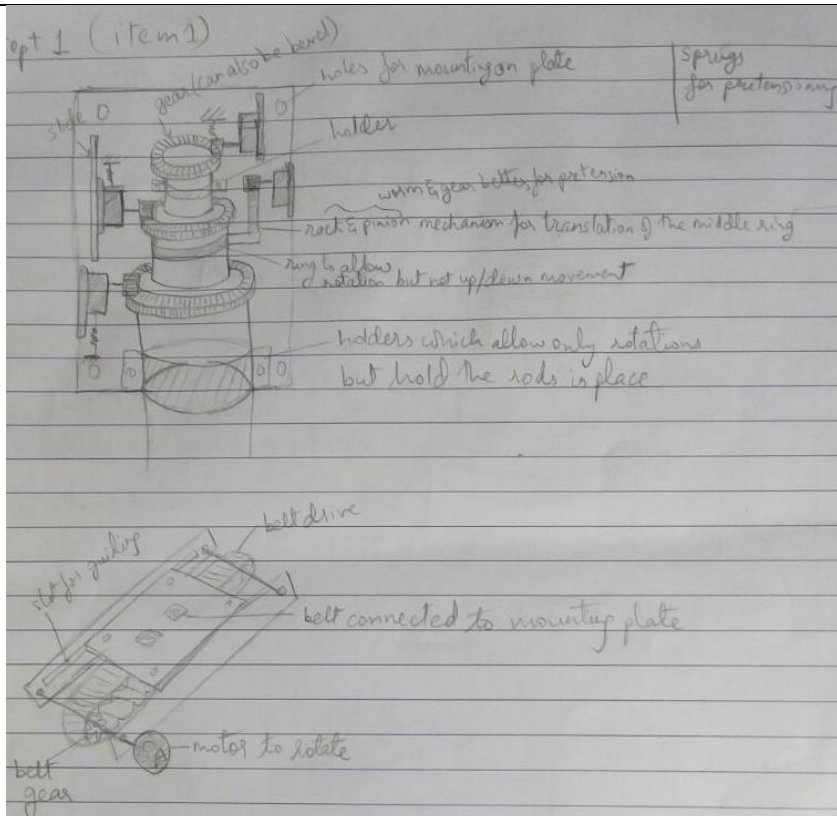
4		<ul style="list-style-type: none"> • Use of spiral gears to rotate the cylinders • A friction wheel mechanism to translate the middle rod • Cable pulley mechanism to move the ZTM
5		<ul style="list-style-type: none"> • Use of direct connection between the cylinder and the actuator to rotate the cylinders • A Linear actuator to translate the middle rod • Magnet mechanism to move the ZTM
6		<ul style="list-style-type: none"> • Use of swivel linkage mechanism to rotate the cylinders • A pulley cable mechanism to translate the middle rod • Linear actuator to move the ZTM
7		<ul style="list-style-type: none"> • Use of screw mechanism to rotate the cylinders • A linear actuator to translate the middle rod • Nut and Bolt (leadscrew) mechanism to move the ZTM

8



- Use of offset bars with motors to rotate the cylinders
- A leadscrew mechanism to translate the middle rod
- Linear actuator mechanism to move the ZTM

9



- Use of gears to rotate the cylinders
- A rack and pinion mechanism to translate the middle rod
- A belt drive mechanism to move the ZTM

10		<ul style="list-style-type: none"> • Use of offset bars to rotate the cylinders • A leadscrew mechanism to translate the middle rod • Linear actuator mechanism to move the ZTM
11		<ul style="list-style-type: none"> • Use of gears to rotate the cylinders • Friction wheel mechanism to translate the middle rod • Pulley and cable mechanism to move the ZTM
12		<ul style="list-style-type: none"> • Use of Pulley and cable to rotate the cylinders • A Linear actuator to translate the middle rod • Rack and pinion mechanism to move the ZTM

Table 20: Combined Concept Ideas

Appendix C

Pugh Matrix

Selection Criteria	Weights	Concept 1	Weighted score	Concept 2	WS
	(0-5)		(WS)		
Cost	2	5	10	4	8
Robustness	3	6	18	4	12
Complexity of System	4	7	28	4	16
Ease of Use	5	7	35	5	25
Structural stiffness	5	7	35	3	15
Controllability/Accuracy	4	8	32	4	16
Compactness of design	4	5	20	4	16
Weight of System	4	3	12	7	28
Safety	3	3	9	3	9
Reliability	3	6	18	3	9
Total Score		57	217	41	154
Total Weighted score		217		154	
Rank		<u>1</u>		10	
Continue with concept?		<u>Y</u>		N	

Selection Criteria	Weights	Concept 3	WS	Concept 4	WS	Concept 5	WS
	(0-5)						
Cost	2	4	8	5	10	6	12
Robustness	3	6	18	3	9	5	15
Complexity of System	4	5	20	4	16	4	16
Ease of Use	5	5	25	4	20	6	30
Structural stiffness	5	6	30	3	15	6	30
Controllability/Accuracy	4	7	28	5	20	5	20
Compactness of design	4	7	28	4	16	3	12
Weight of System	4	4	16	8	32	4	16
Safety	3	6	18	4	12	4	12
Reliability	3	6	18	4	12	6	18
Total Score		56		44	162	49	181
Total Weighted score		209		162		181	
Rank		4		9		6	
Continue with concept?		N		N		N	

Selection Criteria	Weights	Concept 6	WS	Concept 7	WS	Concept 8	WS	Concept 9	WS
	(0-5)								
Cost	2	2	4	4	8	7	14	6	12
Robustness	3	2	6	5	15	7	21	5	15
Complexity of System	4	3	12	4	16	8	32	6	24
Ease of Use	5	4	20	3	15	7	35	5	25
Structural stiffness	5	7	35	4	20	7	35	5	25
Controllability/Accuracy	4	7	28	6	24	7	28	5	20
Compactness of design	4	4	16	5	20	3	12	7	28
Weight of System	4	3	12	5	20	3	12	6	24
Safety	3	2	6	6	18	3	9	6	18
Reliability	3	3	9	5	15	6	18	7	21
Total Score		37	148	47	171	58	216	58	212
Total Weighted score		148		171		216		212	
Rank		11		8		<u>2</u>		<u>3</u>	
Continue with concept?		N		N		<u>Y</u>		<u>N</u>	

Selection Criteria	Weights	Concept 10	WS	Concept 11	WS	Concept 12	WS
	(0-5)						
Cost	2	7	14	5	10	5	10
Robustness	3	5	15	5	15	5	15
Complexity of System	4	7	28	2	8	9	36
Ease of Use	5	6	30	4	20	5	25
Structural stiffness	5	4	20	6	30	7	35
Controllability/Accuracy	4	6	24	5	20	6	24
Compactness of design	4	4	16	6	24	6	24
Weight of System	4	8	32	5	20	5	20
Safety	3	5	15	4	12	4	12
Reliability	3	5	15	5	15	5	15
Total Score		57	209	47	174	57	216
Total Weighted score		209		174		216	
Rank		4		7		<u>2</u>	
Continue with concept?		N		N		<u>Y</u>	

Table 21: PUGH Matrix

Even though concept 1 had the highest score, it used gears, which made gear backlash a huge problem and had to be discarded. Hence concept 8, concept 9 and concept 12 were chosen to develop further.

Appendix D

List of components purchased and site links

For ZTM:

Sr. No.	Item	QTY	Site	Price per piece (euro)	Total (euro)
1	MTSNR8	2	https://uk.misumi-ec.com/vona2/detail/110302641220/?PNSearch=MTSNR8&HissuCode=MTSNR8&searchFlow=suggest2products&Keyword=MTSNR8	12	24
2	KH1026	4	https://uk.misumi-ec.com/vona2/detail/221005158161/?CategorySpec=00000004087%3a%3a%0000001627061%0900000004089%3a%3a%0000001663961	34.32	137.28
3	TTPT22T5150-A-N8	2	https://uk.misumi-ec.com/vona2/detail/110300406820/?CategorySpec=00000432717%3a%3a%0900000005784%3a%3a%0900000005785%3a%3a%3anvd00000000000002%0900000005789%3a%3a%00000001621426	27.89	55.78
4	TTBU325T5-150	3	https://uk.misumi-ec.com/vona2/detail/110302194260/?PNSearch=TTBU325T5-150&HissuCode=TTBU325T5-150&searchFlow=suggest2products&Keyword=TTBU325T5-150	9.3	27.9
5	b_SECBL16	2	Part of SECBL16-466		
6	SUB608ZZ	1	https://uk.misumi-ec.com/vona2/detail/110300108530/?CategorySpec=00000196582%3a%3a%0900000232327%3a%3a%0900000196585%3a%3a%00000001625688%0900000196516%3a%3a%00000001624850%0900000196607%3a%3a%00000001622893%0900000196456%3a%3a%00000001644205	25.90	25.9
7	MTSBR8-452	1	https://uk.misumi-ec.com/vona2/detail/110302642260/?HissuCode=MTSBR8-452&PNSearch=MTSBR8-452&KWSearch=MTSBR8-452&searchFlow=results2type	24.8	24.8

8	SECBL16-466	2	https://uk.misumi-ec.com/vona2/detail/110300043340/?His suCode=SECBL16-466&PNSearch=SECBL16-466&KWSearch=SECBL16-466&searchFlow=results2type	106.4	212.8
---	-------------	---	---	-------	-------

Table 22: List of Purchased Parts for ZTM

For Control Box:

Sr. No.	Item	QTY	Site	Price per piece (euro)	Total (euro)
1	SF-12525	3	https://uk.misumi-ec.com/vona2/detail/221005203296/?CategorySpec=00000425169%3a%3aa%0900000234042%3a%3aa%0900000233997%3a%3aa%0900000234025%3a%3anvd0000000000006%0900000233943%3a%3anvd0000000000007%0900000233964%3a%3anvd00000000000005%0900000233948%3a%3aa	0.64	1.92
2	SB6801ZZ	2	https://uk.misumi-ec.com/vona2/detail/110302272750/?CategorySpec=00000196582%3a%3aa%0900000232327%3a%3ab%0900000196585%3a%3amig00000001623121%0900000196516%3a%3amig00000001628136%0900000196607%3a%3anvd00000000000004%0900000196456%3a%3amig00000001643150%0900000196640%3a%3aa	6.3	12.60
3	54B-030603	3	https://uk.misumi-ec.com/vona2/detail/221000090891/?CategorySpec=00000425169%3a%3aa%0900000233944%3a%3ad%0900000234025%3a%3anvd00000000000008%0900000233943%3a%3anvd00000000000014%0900000233964%3a%3anvd00000000000006	3.94	11.82
4	SCCA6-8	2	https://uk.misumi-ec.com/vona2/detail/110302636320/?ProductCode=SCCA6-8	1.05	2.10
5	n20 motor	2	https://nl.aliexpress.com/store/product/GA12-N20-dc-6V-Hall-Encoder-Motor-With-Code-Disk-3V-Gear-Motor-Electronic-Lock-Motor/1499567_32707648904.html	12.62	30.2
6	WB4-10	3	https://uk.misumi-ec.com/vona2/detail/110100185240/?His suCode=WB4-10&PNSearch=WB4-10&KWSearch=WB4-10&searchFlow=results2type	0.75	2.25

7	Faulhaber Encoder Hollow Cup Gear Motor	1	https://www.aliexpress.com/snapshot/0.html?spm=a2g0s.9042647.0.0.1b7dd8&or derId=89316694131333&productId=32814907261	14.17	14.17
8	LED-0606	2	https://uk.misumi-ec.com/vona2/detail/221000090992/?CategorySpec=00000425169%3a%3ab%0900000234025%3a%3anvd00000000000017%0900000233943%3a%3amig00000001626435%0900000233964%3a%3anvd00000000000014	0.52	1.04
9	JFB-11010	2	https://uk.misumi-ec.com/vona2/detail/221005203274/?CategorySpec=00000425169%3a%3ab%0900000233997%3a%3aa%0900000234025%3a%3anvd000000000000001%0900000233943%3a%3anvd00000000000004%0900000233964%3a%3anvd000000000000001	0.29	0.58
10	GEB-1515	2	https://uk.misumi-ec.com/vona2/detail/221000090868/?CategorySpec=00000425169%3a%3aa%0900000234025%3a%3anvd00000000000003%0900000233943%3a%3amig00000001622111%0900000233964%3a%3anvd00000000000002	2	4

Table 23: List of Purchased Parts for Control Box

The total cost of all these items is 574.93 euro

Additional parts procured after Phase 1 testing:

Sr. No.	Item	QTY	Site	Price per piece (euro)	Total (euro)
1	Velleman VMA409 Dual-controller L298N	3	conrad.nl	8,26	24,78
2	Arduino Uno R3 DIL	1	conral.nl	23,1	23,1
3	Belt Faulhaber Encoder Hollow Cup Gear Motor With Encoder 2342I012 2342L012CR(6.3)	1	https://nl.aliexpress.com	14,17	14,17
4	TTBU225T5-150	2	https://uk.misumi-ec.com	8,20	16,40
5	Castle Creations Max Race Pro SCT 25.2V 3800kV	1	https://www.toemen.nl/castle-creations-max-race-pro-sct-252v-3800kv-p-12364.html	180	180
6	Castle Creations - Castle Link V3 USB programming kit	1	https://www.toemen.nl/castle-creations-castle-link-usb-programming-kit-p-34980.html	31,95	31,95

Table 24: Additional Purchased Parts

Total of additional parts is 282.2euro

Appendix E

List of parts manufactured and method of manufacture. For the Control Box parts refer to Fig.56 and for ZTM parts refer Fig.57.

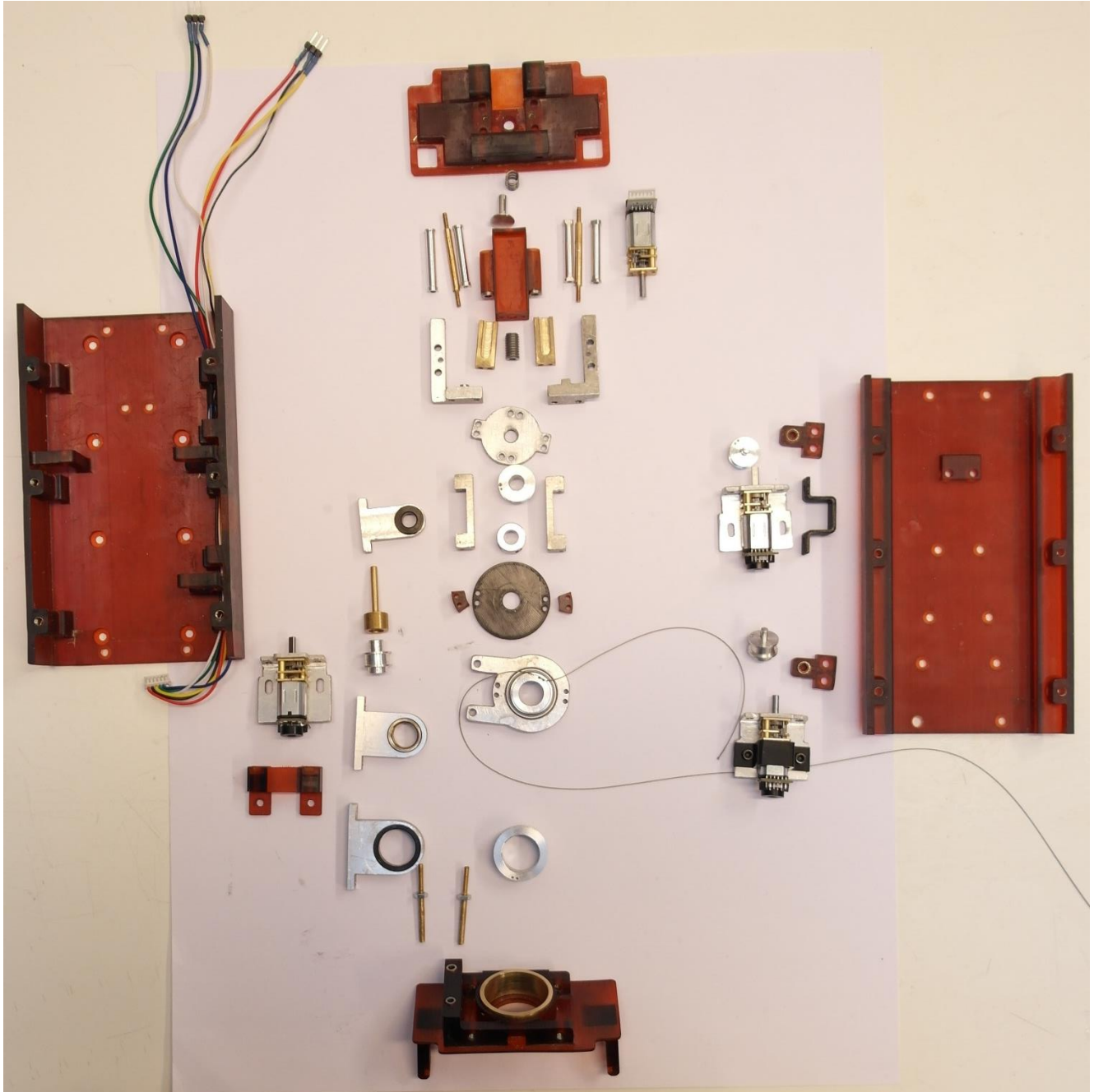


Figure 56: Parts for the Control Box

Control Box Parts:

Part Number	Part Name	QTY	Material	Manufacture
1	rod holder inner	1	Aluminium	water cutting
2	rod holder middle	1	Aluminium	water cutting
3	rod holder outer	1	Aluminium	water cutting

4	linear actuator piece 1	1	Aluminium	water cutting
5	pulley for motor sliding	1	Aluminium	Milling machine and lathe
6	pulley for motors	2	Aluminium	Milling machine and lathe
7	pulley inner rod i1	1	Aluminium	Milling machine and lathe
8	pulley middle rod	1	Aluminium	Milling machine and lathe
9	pulley outer rod	1	Aluminium	Milling machine and lathe
10	leadscrew smaller	1	Steel	Lathe
11	middle rod z translation holding motor	2	Aluminium	water cutting and milling
12	motor bracket	2	Aluminium	Water cutting and bending sheet metal
13	middle rod linear motion guide rod	1	Aluminium	Lathe
14	motor bracket sliding	1	Aluminium	Water cutting and bending sheet metal
15	rod for middle rod guidance	2	Steel	Lathe
16	holder for middle rod translation	4	Aluminium	Lathe
17	din_6902-a_m3-200hv(washer for middle rod movement)	4	Aluminium	buy/Lathe
18	sliding part for middle rod	2	Steel	Lathe
19	linear actuator movepart 3	2	Aluminium	Water cutting
20	linear actuator movepart 1	2	Aluminium	Water cutting and milling
21	linear actuator movepart 2	1	Aluminium	Water cutting
22	bushing for motor middle rod translation	2	Brass	Lathe
23	Sliding middle rod metal part	2	Aluminium	Lathe

Table 25: Control Box Parts Method of Manufacture

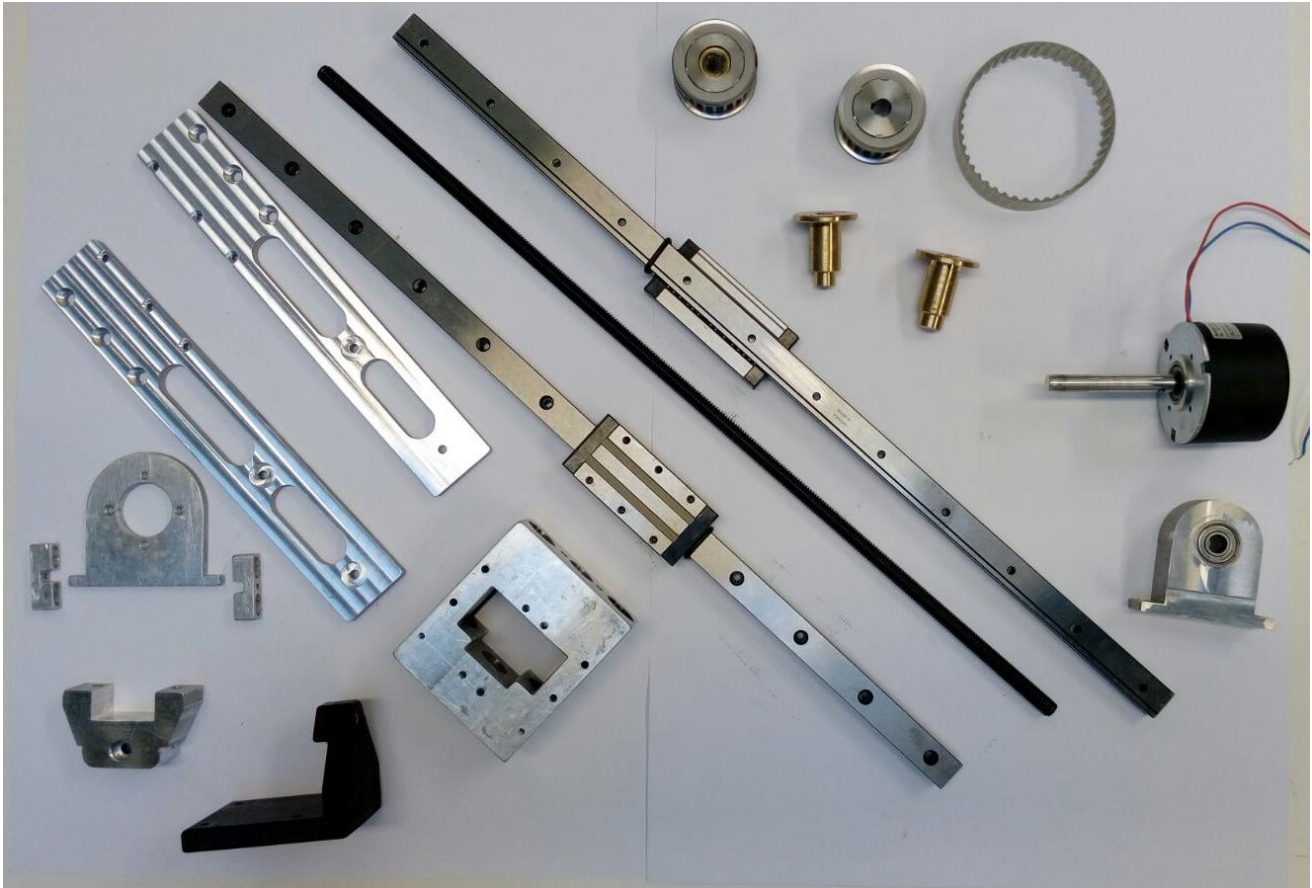


Figure 57: Parts for ZTM

ZTM Parts:

Part Number	Part Name	QTY	Material	Manufacture
1	holder_z translation	1	Aluminium	Water cut
2	Z-translation movement	1	Aluminium	watercut
3	z-translation guide beam	2	Aluminium	lathe
4	timingpulley holder z translation	1	Aluminium	watercut
5	leadscrew cover	1	Aluminium	watercut
6	timing pulley support z translation	1	Aluminium	watercut
7	holder_z translation guide	1	Aluminium	watercut
8	holder_z translation guide 2	1	Aluminium	watercut
9	z translation motor holding block	2	Aluminium	watercut and drill
10	support rod z translation overtube	1	Aluminium	lathe

Table 26: ZTM Parts Method of Manufacture

Appendix F

Arduino Code for control of Control Box dc motors in time. The dc motors will rotate in clockwise direction for a certain duration of time and then reverse its direction for certain amount of time and so on.

```
//Rosnello Fernandes
//dc motor control _PoLaRS
//05-Feb-2018

const int enb = 6; // PWM pin 6
const int in3 = 7;
const int in4 = 8;

const int ena = 9; // PWM pin 9
const int in1 = 10;
const int in2 = 11;

const int ena1 = 3; // PWM pin 3
const int in11 = A1;
const int in21 = A2;

const int enb1 = 5; // PWM pin 5
const int in31 = A3;
const int in41 = A4;

const int button = 2;
const int button2 = 4;
const int button5 = 12;
const int button6 = A5;

int buttonState = 0;
int buttonState2 = 0;
int buttonState5 = 0;
int buttonState6 = 0;

void setup() {
  pinMode(in3, OUTPUT);
  pinMode(in4, OUTPUT);
  pinMode(enb, OUTPUT);
  pinMode(in1, OUTPUT);
  pinMode(in2, OUTPUT);
  pinMode(ena, OUTPUT);
  pinMode(in11, OUTPUT);
  pinMode(in21, OUTPUT);
  pinMode(ena1, OUTPUT);
  pinMode(in31, OUTPUT);
  pinMode(in41, OUTPUT);
  pinMode(enb1, OUTPUT);
  pinMode(button, INPUT_PULLUP);
  pinMode(button2, INPUT_PULLUP);
  pinMode(button5, INPUT_PULLUP);
  pinMode(button6, INPUT_PULLUP);

  Serial.begin(9600);
}

void sped() {
  int potValue = analogRead(A0); // Read potentiometer value
  int pwmOutput = map(potValue, 0, 1023, 0, 255); // Map the potentiometer value from 0
to 255
  analogWrite(ena, pwmOutput); // Send PWM signal to L298N Enable pin
  // Read button - Debounce

  analogWrite(enb, pwmOutput); // Send PWM signal to L298N Enable pin
  // Read button - Debounce
```

```

    analogWrite(enal, pwmOutput); // Send PWM signal to L298N Enable pin
    // Read button - Debounce

    analogWrite(enbl, pwmOutput); // Send PWM signal to L298N Enable pin
    // Read button - Debounce
}

void loop() {

    buttonState = digitalRead(button);
    Serial.println (buttonState);
    Serial.print("button1 = ");

    buttonState2 = digitalRead(button2);
    Serial.println (buttonState2);
    Serial.print("button2 = ");

    buttonState5 = digitalRead(button5);
    Serial.println (buttonState5);
    Serial.print("button5 = ");

    buttonState6 = digitalRead(button6);
    Serial.println (buttonState6);
    Serial.print("button6 = ");

    if (buttonState == HIGH){
        sped();
        //turn in one direction
        digitalWrite(in3, HIGH);
        digitalWrite(in4, LOW);

        delay(1000); //time to wait before reversing direction
        //Change direction
        digitalWrite(in3, LOW);
        digitalWrite(in4, HIGH);

        delay(1500);
    }

    if (buttonState2 == HIGH)
    {
        sped();
        //turn in one direction
        digitalWrite(in1, HIGH);
        digitalWrite(in2, LOW);

        delay(1000); //time to wait before reversing direction
        //change direction
        digitalWrite(in1, LOW);
        digitalWrite(in2, HIGH);
        delay(1000);
    }

    if (buttonState5 == HIGH)
    {
        sped();
        //turn in one direction
        digitalWrite(in11, HIGH);
        digitalWrite(in21, LOW);

        delay(1000); //time to wait before reversing direction
        //change direction
        digitalWrite(in11, LOW);

```

```

digitalWrite(in21, HIGH);
delay(1000);
}

if (buttonState6 == HIGH)
{
    sped();
    //turn in one direction
    digitalWrite(in31, HIGH);
    digitalWrite(in41, LOW);

    delay(800); //time to wait before reversing direction
    //change direction
    digitalWrite(in31, LOW);
    digitalWrite(in41, HIGH);
    delay(800);
}

else
{
    //do not run motor
    digitalWrite(in3, LOW);
    digitalWrite(in4, LOW);
    digitalWrite(in1, LOW);
    digitalWrite(in2, LOW);
    digitalWrite(in11, LOW);
    digitalWrite(in21, LOW);
    digitalWrite(in31, LOW);
    digitalWrite(in41, LOW);
    delay(20);
}
}

```

Appendix G

Experiment 1: Bead for holding cable together

Introduction: The use of beads to hold the cables together needs to be tested for how much tension or pull force it can hold without the cables slipping out of it. This would depend on several factors like how much compression force is used to press the beads the length of each bead, the bead hole diameter, the manner in which the cables are pressed inside the bead etc. There were 2 methods tested for holding the cable in the beads.

Method 1: The cables are inserted from the opposite ends of the bead and pass out through the opposite ends (Fig.58).



Figure 58: Method 1

Method 2: The cables are inserted from the same side of the bead and pass out together from the other end (Fig.59).

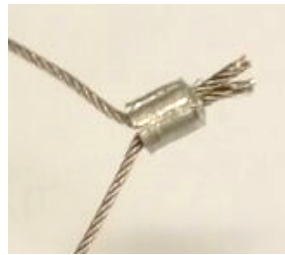


Figure 59: Method 2

Methods and Materials: An effort is made to keep the factors that change as stable/similar as possible. The lengths of the beads were kept between 1-3mm, the bead hole diameter was 1.1mm, bead diameter was around 2mm and the compression for pressing in the bead was done by a single person using the same tool with maximum force with which it could be compressed. However, there can be other factors which are unknown and may influence the bead holding force.

Hold one end of the cable at a strong support and the other end attached to a pull-push gauge Model ANF-50 (Fig.60). Pull on the pull-push gauge to measure the force reading. Check how much is the maximum force it reads before the cable slips out of the bead. Make similar measurements for the second manner of attaching the beads.



Figure 60: Experiment Setup

Results:

Bead attachment method	Force needed to pull out cable	Length of bead
Method 1	50N	2.9mm
	35N	1.1mm
Method 2	98N	2.2mm
	95N	2.6mm

Table 27: Bead Pull Forces

Discussion: The tests were conducted by using the beads made in the workshop, these were of varied lengths as it was difficult to make tiny beads of the same length and diameter. However, the results of the experiment showed that a larger cable length can hold a higher force before the cable slips out of the bead and vice versa. The manner of attaching the cable also plays a large role in the amount of force the bead can handle before the cables slips out. It was found that the method 2 was superior to method 1 in holding larger force.

Conclusion: Method 2 has higher force holding capability than Method 1.

Experiment 2: Movement range of cable pulley system

Introduction: The amount by which pulleys can be rotated with the cable system needed to be checked as a movement range of at 150-180 degrees is desired to move the SATA instrument tip in its complete range.

Methods and Materials: An experimental setup was created by 3-D printing the pulleys and the support base (Fig.61). The dc motor (6v, 530rpm, 0.019Nm) was inserted in the slot provided and the pulleys were mounted on their shafts. The cable was wound on the pulley and the open ends of the cable were connected by method 2 (as it would hold higher forces and was easier to tension by one person). The support base consisted of 2 parts, these were able to be pushed apart to increase the cable tension. Once the setup was completed the dc motor was turned in one direction, which caused the pulley to rotate, after completing one rotation the direction was reversed. It was tried to increase the rotations in steps of 90 degrees and check how many rotations can be completed by the pulley before it stopped due to slipping or cable entanglement or any other problem.

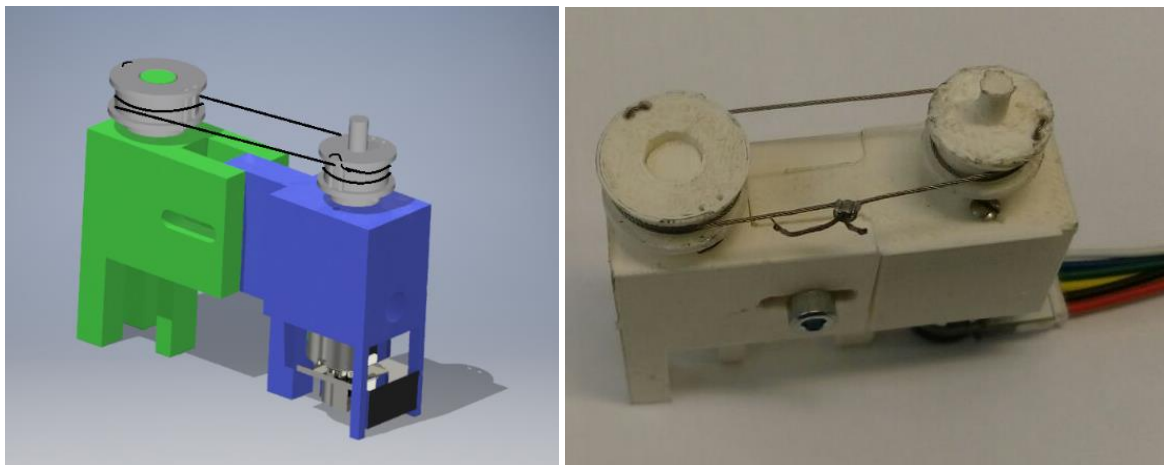


Figure 61: Test Setup for Cable Connections

Results: The driven pulley was able to rotate with the driving pulley after a small initial slip. This slip happened in both the directions and increasing the tension in the cable only decreased the slip but the tiny slip was still present.

After moving the pulley through around one and a half ($360+180$ deg.) rotation, the cable would not move further as the looping of the cable though the pulley holes at the top (cable attachment to pulley) prevented the pulley from turning more. A similar result was seen in the opposite direction, however in the opposite direction the slip was a bit more and the number of rotations were around one and quarter ($360+90$ deg.).

Discussion: It is seen that the setup was able to demonstrate that the pulley system with cables can rotate 180 degrees, however there is still the problem of slip which does not go away from the system even if the cable is pulled tight.

The movement of the pulley is not the same in both the directions as the pulling of the cable in one direction causes the cable to slack in the other direction and this causes a larger slip in the reverse direction. However, the pulley is still able to complete more than 1 revolution in both directions.

Conclusion: The range of motion of the pulley is sufficient to achieve movement range of 150-180 degrees, even with slippage.

Experiment 3: Determination spring constant (k) of springs from workshop and selection of spring

Introduction: The calculations from Section 3.2.4 indicated that the spring to be used had to have a k value of 2.5N/mm, hence we needed to find a spring with a similar k value.

Methods and Materials: Initially 7 springs were chosen, however 2 of the 7 springs had the difference between their undeformed lengths and deformed lengths less than 6.5mm (less than the maximum deformation needed) and hence were discarded (Fig.62). The springs were put inside the brass housing and the steel support. The length of this system undeformed and after deformation was measured (Fig.63). The force was measured using a pull-push gauge Model ALF-50. With the force and the difference in the lengths of the spring after and before deformation, the k value can be obtained. The springs with different k values were inserted in the Control Box to test for the push back of the middle rod manually and by motor to find out the best spring to use.

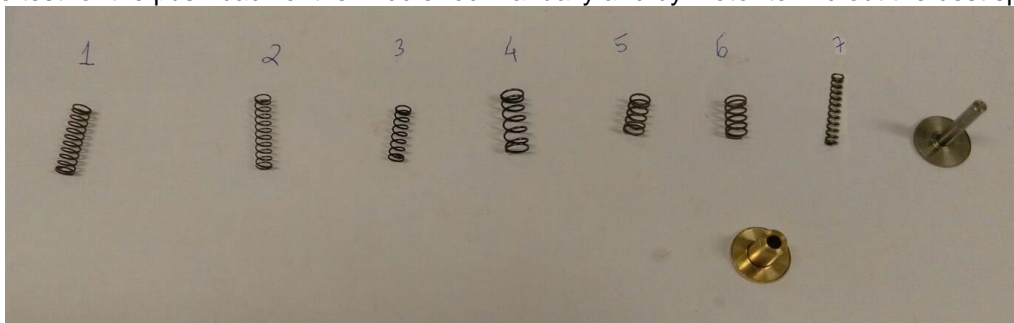


Figure 62: Springs from Workshop



Figure 63: Test Setup

Results: The Table 28 shows the spring dimensions and k value.

Spring number →	1	2	3	4	5
Undeformed length experiment	27.12mm	29.30mm	24.15mm	24.90mm	27.5mm
Deformed length experiment	15.50mm	14.96mm	14.36mm	14.69mm	17.2mm
Force registered on push pull gauge	7N	6N	9N	16N	30N
K	0.6N/mm	0.41N/mm	0.91N/mm	1.56N/mm	2.91N/mm
Free length	17mm	18.2mm	13.41mm	15.22mm	18mm
Deformed length	4.88mm	4.50mm	3.45mm	3.66mm	7.8mm
Outer diameter	4.55mm	4.12mm	4.05mm	6.04mm	4.12mm
Inner diameter	3.63mm	3.41mm	3.22mm	5.01mm	3.2mm
Thickness	0.4mm	0.31mm	0.4mm	0.45mm	0.6mm

Table 28: Spring Values

Discussion: Choosing a spring from the list was by trial and error, once the spring was fitted inside the Control Box, the middle rod translation mechanism needed to be pushed back to check if it was possible to push it back. Apart from that, the middle rod translation mechanism was also activated by using the motor to check if the motor would cause the spring to be compressed.

Conclusion: Spring 5 was selected to be used in the Control Box, as it would cause the spring to be pushed back the least when the motor was activated and the manual push back also did not need a lot of force.

Experiment 4: Translating the movement speed of pitch and yaw of the SATA instrument tip to SATA instrument tube rotation speed

Introduction: The speed needed for the gripper to pitch, yaw and rotate are mentioned in the requirements (Section 2) in terms of the instrument tip movements, however they need to be converted to SATA instrument cylinder rotation speed, so that the dc motors used in the Control Box to turn the CBC rods can be tested for the speed.

Methods and Materials: It is seen that the range of the pitch and yaw of the handheld SATA instrument is 120 degrees, which corresponds to a rotation of 180 degrees of the cylinders. The speed of pitch and yaw in literature is given as 0.5 rad/s (28.64 deg/s). Hence to cover the pitch and yaw of the SATA instrument (120 degrees) it will take around 4.1 seconds. Hence, the rotation of the SATA cylinders (180 deg) should take 4.1 seconds, giving a speed of 43.9 deg/s (0.76 rad/s) for the rotation of the SATA cylinders for pitch and yaw. The rotation speed of the instrument should remain the same as mentioned in the literature as the instrument tip is rotated by the innermost cylinder of the SATA instrument (3 or 4 rad/s) (171.88 deg/s or 229 deg/s).

Results: The speeds of middle, outer and innermost cylinder of the SATA instrument in relation to the pitch, yaw and rotation of the gripper tip were found (Table 29):

Cylinder	Speed of Instrument tip	Range of movement of Instrument tip	Range of Cylinders	Speed of Cylinders
Middle (pitch)	0.5 rad/s	120 deg	180 deg	0.76 rad/s
Outer (yaw)	0.5 rad/s	120 deg	180 deg	0.76 rad/s
Inner (rotation)	3-4 rad/s	180 deg	180 deg	3-4 rad/s

Table 29: Speed Conversion Table

Discussion: The speeds of the rotation of the instrument tip from literature were converted to the SATA instrument cylinder rotation speeds. However, it is important to note that the measurements of the instrument movement range of the SATA Instrument were done physically and hence the measurements are approximate values. It can be that the range of the instrument tip is a value between 121deg. or 119 deg. instead of 120 deg. These values of rotation speeds obtained will be used to check if the requirements of the speed of instrument movement have been met by using the motors.

Conclusion: The speeds of Pitch, Yaw and Rotation of the SATA instrument movement at the gripper were converted to the cylinder rotations of the SATA instrument.

Experiment 5: Timing belts and timing pulley selection

Introduction: Since the size of the timing belts and pulleys were too small it was difficult to find these from online stores. Hence it was decided that we would make our own timing belts and pulleys for the application.

Methods and Materials: Fix the timing belt with a certain circumference and the number of teeth, obtained by calculating the center distance between the pulleys and obtaining the circumference of the timing belt. The number of teeth for the circumference was obtained by trial and error, by checking the number of teeth that can fit in the circumference. The distance between the teeth was varied, until one set of motor pulley and the timing belt could mesh (Fig.64). The other timing pulleys were designed trying to keep the same diameters and changing the number of teeth, to match one of the printed belts. When a match was found the number of teeth was noted.



Figure 64: Timing Pulleys and Belts Prototyped

Results:

Outer timing belt circumference =96mm and number of teeth=34.

Middle timing belt circumference =91mm and number of teeth=33.

Inner timing belt circumference =85mm and number of teeth=32.

Diameter of the timing pulleys	Number of teeth tested	'Number of teeth' matching with timing belt
Motor pulley 10mm	12,13,14,15,16	14
Inner rod pulley 13mm	14,15,16,17,18	17
Middle rod pulley 14mm	17,18,19,20,21	18
Outer rod pulley 19mm	19,20,21,22,23	23

Table 30: Timing Pulley and Belt Selection



Figure 65: Timing Belt and Pulleys Selected

For the timing belt to be used (Fig.65):

The motor timing pulley of 10mm diameter needs to have 14 teeth.

The motor timing pulley of 13mm diameter needs to have 17 teeth.

The motor timing pulley of 14mm diameter needs to have 18 teeth.

The motor timing pulley of 19mm diameter needs to have 23 teeth.

Discussion: The timing belts were made by trial and error. The design of the timing belt and the pulley was not perfect and this can be further improved by using proper timing belts and pulleys.

Conclusion: The timing belts and pulleys diameters and teeth were obtained.

Experiment 6: Timing belts force test

Introduction: The timing belts should be able to hold the tension in the belts without breakage.

Methods and Materials: Using a pull-push gauge Model ANF-50 to pull the cable from one end and hold the other end (Fig.66). Note the force at which the belt breaks.



Figure 66: Setup for timing belt force test

Results: The timing belt broke at a force of = 98 N

Discussion: The forces in the timing belt need to be able to handle the torque of the motors. This force is around 50N, it is seen that the timing belt can hold more than the needed force.

Conclusion: The timing belt can be used in the system without breakage.

Appendix H

Design of cable pulley system

For the cable attachment system a small design process was carried out. This involved brainstorming solutions or ideas to the problem of cable attachment. Which provided a few options for the cable attachment, as the pulleys were small in size this limited the mechanisms that could be used to attach the cable.

Three solutions were selected from a solution list and prototyped in the 3-D printer (Fig.67, Fig.68, Fig.69). It was noticed that 2 of these options needed a screw to hold the cables in place (Fig.67, Fig.68). While one relied on the friction and the curve of the cable to hold it in place. The use of screws would provide a better hold for the cables but after testing the concepts it was found that even concept 3 without the screw was able to hold the cable with sufficient strength (Fig.69, Fig.70).

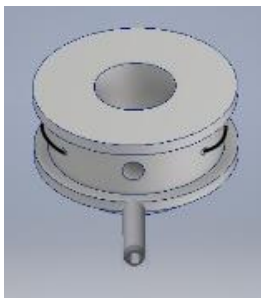


Figure 67: Concept 1

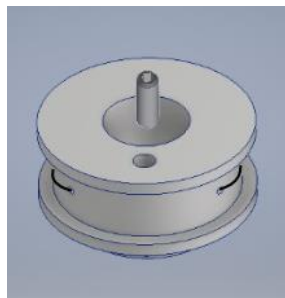


Figure 68: Concept 2

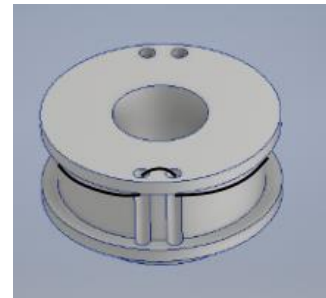


Figure 69: Concept 3

As it looped the cable and did not use any screws to hold the cables in place. The cables were held in place by the steep angle from the cable passing through the 2 holes. It was decided that this attachment system would be used for the cable system as it was simple.



Figure 70: Pulley with Cable Loop Holes

The cables were held together on the open ends by means of a bead (Fig.71), which after passing the wires through it was pressed by means of a pliers to crush the metal and secure the open ends of the cable. This was also tested to ensure that the cables will not slip through if pulled.



Figure 71: Beads for Cable Attachment

There were 2 methods by which the cables can be passed though the beads:

Method 1: Entry through the same side hole and exiting together through the other end.

Method 2: Entry through the opposite side holes and exiting separate through the other ends.

Experiment were carried out to find out which of the 2 attachment methods would be suitable to hold the open ends of the cable together (Appendix G- Experiment 1).

The results showed that method 2 was superior in terms of holding higher forces, however, it was decided to use method 1 as the joining of the 2 cables in this manner was smoother and did not interfere with the components in the Control Box. The maximum force that was calculated in the cables by using the highest torque motor i.e.41rpm with 0.254Nm:

Since the outer rod has a larger diameter pulley ($r = 9.5$) the torque is the highest at this pulley. The torque calculated at the outer end by using 41rpm motor is $T = 0.465Nm$.

$$T = F * r$$
$$0.465 = F * 9.5$$

Hence the $F = 48.9N$

The beads in method 1 can hold a maximum of 50N if the length of the bead is around 3mm. Hence the force can be handled by the bead.

Therefore we use the method 1 to secure the open ends of the cable.

Design of timing pulley and belt system

The design of the timing pulley and belt was done by lasercutting the teeth of the timing pulley and 3-D printing the belt. The manner in which the timing pulleys would be attached to the system was also designed. The timing pulley was made of 3 components (Fig.72):

- a. Timing pulley teeth
- b. Timing pulley base
- c. Timing pulley cover

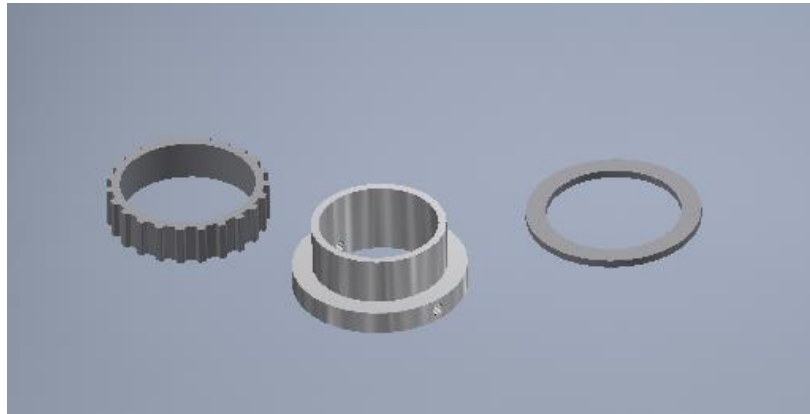


Figure 72: Timing Pulley Teeth, Timing pulley base, Timing pulley cover (Left to Right)

The concept idea was first prototyped by 3-D printing using PLA and lasercutting using acrylic material. The prototype is shown in Fig.73.



Figure 73: Timing Pulley Prototype Design

The timing pulley teeth are lasercut using aluminum and fitted on the timing pulley by using resin glue. A cover is then placed on top of the modified pulley to complete the timing pulley. The cover prevents the belt from coming off the timing pulley (Fig.74).



Figure 74: Completed Timing Pulley

The CAD models for the timing pulley and belt were obtained by looking at existing pulleys and using trapezoidal tooth profile. The pulley sizes were obtained from existing timing pulleys online and the sizes of the belts were determined by trial and error (Appendix G- Experiment 5). The completed timing pulleys were tested if the belt and the timing pulley fit.

Appendix I

Assembly of the Prototype

The Assembly of the prototype (Control Box and the Z Translation Mechanism (ZTM)) has to be done in a certain manner so that all the components can be fitted in it.

The assembly is divided into 2 parts:

1. Assembly of the Control Box
2. Assembly of the ZTM.

1. Control Box Assembly:

The assembly of the Control Box is made up of 2 sub- assemblies i.e.steps 1 to 9 (Fig.75) and steps 10 to 21 (Fig.76), which have to be assembled together to obtain the final assembly.

Note: Make sure that the 2 bolts at the front of the Control Box, needed to attach the Control Box to the slides are placed in the Control Box before starting the assembly of the Control Box.

1. Mount the motors(33,41) in the motor brackets(34 with 35,42 with 43). The motor is held in position by using tiny screws that fit on the motor head.
2. Mount the inner screw of upper motor (33), so that it can swivel over the screw. Using this swiveling action mount the motor assembly of lower motor (41) on the back box part (19). Now it should also be possible to mount the pulley support (66) and the motor pulley to this motor (41).
3. Fix the remaining screw of the upper motor (33) in the Control Box and fix the pulley and the pulley support (65) in the Control Box. Now the 2 motors (33,41) are in place with the pulleys and the pulley holders. Test to make sure the pulley rotate freely and are not obstructed by the pulley holder or the motor screws.
4. On the upper Control Box part (18), mount the four supports (26) and two sliding rods (60) in the upper Control Box part (18).
5. Insert the middle rod translation motor (59) in the motor box (27) and fix it in place by using the two screws on its head.
6. Create the motor support assembly by fixing together the two L shaped parts (28), which hold the motor in place and guide the translation movement of the middle rod.
7. Place the spring (24) and the spring guide (25) in position in the upper Control Box part.
8. Slide the motor box (27) with the motor (59) in through the sliding rods (60) attached to the upper Control Box part (18) so that the spring (24) can be pushed in and the spring mechanism (24,25) will push it back .
9. Mount the L shaped part assembly (28) in place over the four supports (26) and sliding rods (60). Now the motor box (27) should be pushing on the L shaped assembly (28) due to the push from the spring assembly (24,25).

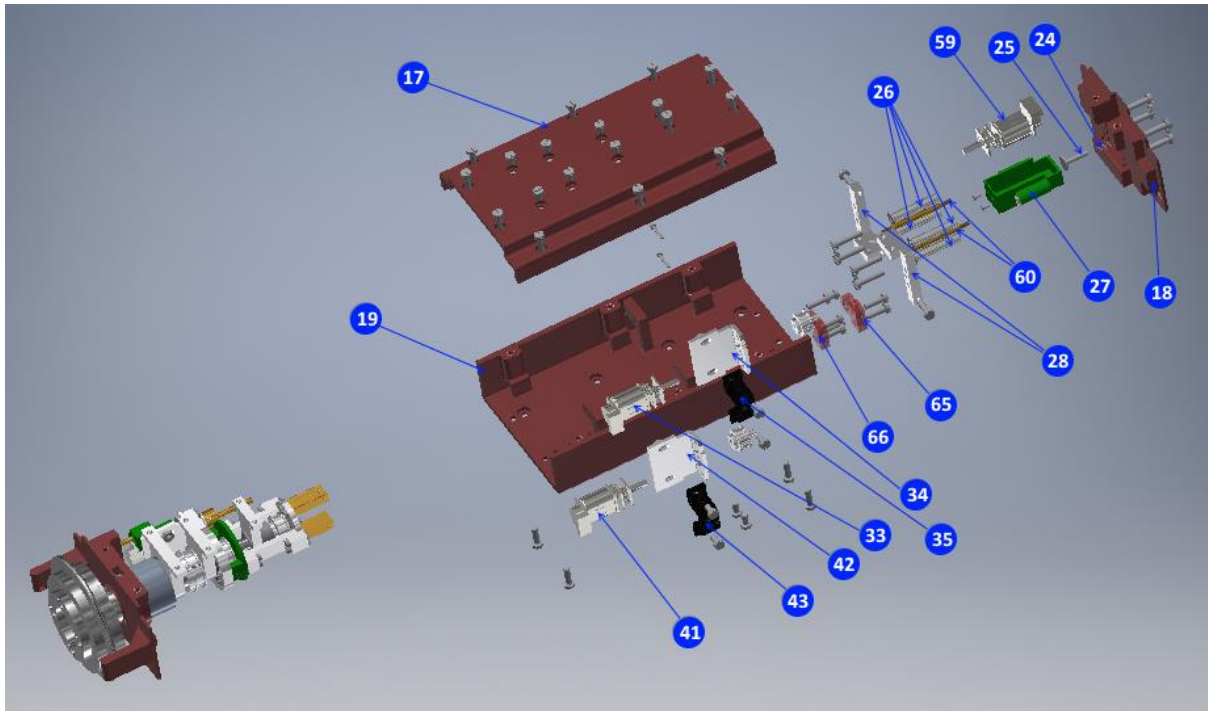


Figure 75: Control Box Exploded View

10. On the lower Control Box part (20), combine the CBC coupling parts (21,22,23) together so that it can be inserted through the lower Control Box part (20) hole. Then attach the holding piece of the CBC (67) along with the bushing (45). This secures the outer rod (21) and the middle rod (22) of the CBC.
11. Mount the outer rod holder (44) with the in it bushing on the Outer CBC, after this mount the outer rod pulley (40).
12. Fix the middle rod motor (49) to the motor bracket (50) with motor holder (47) along with the sliding guide rods (46).
13. Create the sliding middle rod assembly by assembling the middle rod pulley (37) sandwiched between the motor-linear coupler part (52) and circular disk (36). The middle rod pulley is prevented from being crushed by adding the two spacers (53) between the 2 sandwiching parts. Mount the support pillars (57) on the circular disk along with the nut plate (29) with the tiny leadscrew (61) in it.
14. To this sliding middle rod assembly add the previously created middle rod motor assembly (49,50,47,46) and add the middle rod pulley (51) and the translating rod (54).
15. Slide the completed assembly from the previous step over the middle CBC rod (22) after sliding the middle rod holder (48) with the bushing in it.
16. There is a gap between the support pillars(57) ends i.e. between the circular disk (36) and nut plate (29) . Mount the inner rod holder (55) in this gap, followed by the shaft holder (56) and the inner rod pulley (32) on the inner CBC rod (23).
17. Make sure that the sliding middle rod assembly step 15 has its sliding guide rods (46) sliding inside the holes in the lower Control Box part (20), created to guide it.
18. Mount the nuts on the backside of the back Control Box part (19) so that the lower Control Box part (20) and upper Control Box part (18) and the L shaped assembly part (28) are fixed in place.
19. Mount the Control Box on the Z Translation Mechanism by using nuts and bolts on the back Control Box part (19) with the nuts inside the box and the bolts inserted from the outside underneath the sliders (5).
20. The wires of the motors should be routed through the cable routing route provided in the back Control Box part (19).
21. Make sure that all the rod holders of the three CBC rods are facing upward and mount the upper Control Box cover (17) to fix them in place and close the Control Box.

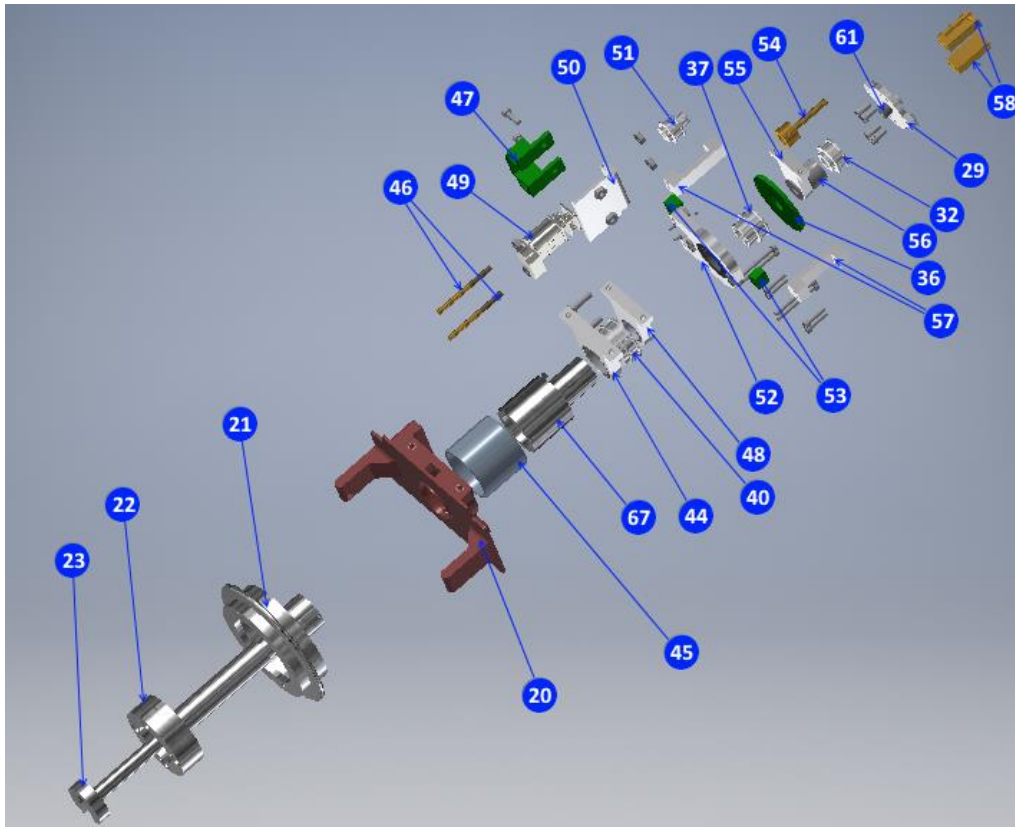


Figure 76: Control Box Semi Assembly Exploded View

2. ZTM Assembly (Fig.77):

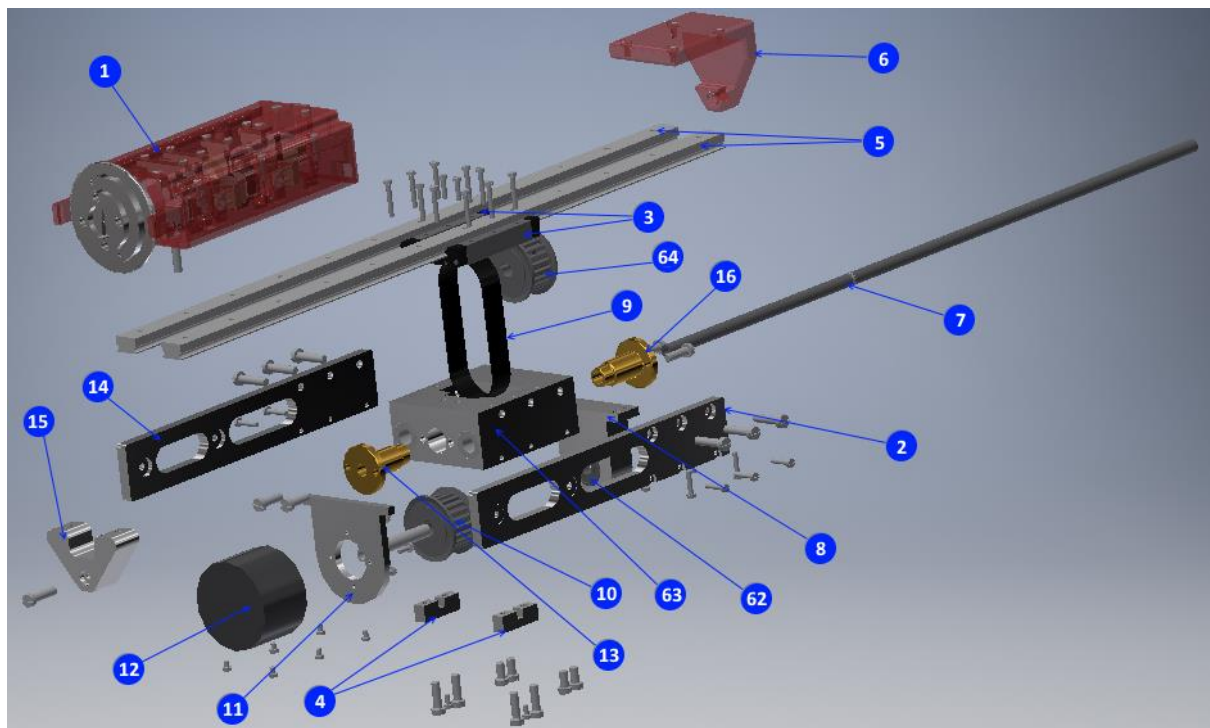


Figure 77: ZTM Exploded View

1. Mount the slide moving part (3) on the main block (63).By using bolts through the holes provided on the lower side of the main part.

2. Mount the side holders (14,2) on the main block (63) making sure that the bolts used are flush with the surface.
3. Mount the driven pulley (64) inside the gap provided in the main block (63) along with the belt (9)
4. Fix the side movement stoppers (16,13) in the holes provided on the main block (63) and fix them in place so that the driven pulley (64) does not move linear but only rotates.
5. Mount the leadscrew (7) inside the driven pulley (64) which has a threaded center, through the main part (63) and fix the leadscrew (7) by using the back end guide holder (6) on the back of its the leadscrew (7) end.
6. Mount the belt (9) over the driving pulley (10) and the driving pulley (10) over the motor shaft (12). The motor (12) is fixed in the main part (63) by using the motor plate (11) which sits on the lower portion of the main part (63) and is fixed to the main part (63) by means of two small blocks (4).
7. On the other end of the motor shaft, the support is provided by motor pulley shaft holder (8). There is a bearing (62) inside this part (8), which ensures that the rotation of the motor is not hindered. It also makes sure that the forces due to the tension in the belt will not cause the motor shaft to bend.
8. On this assembly of the Z Translation Mechanism and the Control Box (1) can be mounted and the front end guide holder can be attached to the slide fixed part (5), with its bolts mounted on the slide fixed part (5) from inside the Control Box (1).

Note: Once this setup is completed the cables can be inserted in the pulley holes. The method of cable attachment/ wrapping of the cable over the pulley is done as shown in the Fig.78

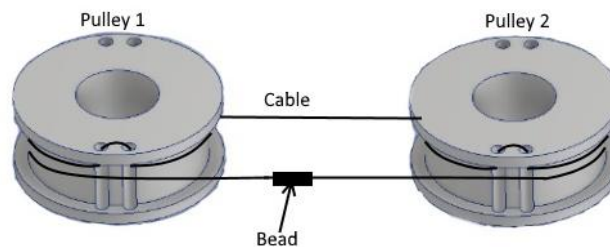


Figure 78: Cable Wrapping over Pulley

The cable is passed through the 2 holes and then wrapped around the back of the pulley. The 2 cable ends coming out of the 1st pulley are inserted in the same way on the 2nd pulley. The bead is used to fix the 2 open ends together.

Note: In the case of the timing belt and pulley, the timing belt needs to be fitted on the timing pulley of the motors before the assembly of the system is started. i.e. before step 2 of the Control Box assembly. Similarly the timing belt of the middle rod pulley has to be fitted on before the middle timing pulley assembly is started. i.e. before step 13 of the Control Box assembly.

Appendix J

Resolution of dc Motors used in the Control Box and ZTM need to be determined.

Control Box Motors

The resolution of the dc motors used in the Control Box are measured by using an encoder (consisting of a hall sensor and magnetic disk) and arduino microcontroller. The motor shaft is turned through 360 degrees manually (Fig.79) and the code measures the number of times the signal from the encoder is 1 or when there is a peak. When the number of counts for 1 complete rotation of the dc motor shaft is obtained, we can calculate the how much the motor shaft will rotate for 1 step of the encoder. We can also calculate the number of counts for 1 rotation of the dc motor (without the gearbox). However, it is important to note that this measurement is not very accurate as there are errors due to moving the motor shaft manually through 360 degrees.

In another test for checking the error, the code directs the motor to stop rotating when the encoder reads 1000 steps. However, due to the motor inertia, the motor rotates a bit longer and the encoder counts a bit more than 1000 before stopping. This error would be decreased when there is load on the system as the inertia effects will be negligible compared to the forces on the timing pulley and belt.

The arduino code used is the same for all the dc motors tested:

```
//Rosnelo Fernandes
//Motor resolution and error test

#define encoder0PinA 2
#define encoder0PinB 4

#define ena 6 // PWM pin 6
#define in1 7
#define in2 8

volatile long encoder0Pos=0;
long newposition;
long oldposition = 0;
unsigned long newtime;
unsigned long oldtime = 0;
long vel;

void setup()
{
  pinMode(encoder0PinA, INPUT);
  digitalWrite(encoder0PinA, HIGH); // turn on pullup resistor
  pinMode(encoder0PinB, INPUT);
  digitalWrite(encoder0PinB, HIGH); // turn on pullup resistor
  attachInterrupt(0, doEncoder, RISING); // encoDER ON PIN 2
  Serial.begin (9600);
  // Serial.println("start");
  // Serial.print(" "); // a personal quirk

  pinMode(in1, OUTPUT);
  pinMode(in2, OUTPUT);
  pinMode(ena, OUTPUT);
}

void loop()
{
  newposition = encoder0Pos;
  //newtime = millis();
  //vel = (newposition-oldposition) * 1000 /(newtime-oldtime);
  //Serial.print ("speed = ");
  //Serial.println (vel);
  Serial.print(" ");
  Serial.print ("position = ");
```

```

int sensorValue = digitalRead(newposition);
Serial.println (encoder0Pos);
oldposition = newposition;
//oldtime = newtime;
delay(1);
analogWrite(ena,255); //set speed

if (newposition<=1000)// set time to stop/steps/count encoder
{
    digitalWrite(in1, HIGH);
    digitalWrite(in2, LOW);
}
else
{
    digitalWrite(in1, LOW);
    digitalWrite(in2, LOW);
}
}

void doEncoder()
{
    if (digitalRead(encoder0PinA) == 1) {
        encoder0Pos++;
    } else {
        encoder0Pos;
    }
}
}

```



Figure 79: Motor Marker for Rotation

The serial monitor of the arduino was used to read out the counts of the encoder. The plot of the data from the encoder can be also seen in the serial plot (Fig.80), but it is difficult to read. Hence the encoder count was read from the Arduino Serial monitor (Fig.81).

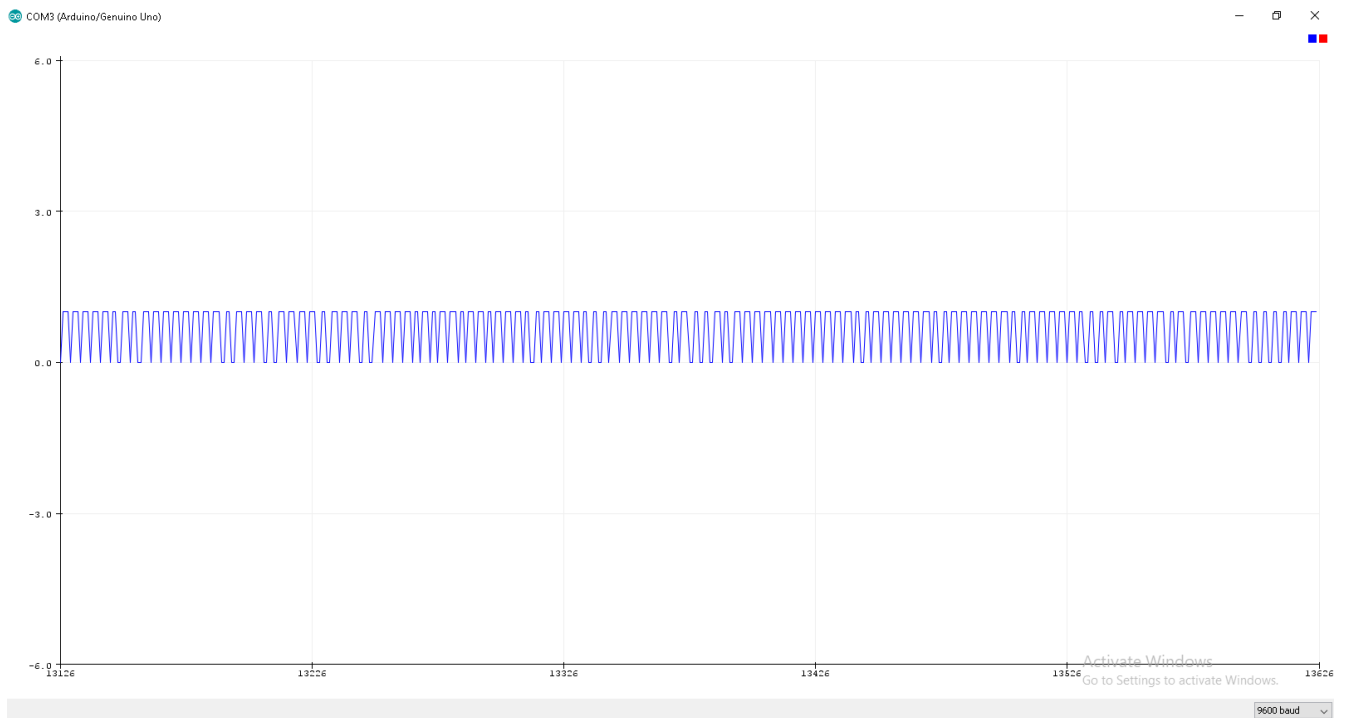


Figure 80: Encoder Step Plot in Serial Plotter

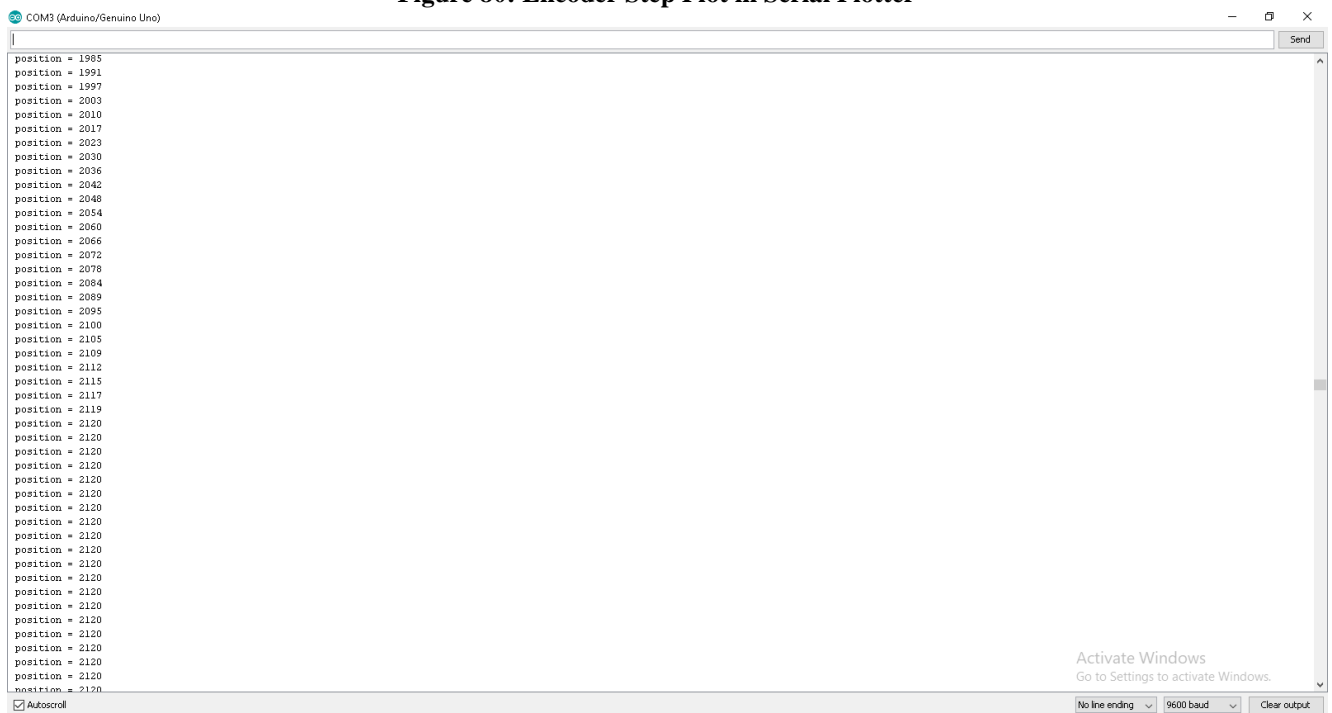


Figure 81: Encoder Step Count in Serial Monitor

The motors used in the Control Box are:

1. 1.1135 W power Motor, with Speed: 155 rpm, Torque: 0.0686 Nm with a gear-ratio of 100:1.
2. 1.0673 W power Motor, with Speed: 52 rpm, Torque: 0.196 Nm with a gear-ratio of 298:1.
3. 1.0519 W power Motor, with Speed: 41 rpm, Torque: 0.245 Nm with a gear-ratio of 380:1.

Table 31 provides the resolution of the encoder step and the error (extra counts).

Motor ↓	Encoder count for 1 rev of motor shaft (with gearbox)	Encoder count for 1 rev of motor shaft (no gearbox)	Relation between 1 count and degree(with and without gearbox)	Encoder count when stopped at 1000 counts	Extra counts when completely stopped
Speed : 155 rpm Torque : 0.0686Nm Gear ratio : 100:1	a.711 b.722 c.696 d.707 e.710 Average:709.2	7.09	50.7 degrees (without gearbox) 0.507 degrees (with gearbox)	a.1126 b.1127 c.1126 d.1128 e.1127 Average:1126.8	126.8
Speed : 52 rpm Torque : 0.196Nm Gear ratio : 298:1	a.2463 b.2511 c.2479 d.2456 e.2360 Average:2453.8	8.23	43.7 degrees (without gearbox) 0.146 degrees (with gearbox)	a.1166 b.1163 c.1164 d.1162 e.1164 Average:1163.8	163.8
Speed : 41 rpm Torque : 0.245Nm Gear ratio : 380:1	a.2092 b.2080 c.2097 d.2090 e.2071 Average:2086	5.4	65.4 degrees (without gearbox) 0.17 degrees (with gearbox)	a.1135 b.1135 c.1136 d.1136 e.1137 Average:1135.8	135.8

Table 31: Motor Resolution and Error

The number of counts per revolution of the motor shaft (with gearbox) are read out from the arduino serial monitor. Given the gear ratio, we can obtain the number of counts for the motor shaft (without gearbox) as:

$$count(without\ gearbox) = \frac{count(with\ gearbox)}{gear\ ratio}$$

Hence, for the first motor (155rpm),

$$count(without\ gearbox) = \frac{709.2}{100} = 7.09$$

The relation between 1 encoder count and the degrees the shaft moves can be obtained as:

$$1\ count(without\ gearbox) = \frac{360\ deg}{count(without\ gearbox)}$$

$$1\ count(with\ gearbox) = gear\ ratio * 1\ count(without\ gearbox)$$

Hence, for the first motor (155rpm),

$$1\ count(without\ gearbox) = \frac{360\ deg}{709.2} = 0.507\ deg/count$$

$$1\ count(with\ gearbox) = 100 * 0.507 = 50.7\ deg/count$$

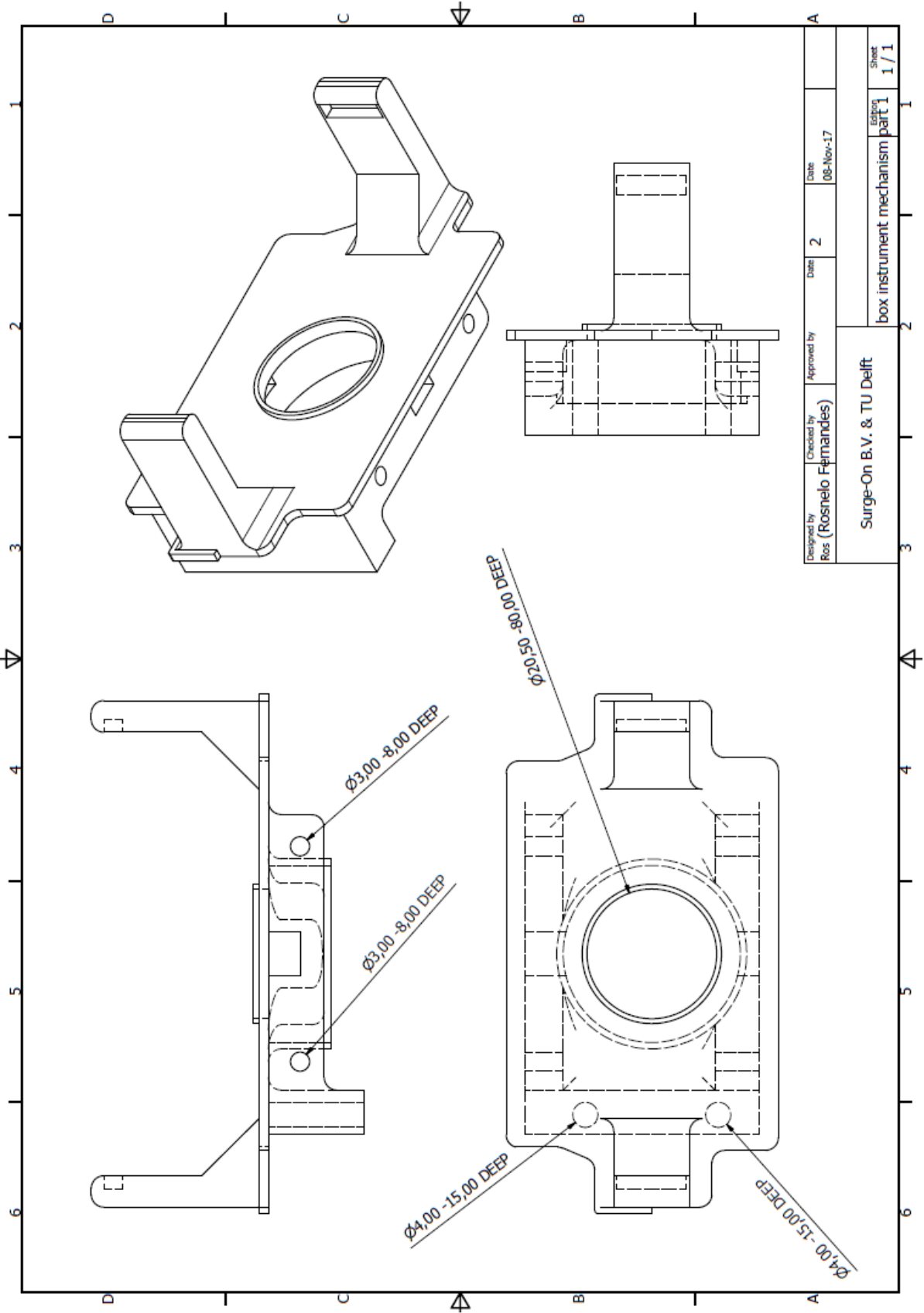
Since this motor is used for linear movement using a leadscrew with 0.5mm pitch, the smallest step that it can take is when the motor moves the shaft by 50.7deg, this would move the leadscrew by,

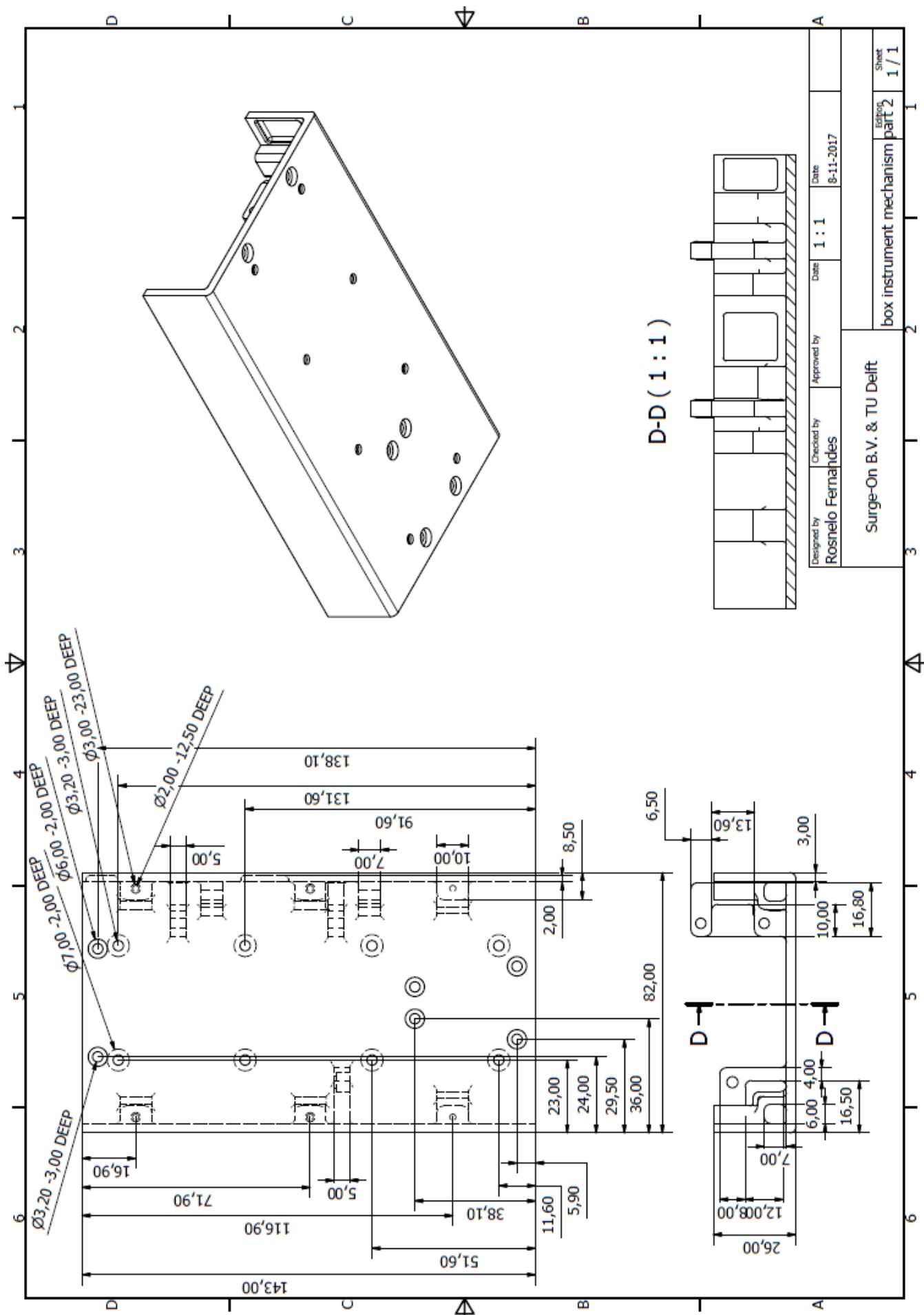
$$linear\ step = \frac{360}{0.5 * 50.7} = 0.07mm$$

Hence the smallest step that can be taken by the leadscrew is 0.07mm for every count of the encoder.

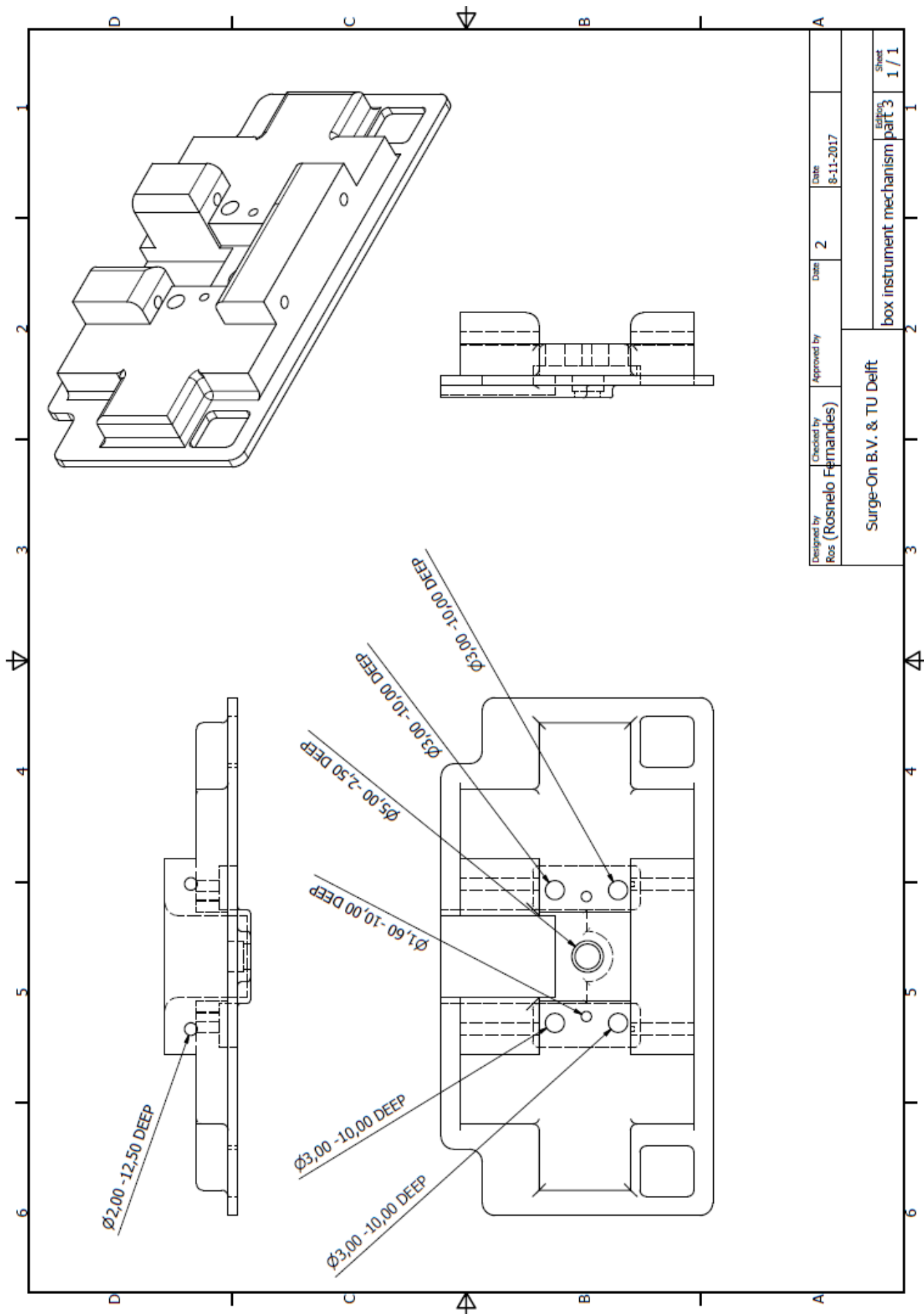
Appendix K

Control Box Drawings:

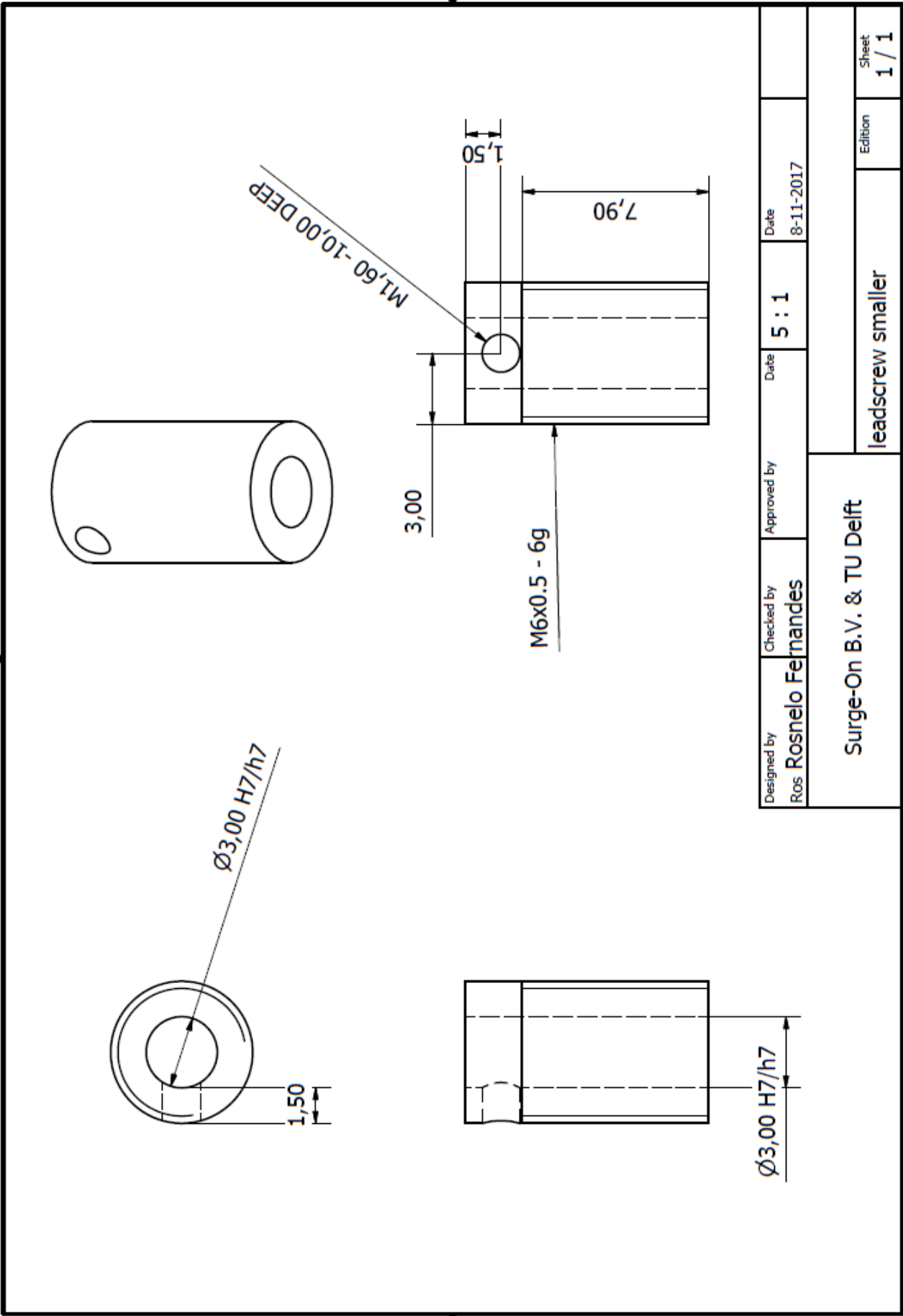


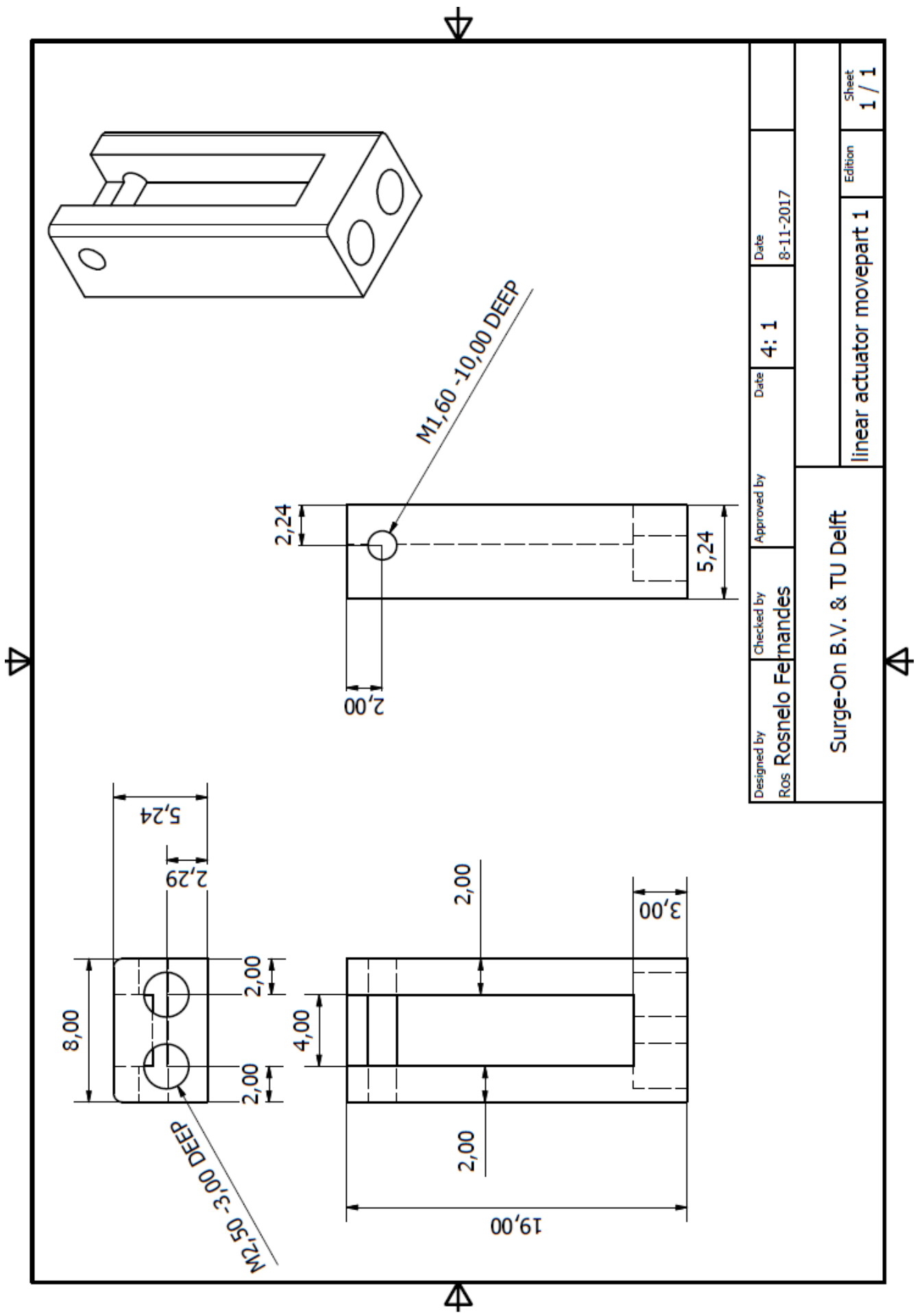


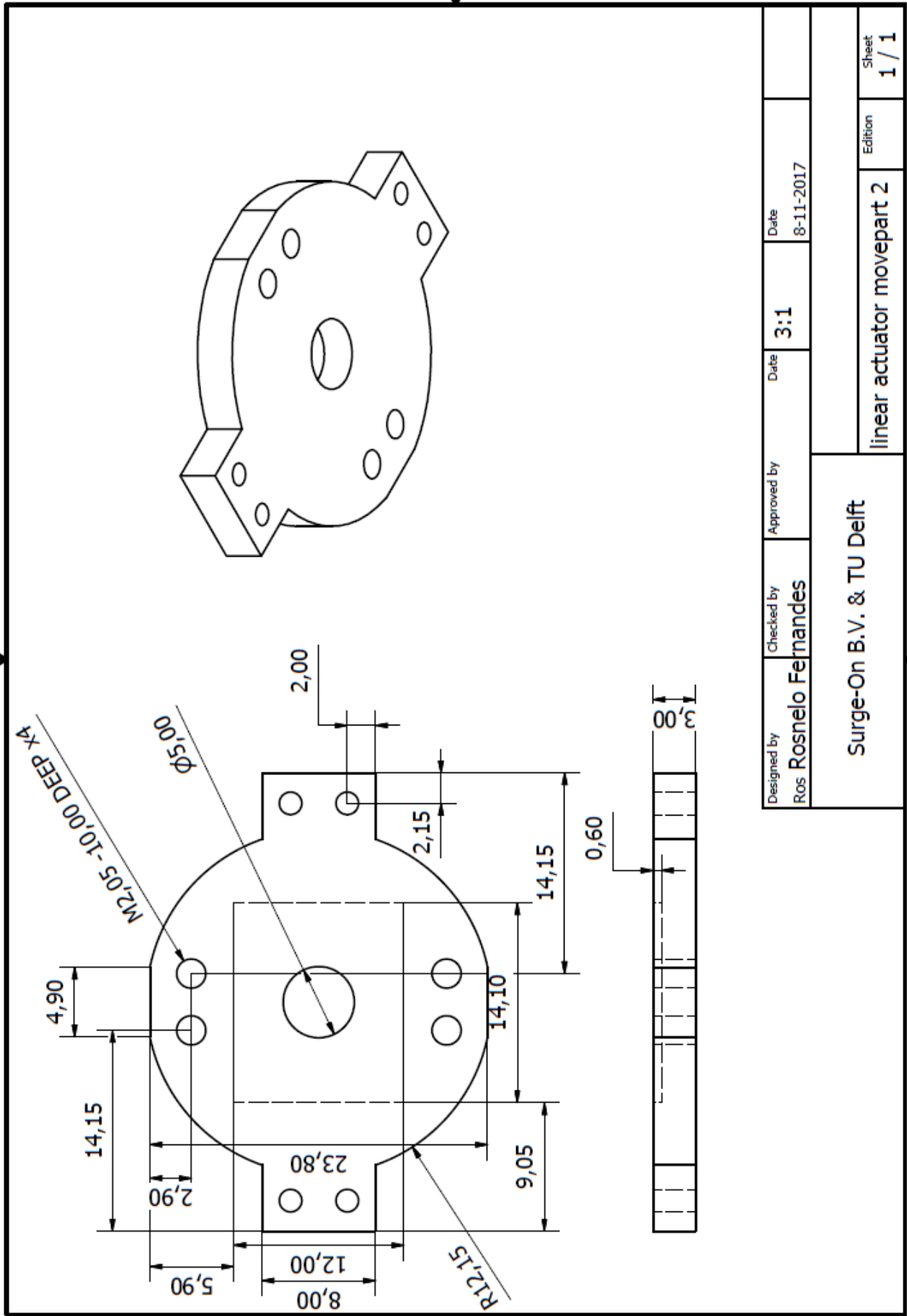
Designed by Rosnelo Fernandes	Checked by	Approved by	Date 8-11-2017	Sheet 1 / 1
box instrument mechanism part 2				
Surge-On B.V. & TU Delft				

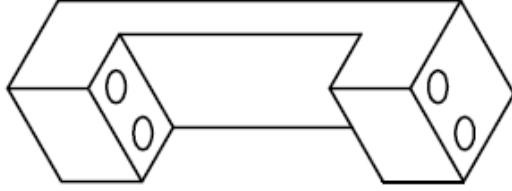
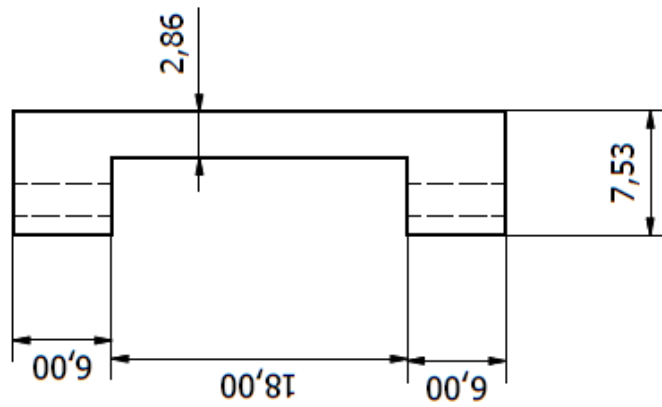
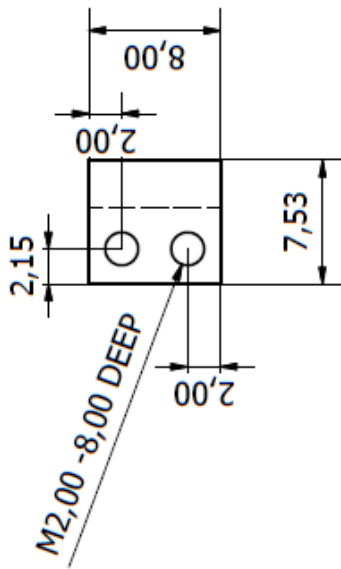


Designed by Ros (Rosnelo Fernandes)	Checked by	Approved by	Date 2	Date 8-11-2017	
Surge-On B.V. & TU Delft					
box instrument mechanism part 3					Sheet 1 / 1

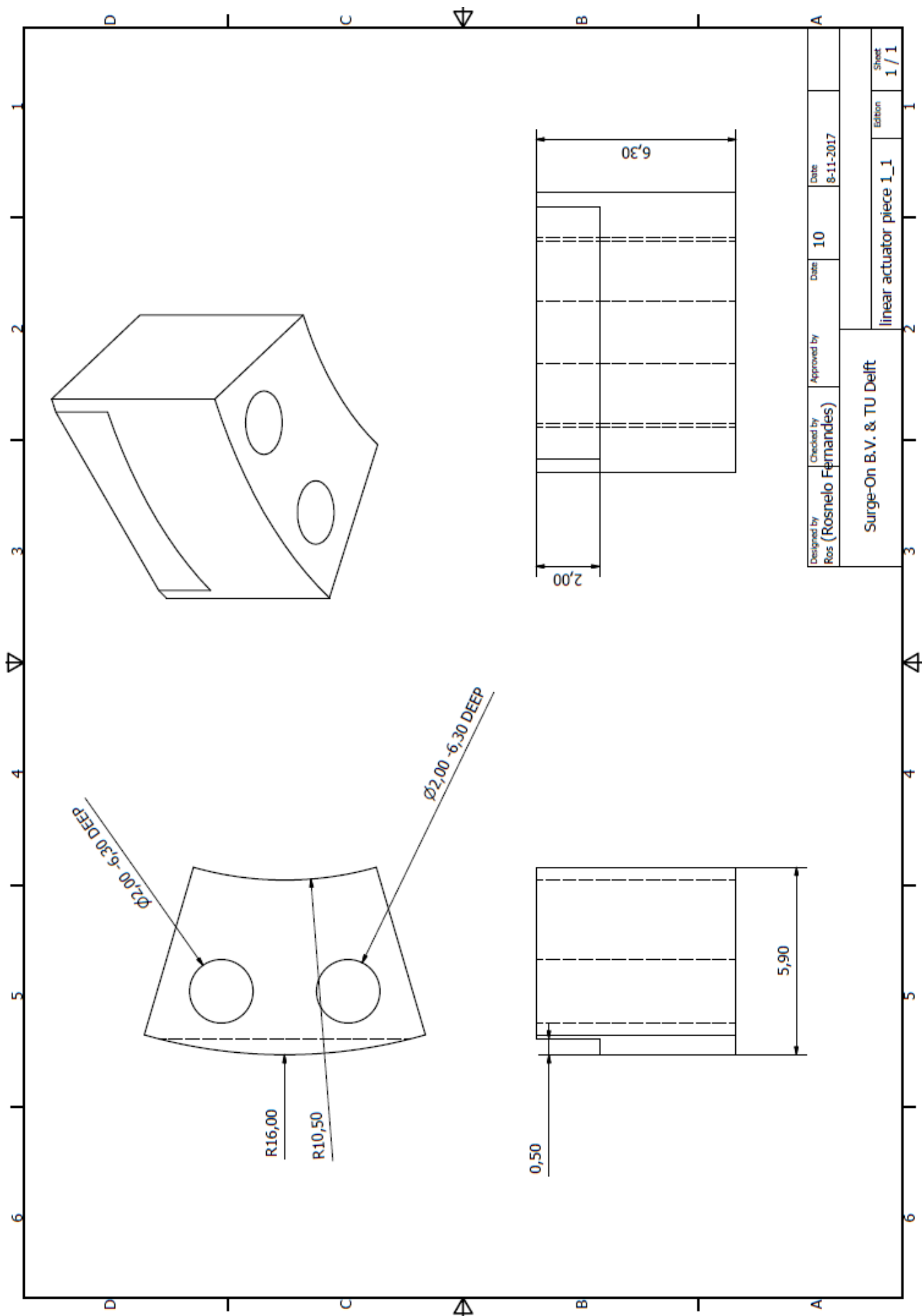


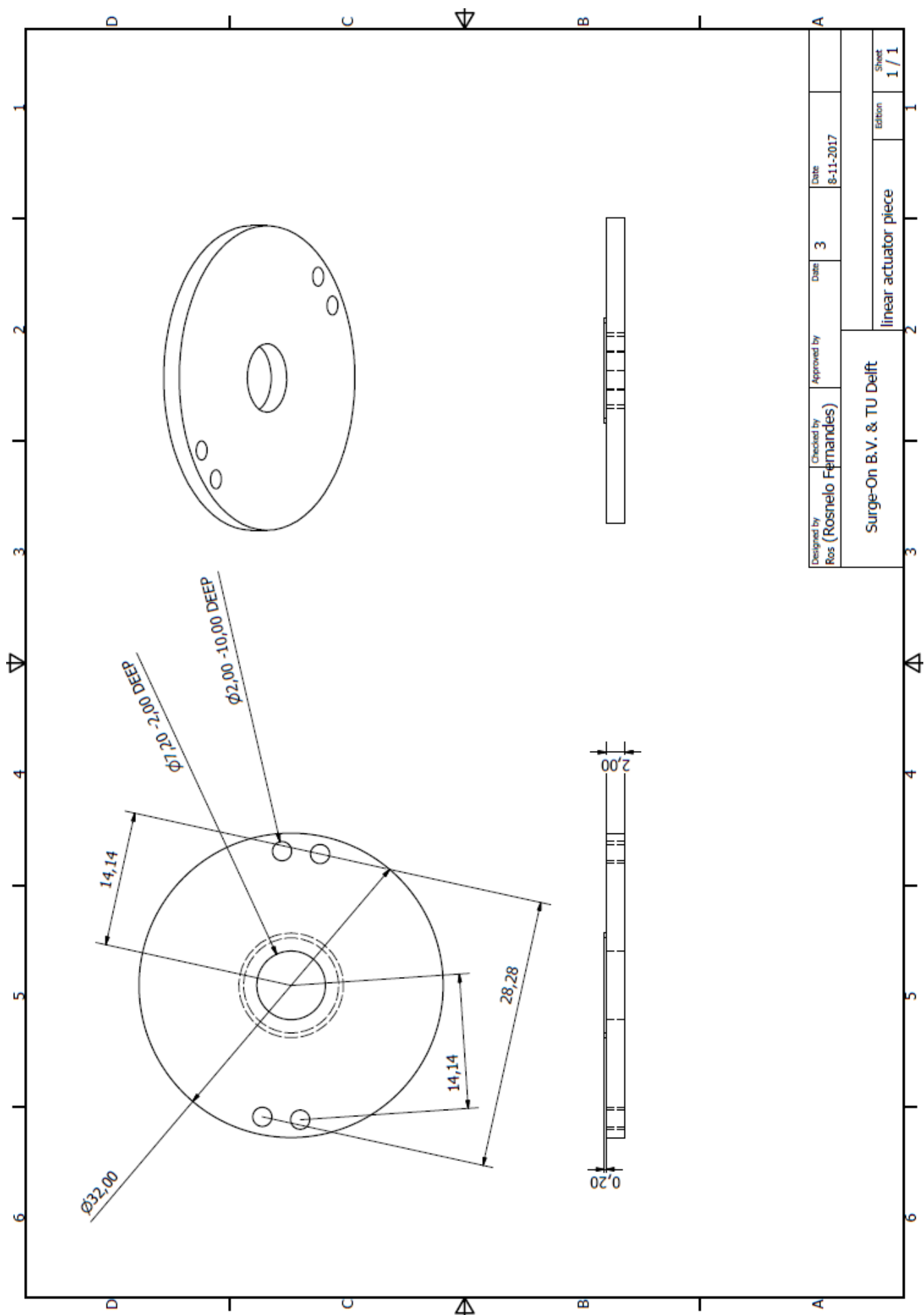


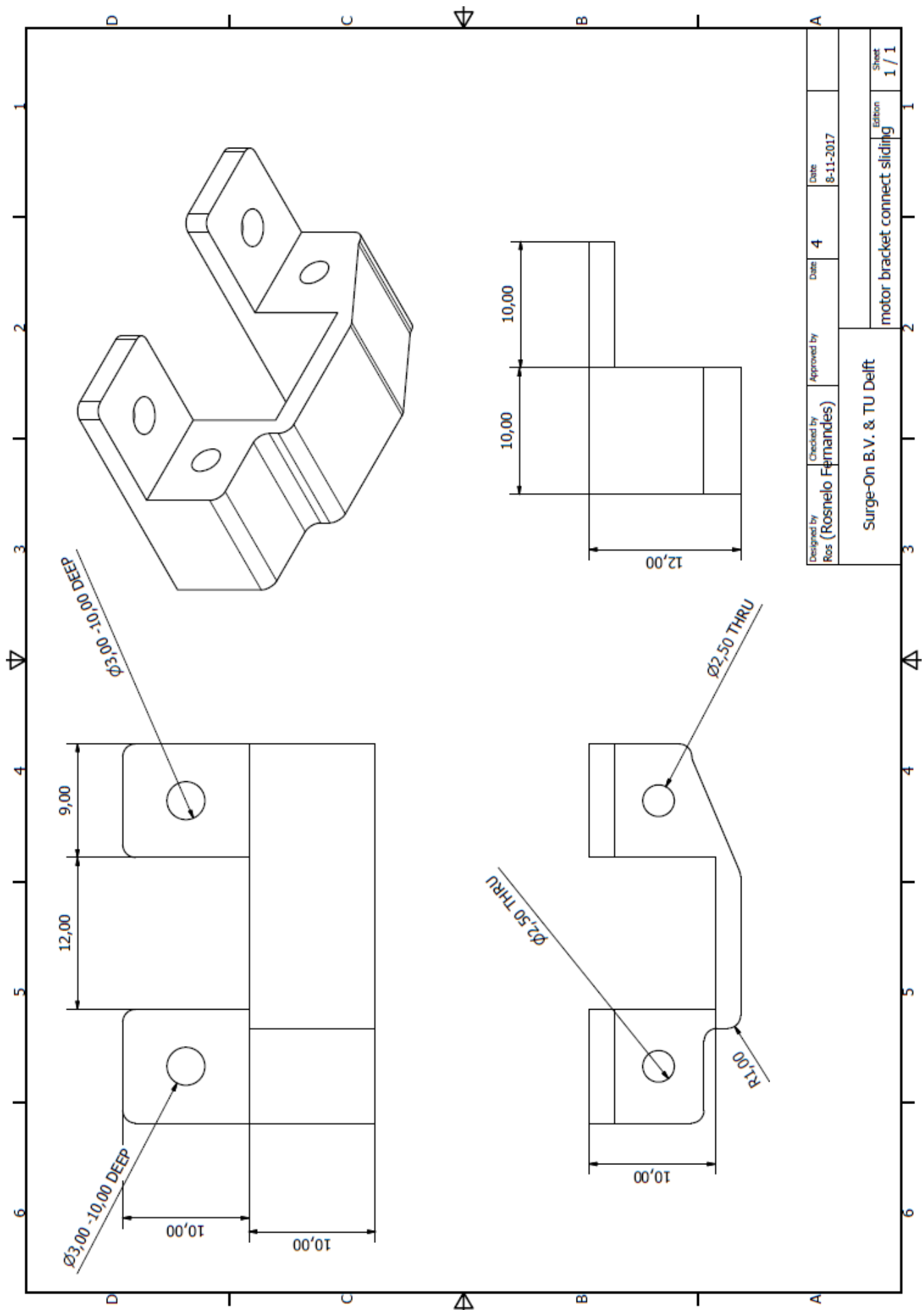


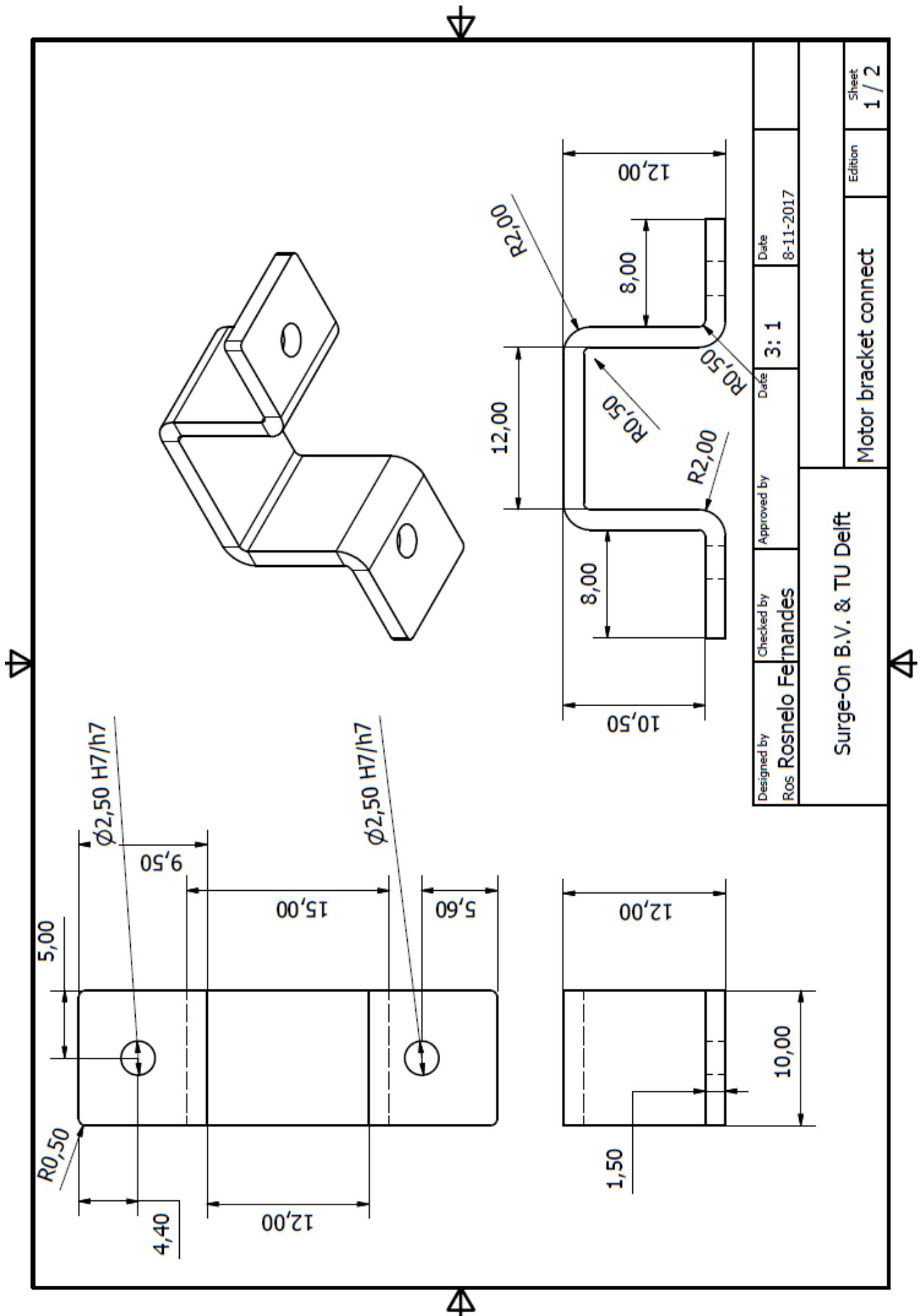


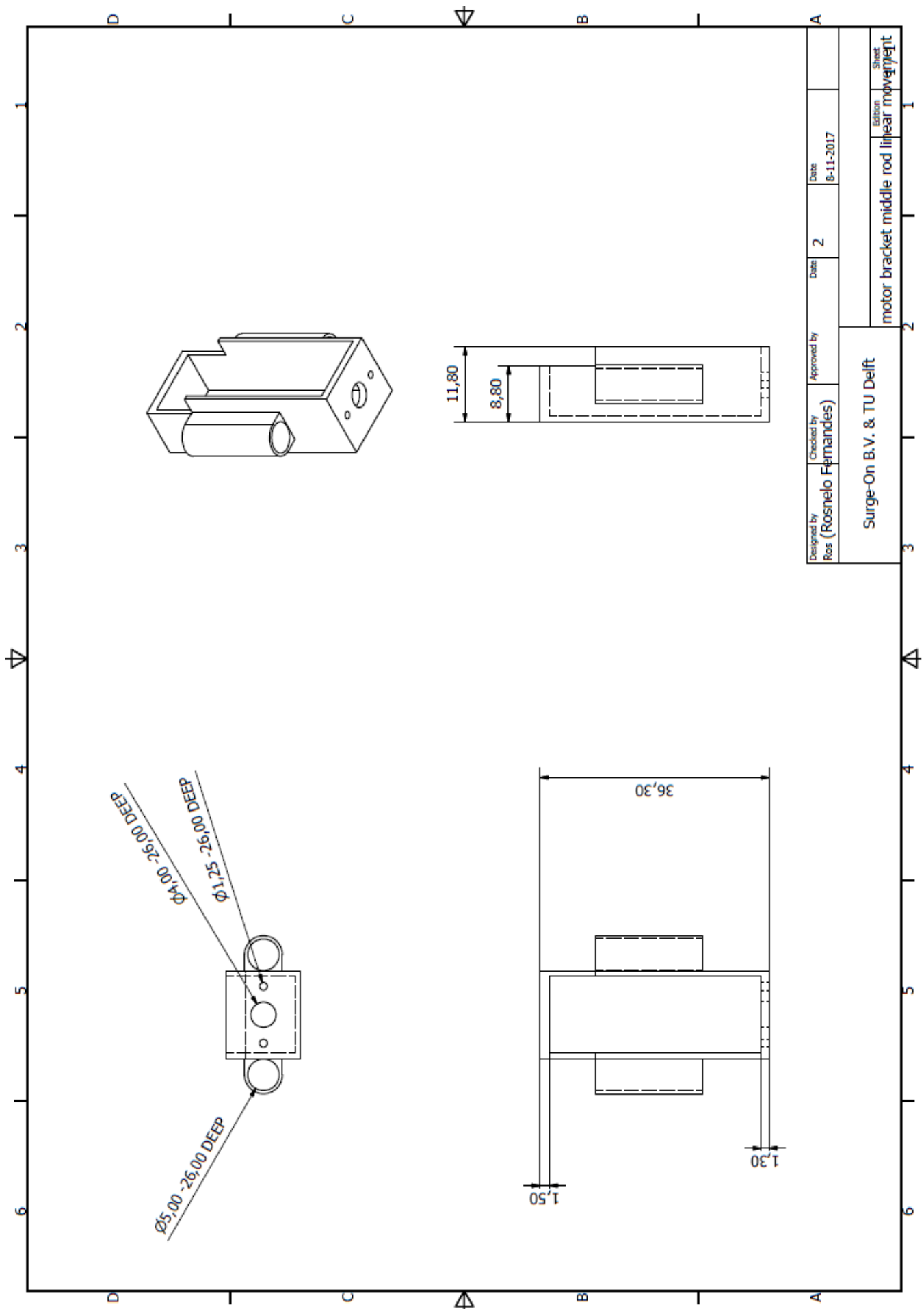
Designed by Ros Rosnelo Fernandes	Checked by	Approved by	Date	2.5 : 1	Date	8-11-2017
Surge-On B.V. & TU Delft						linear actuator movepart 3
						Sheet 1 / 1

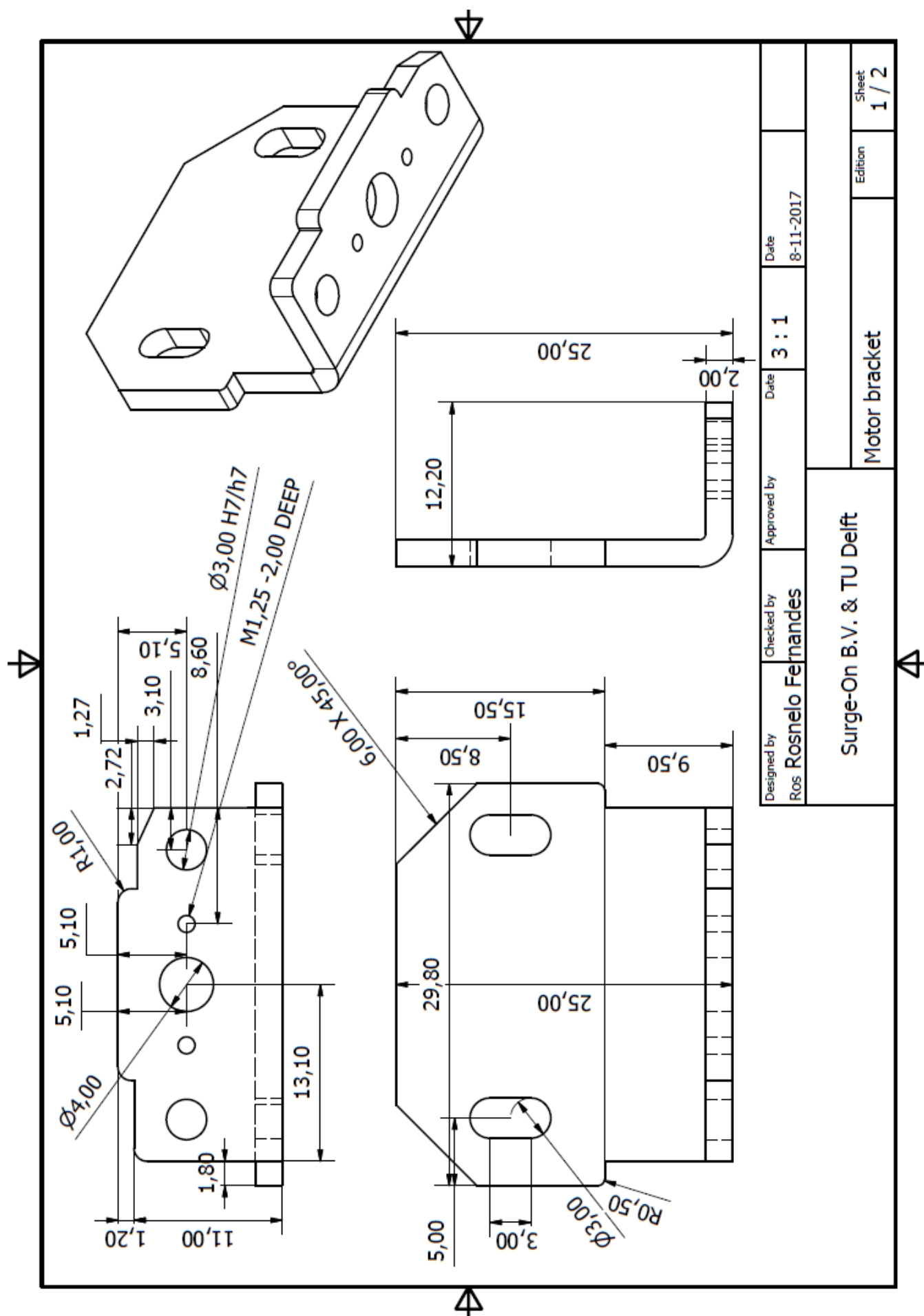


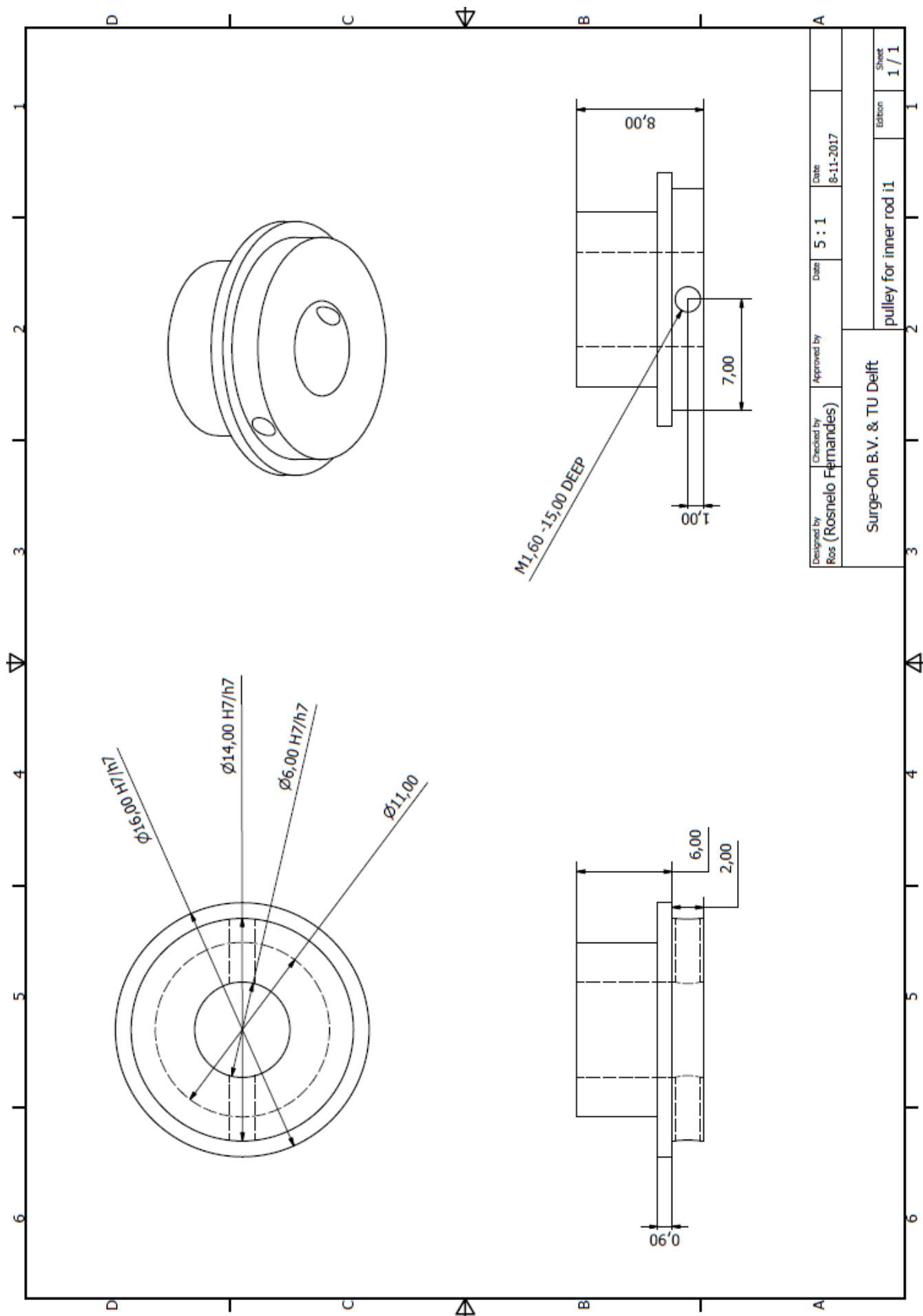


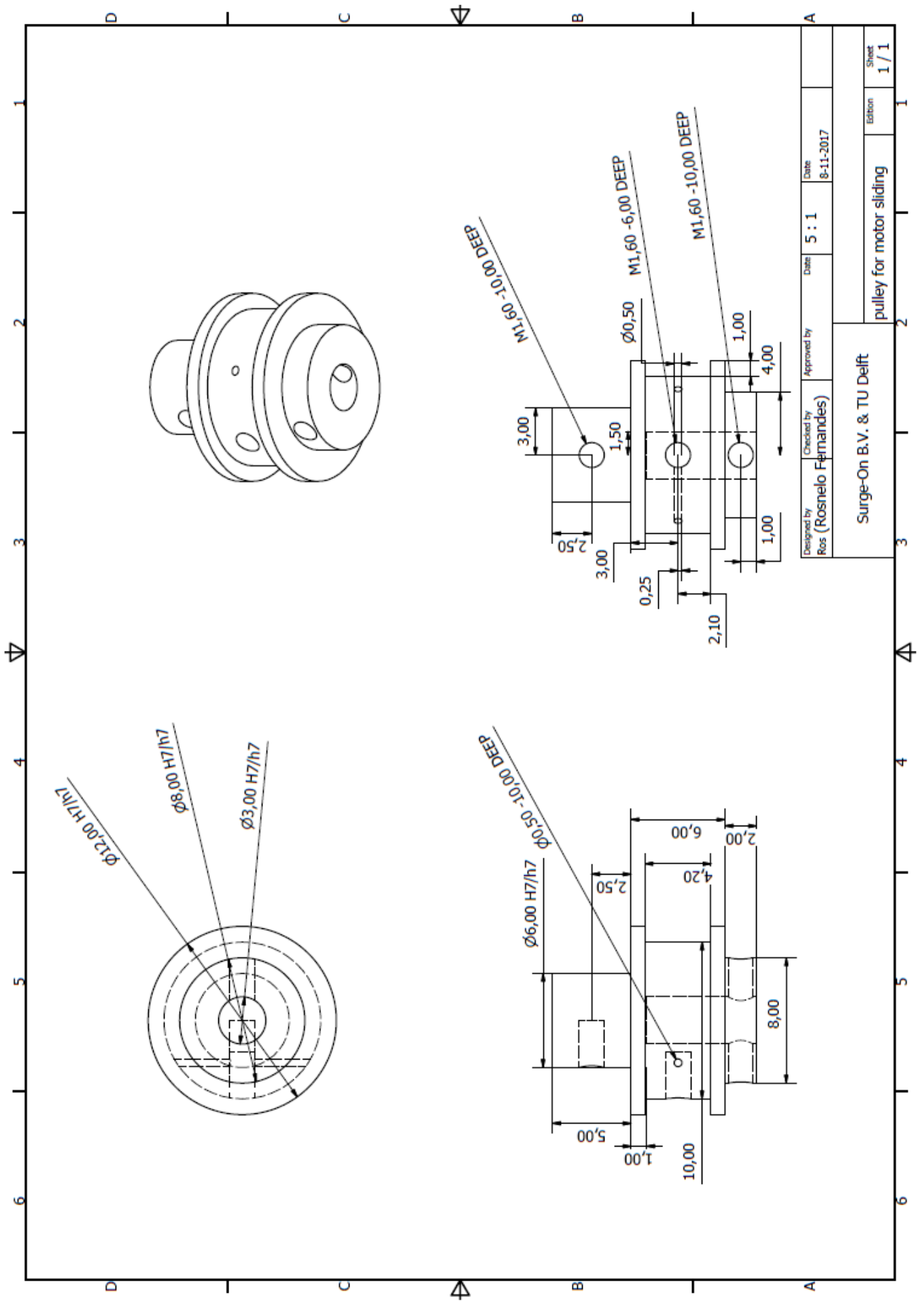


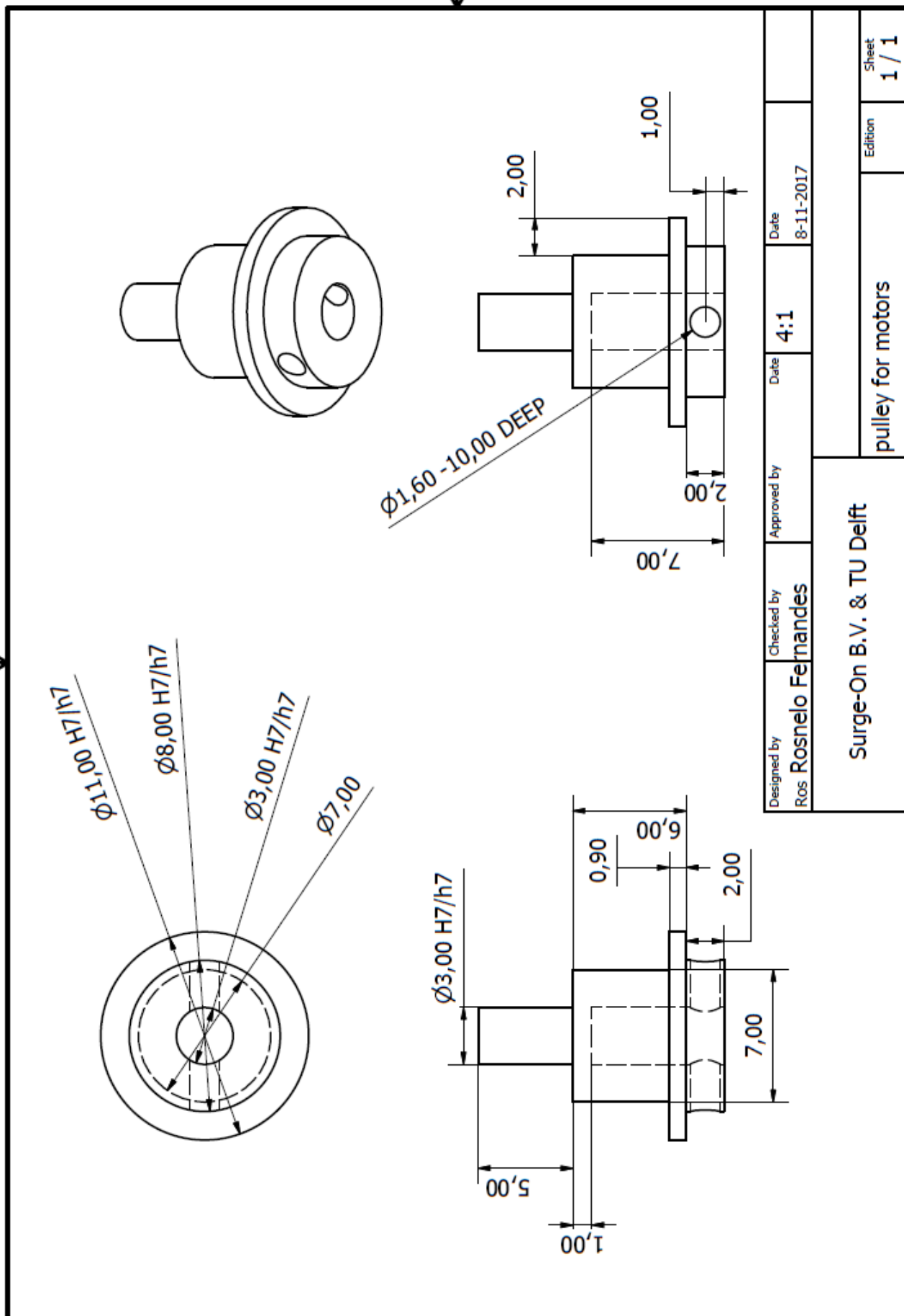


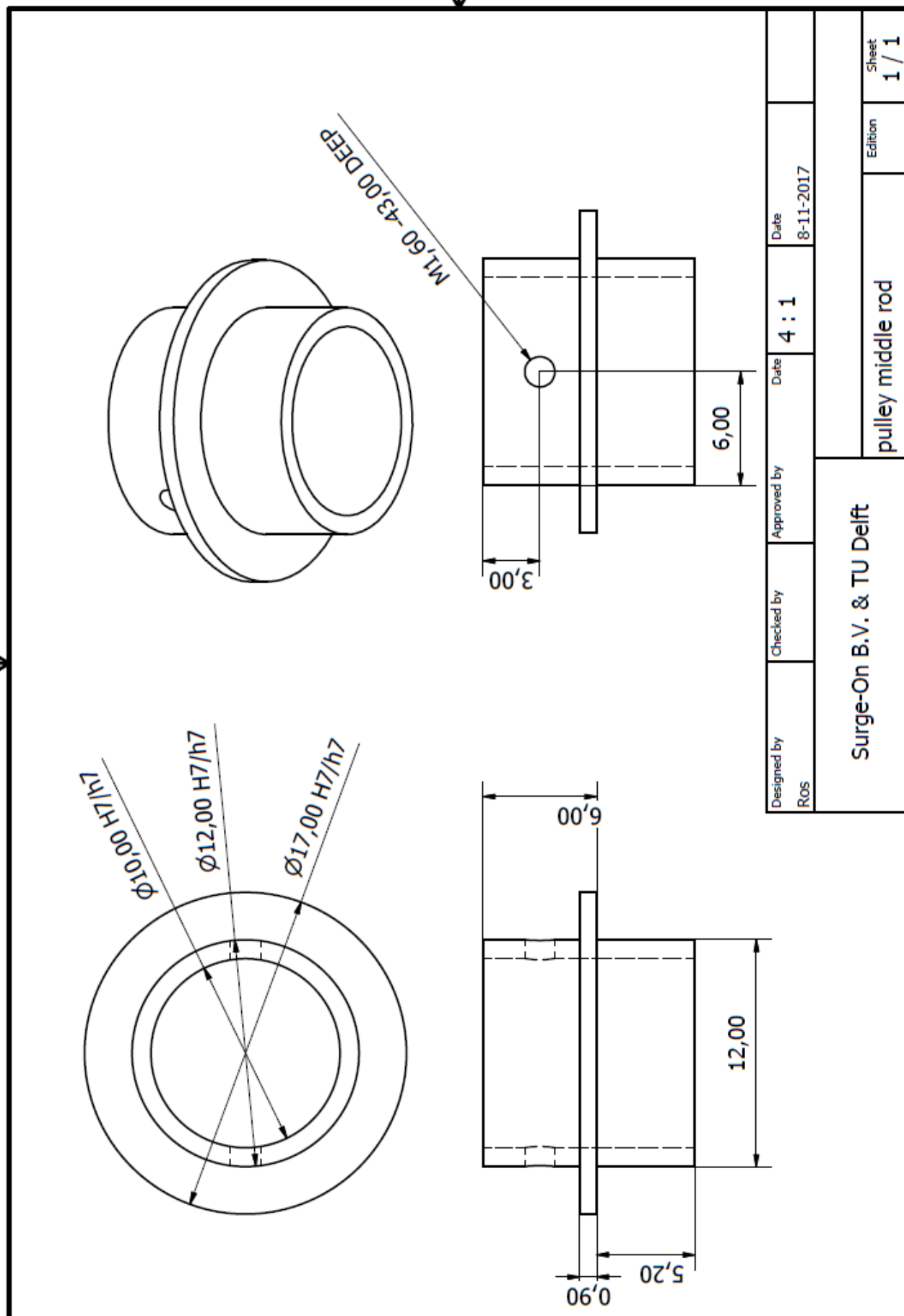


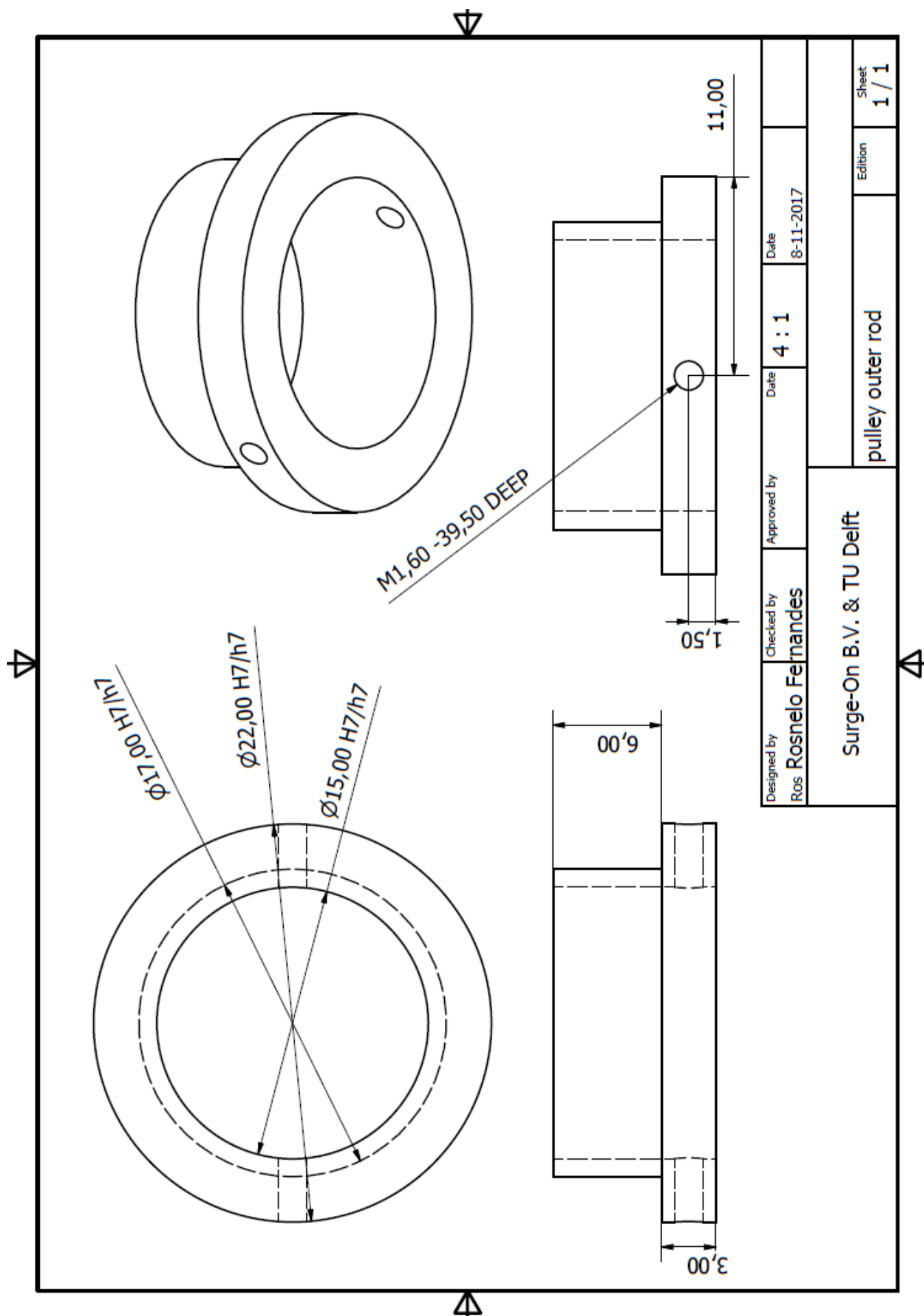


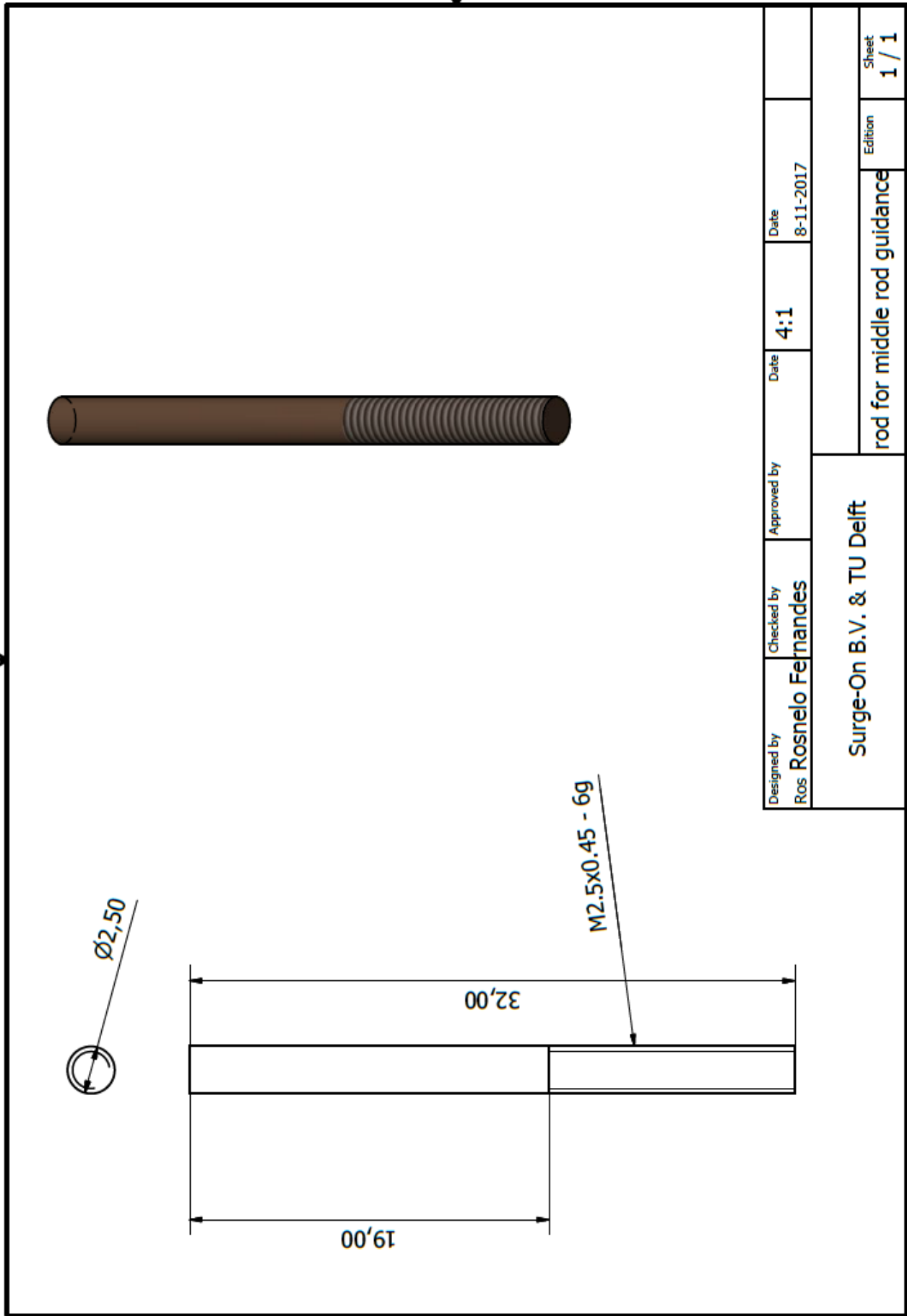




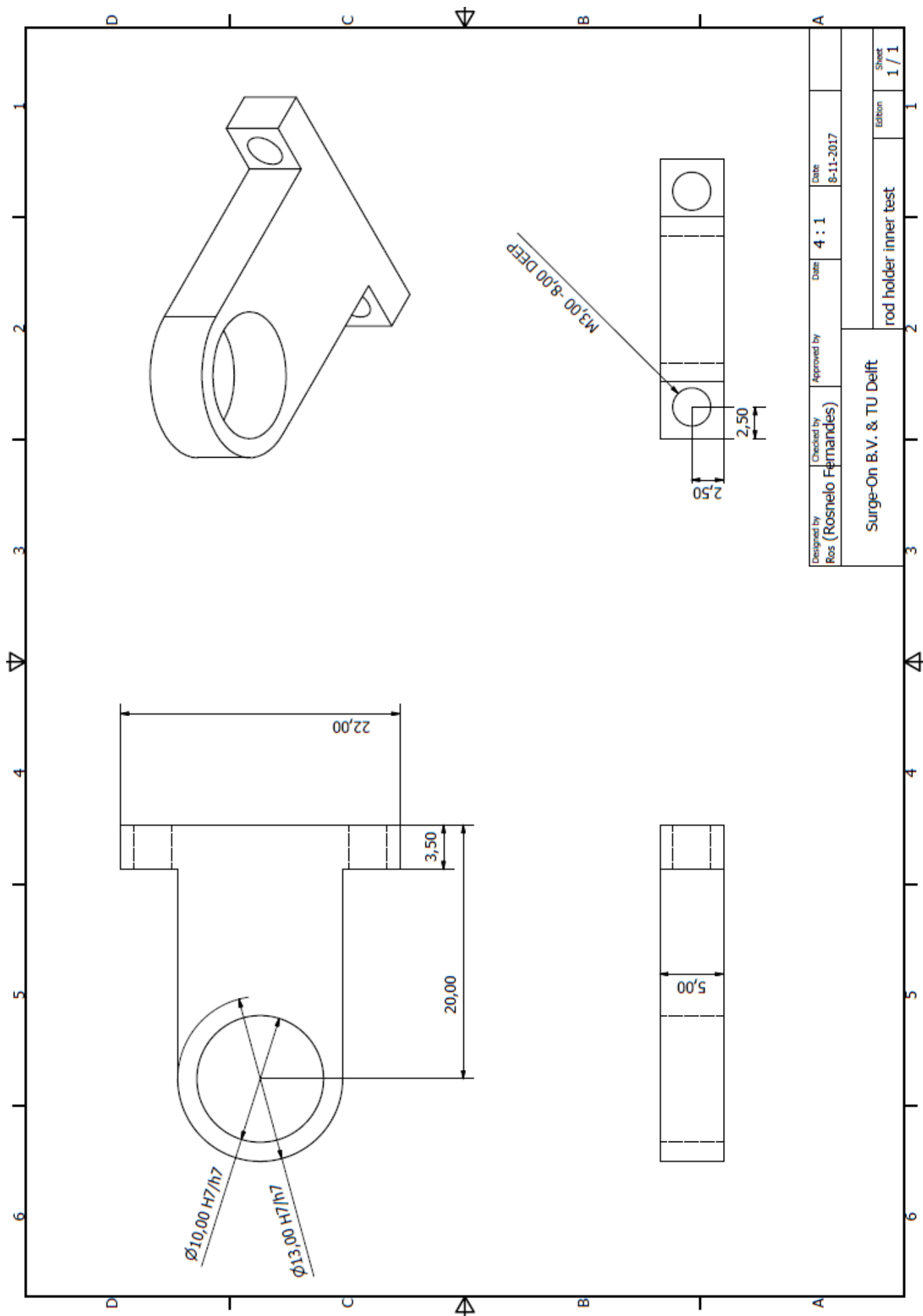


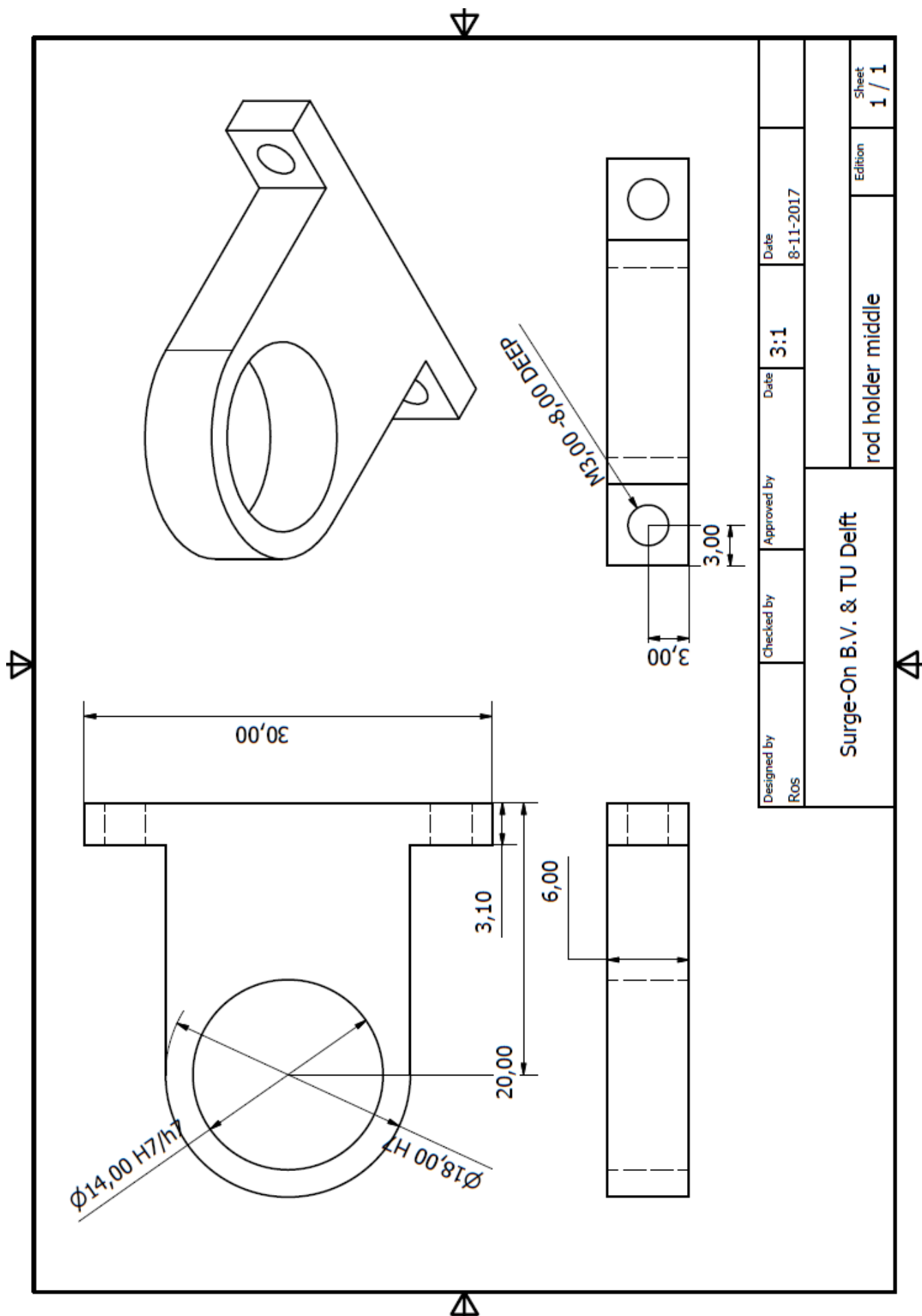


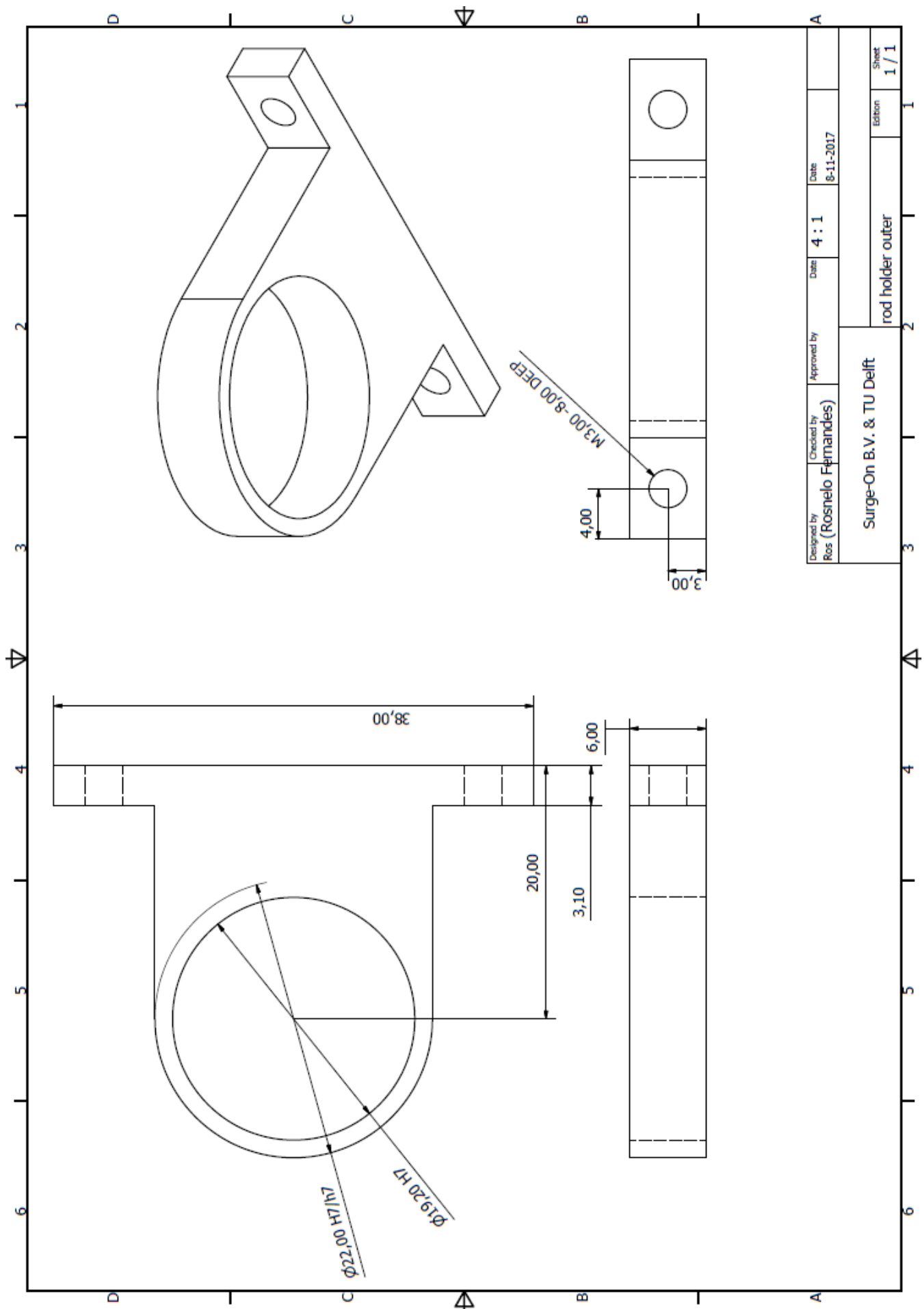


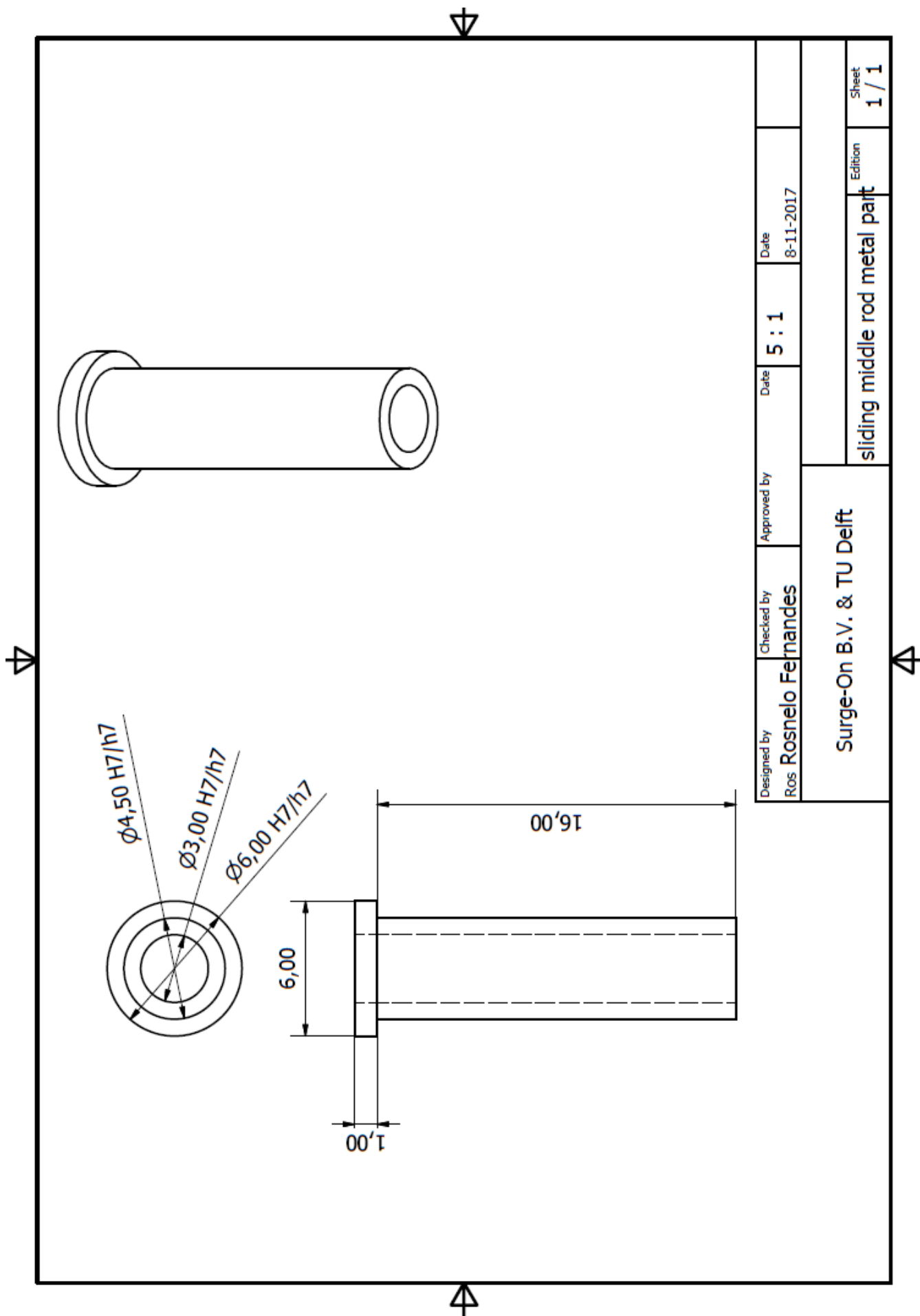


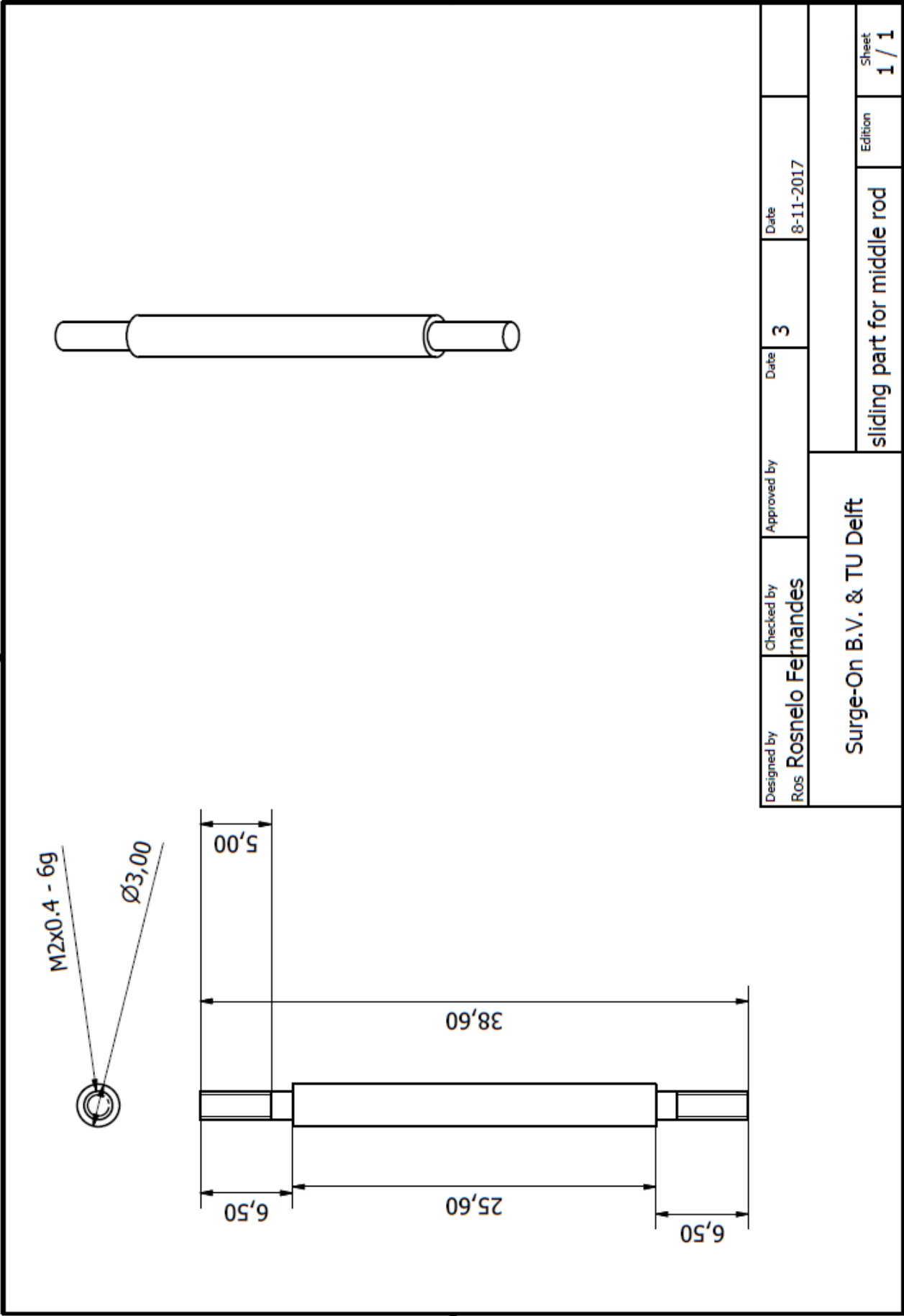
Designed by Ros Rosnelo Fernandes	Checked by Fernandes	Approved by	Date 4:1	Date 8-11-2017	
Surge-On B.V. & TU Delft			rod for middle rod guidance		
			Edition	Sheet 1 / 1	



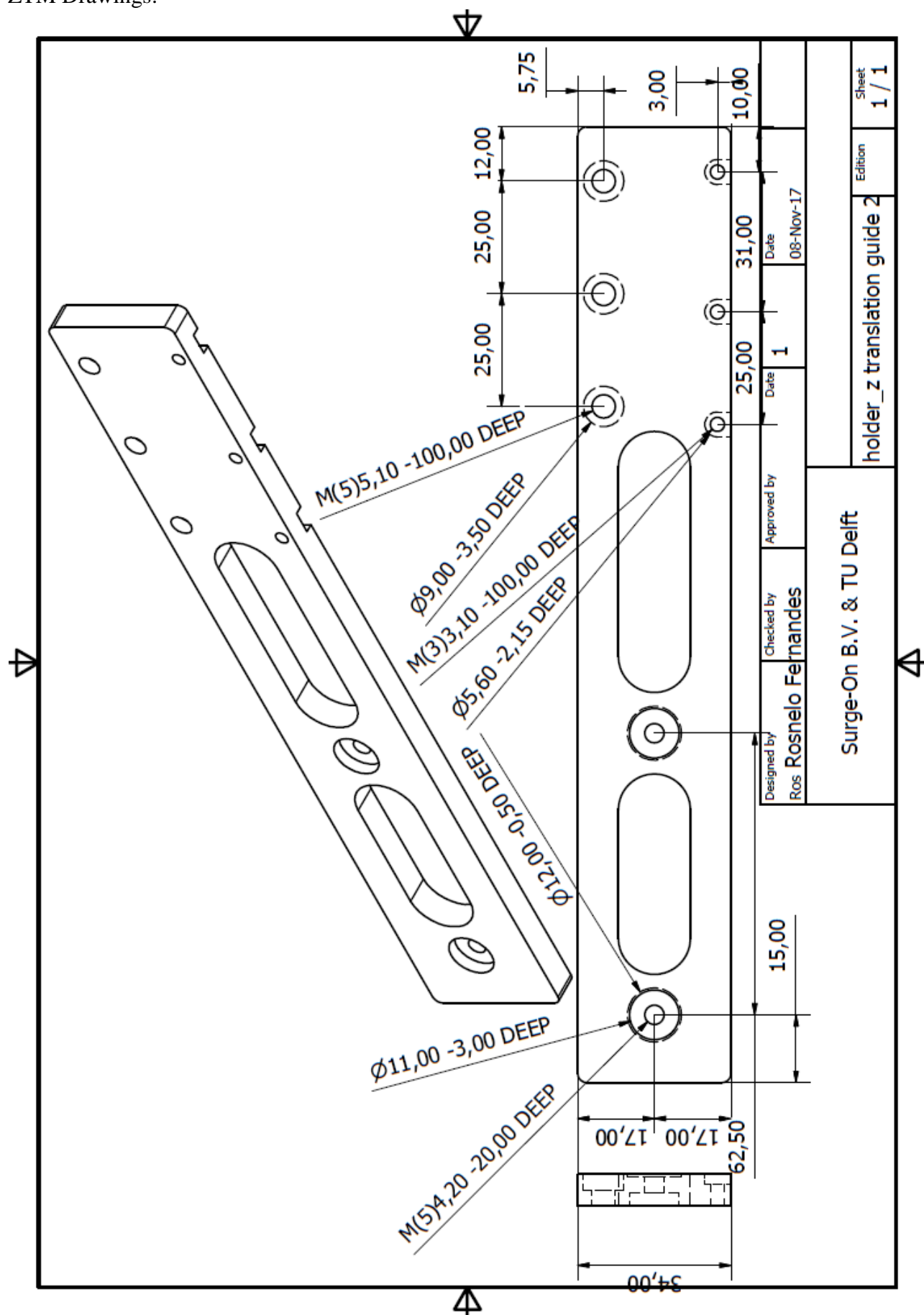


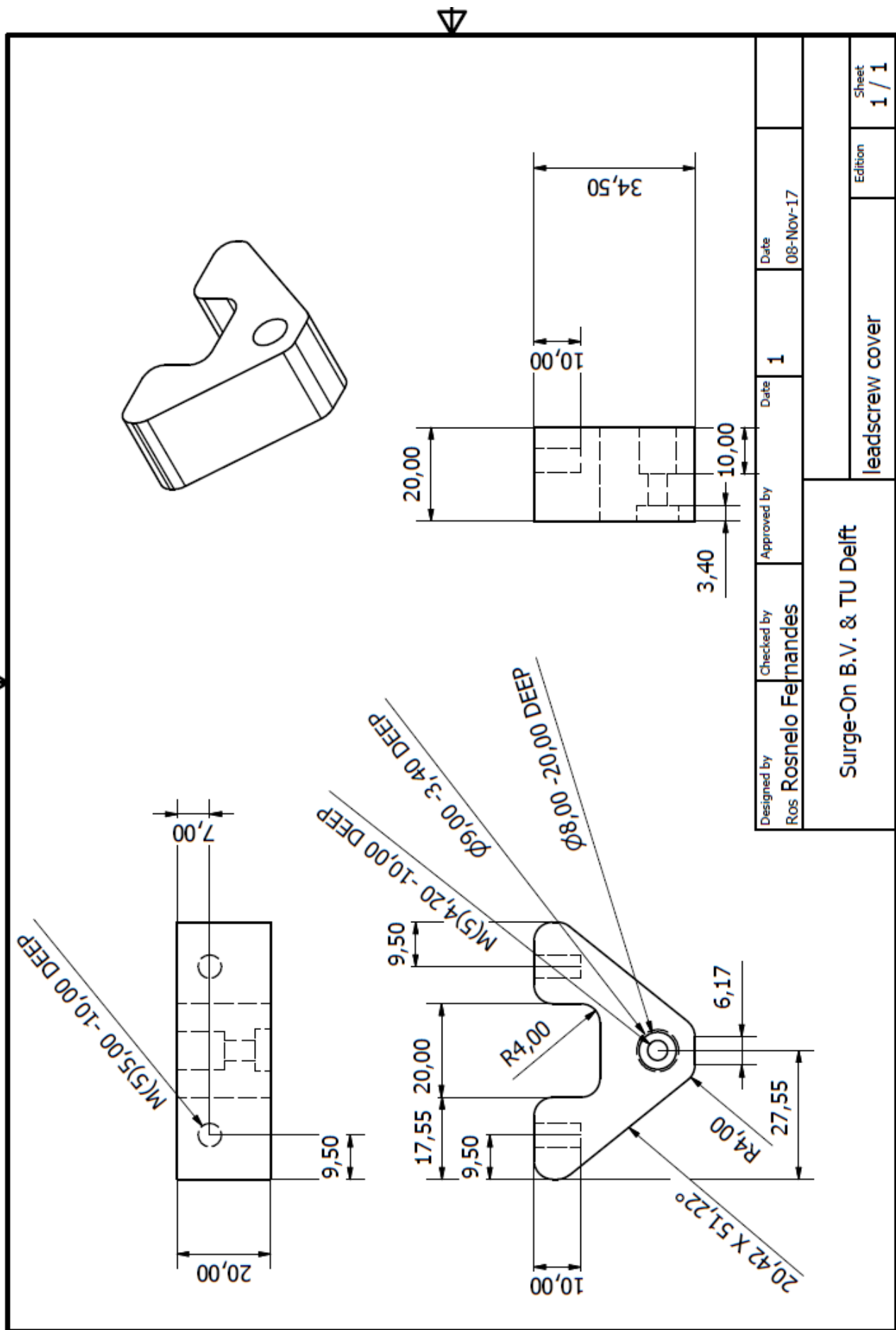


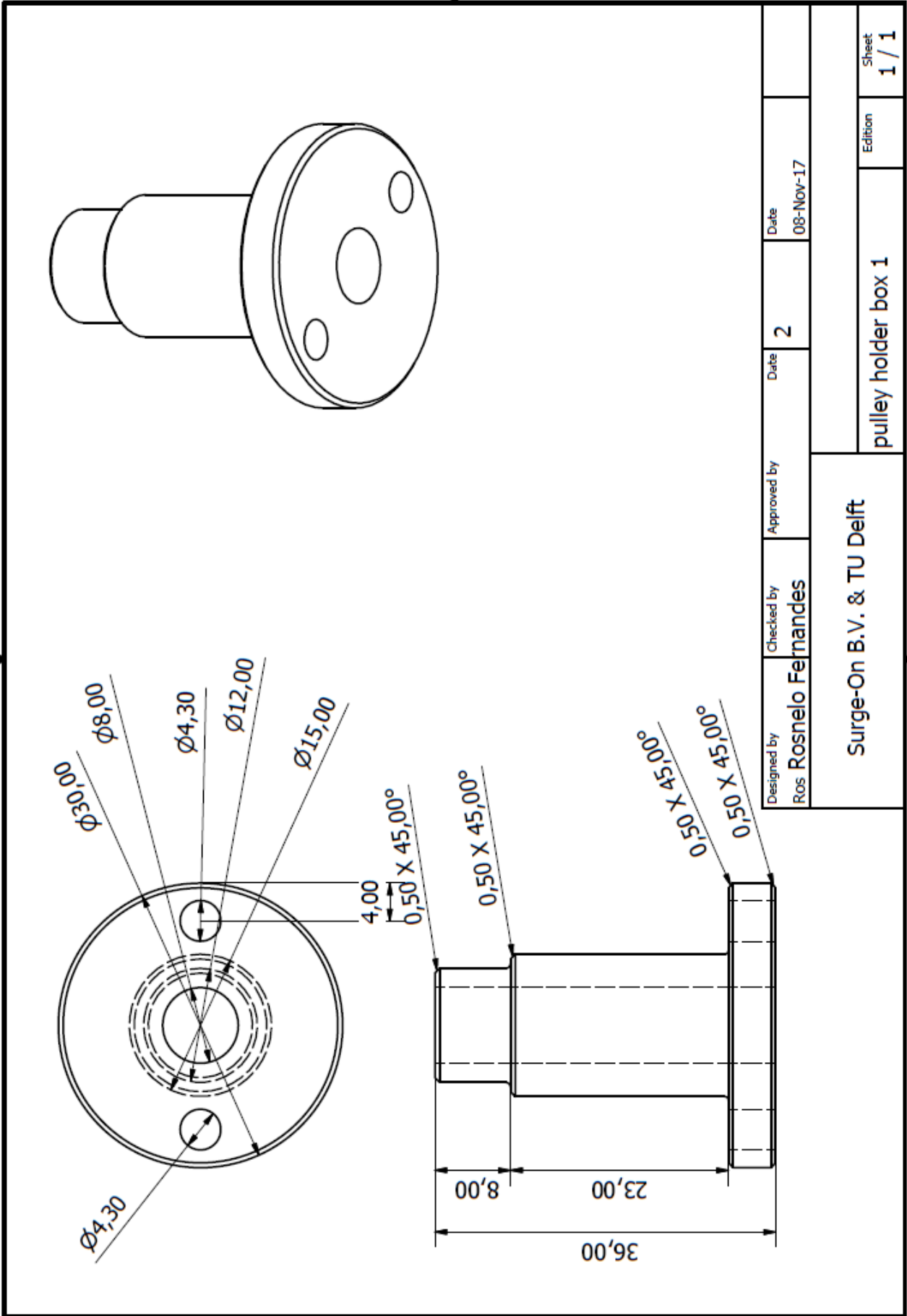


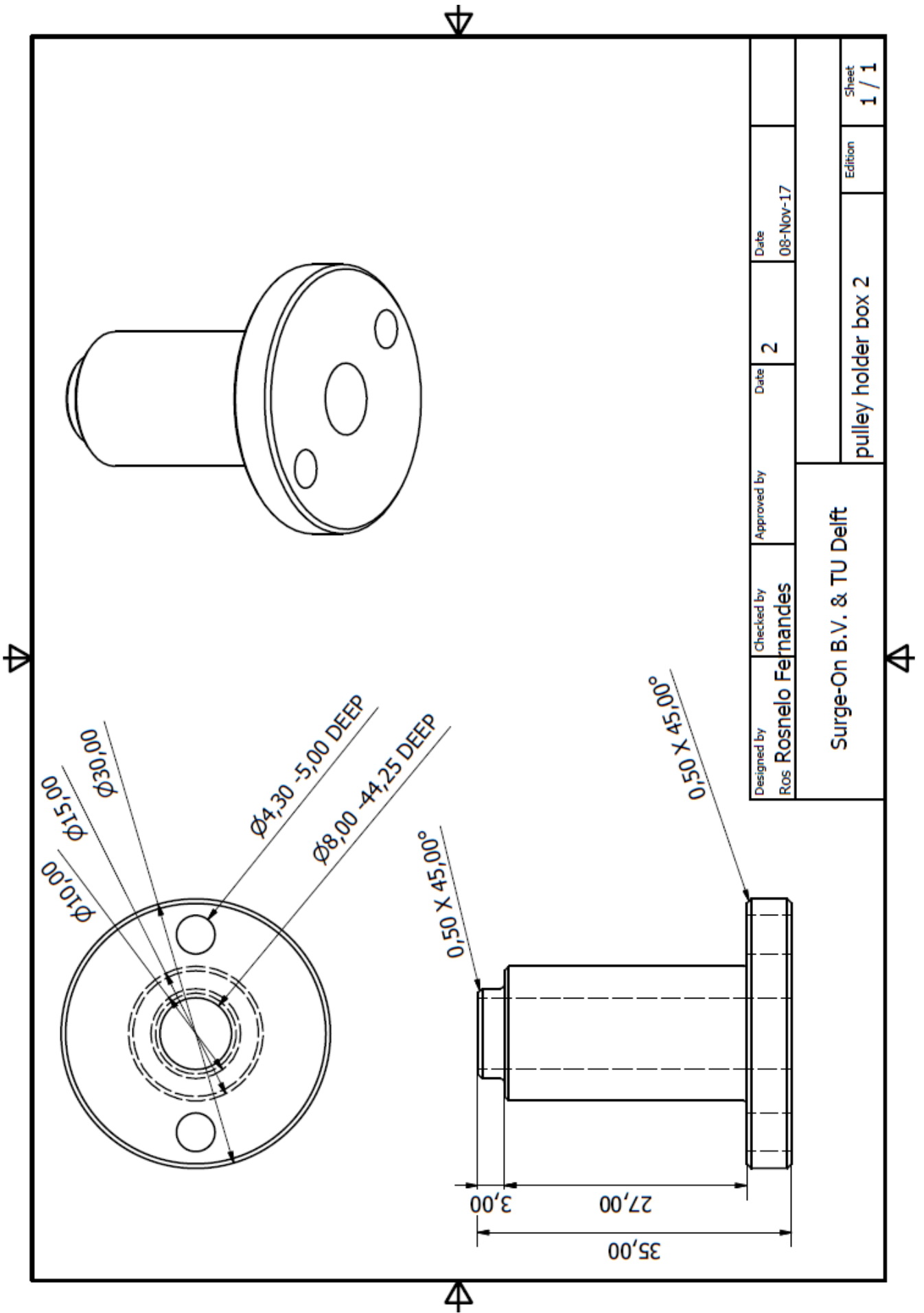


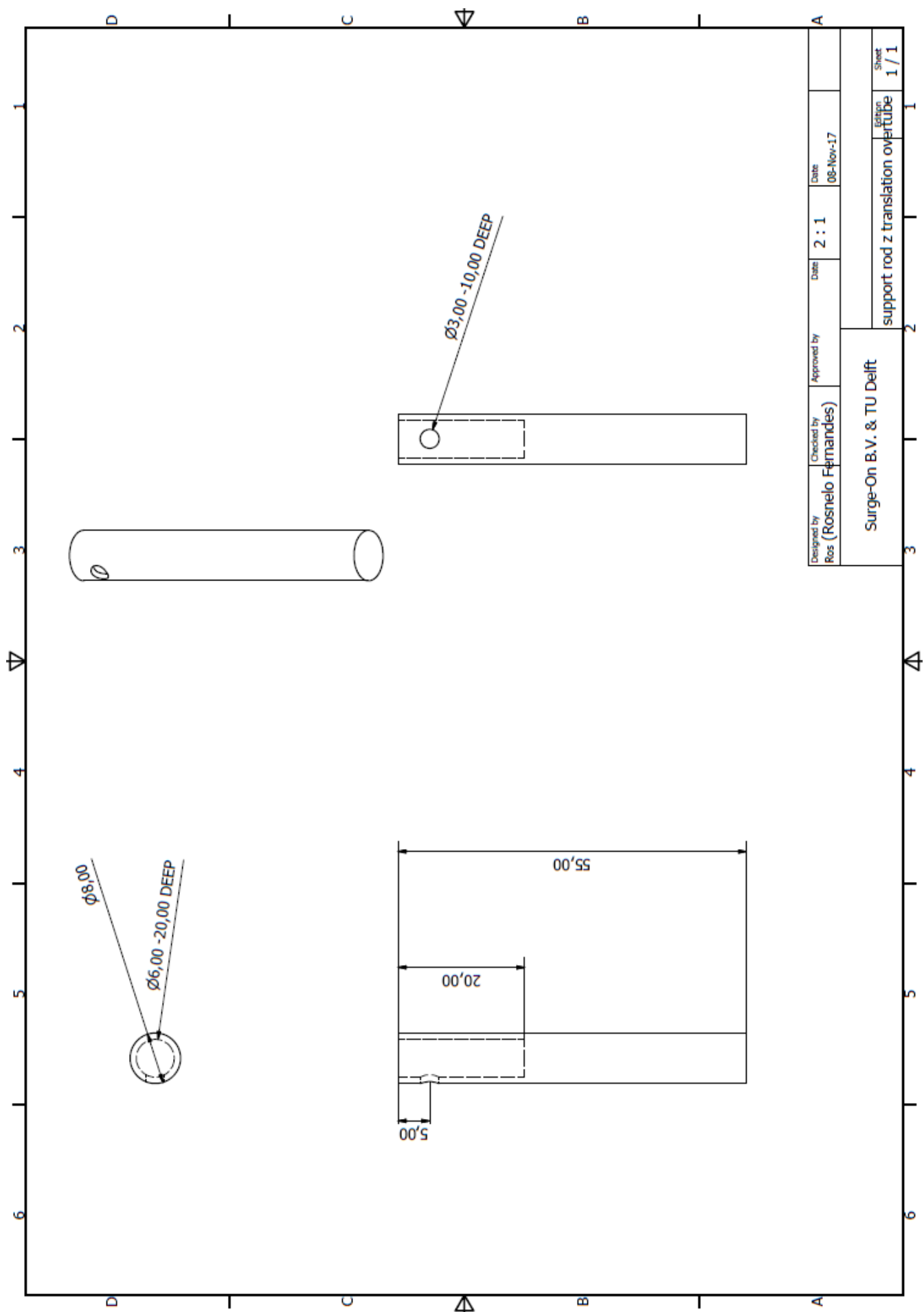
ZTM Drawings:



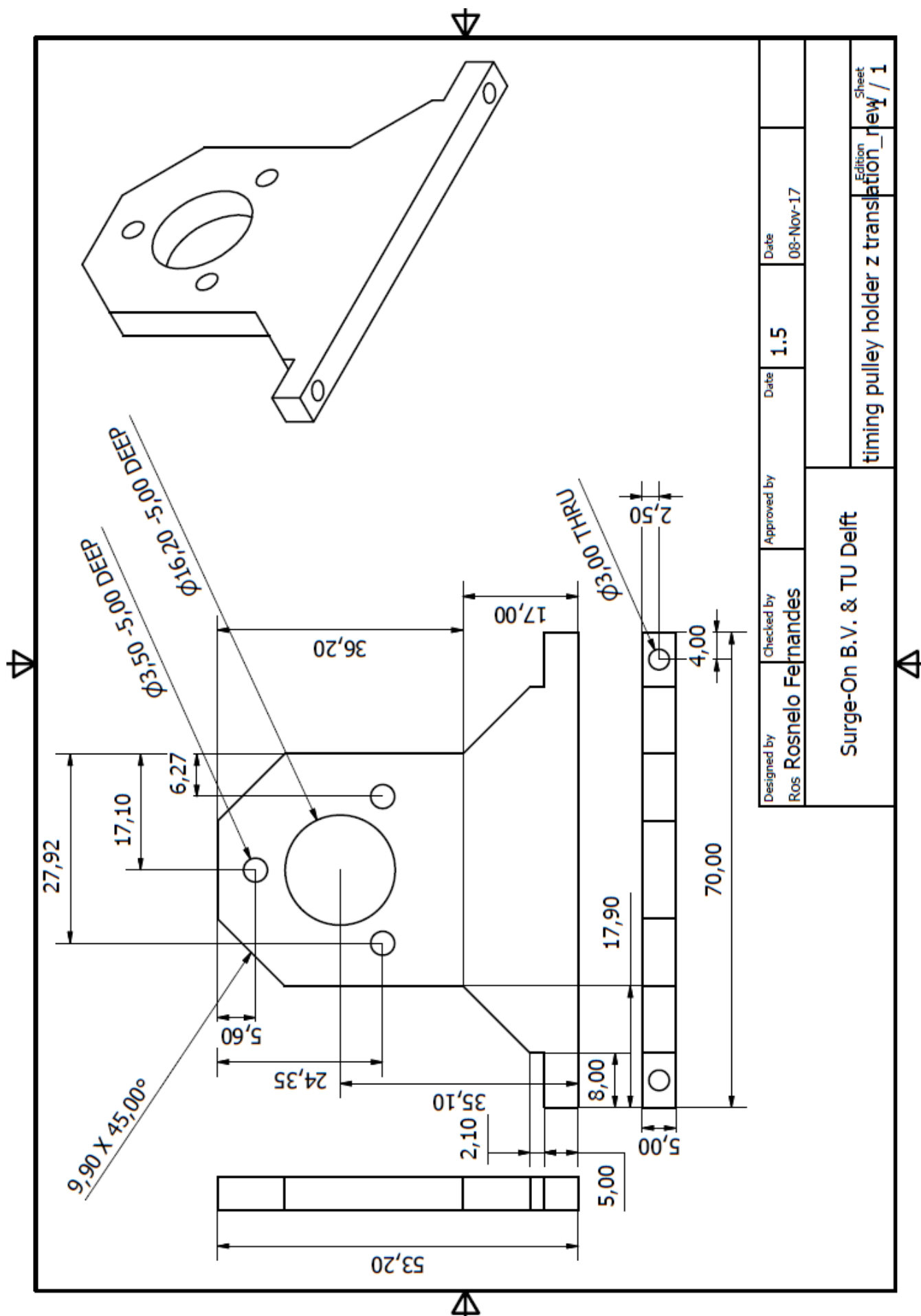


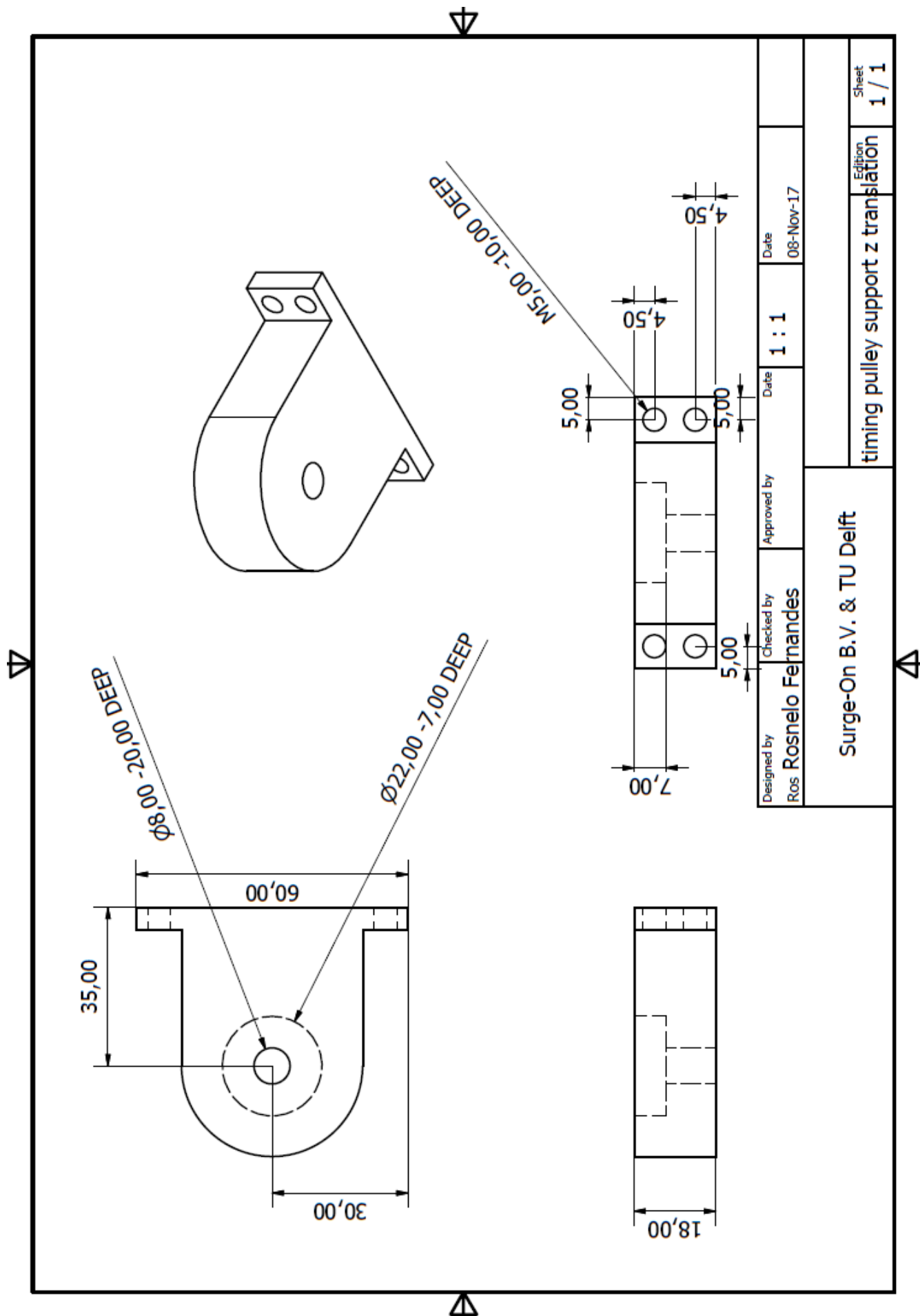


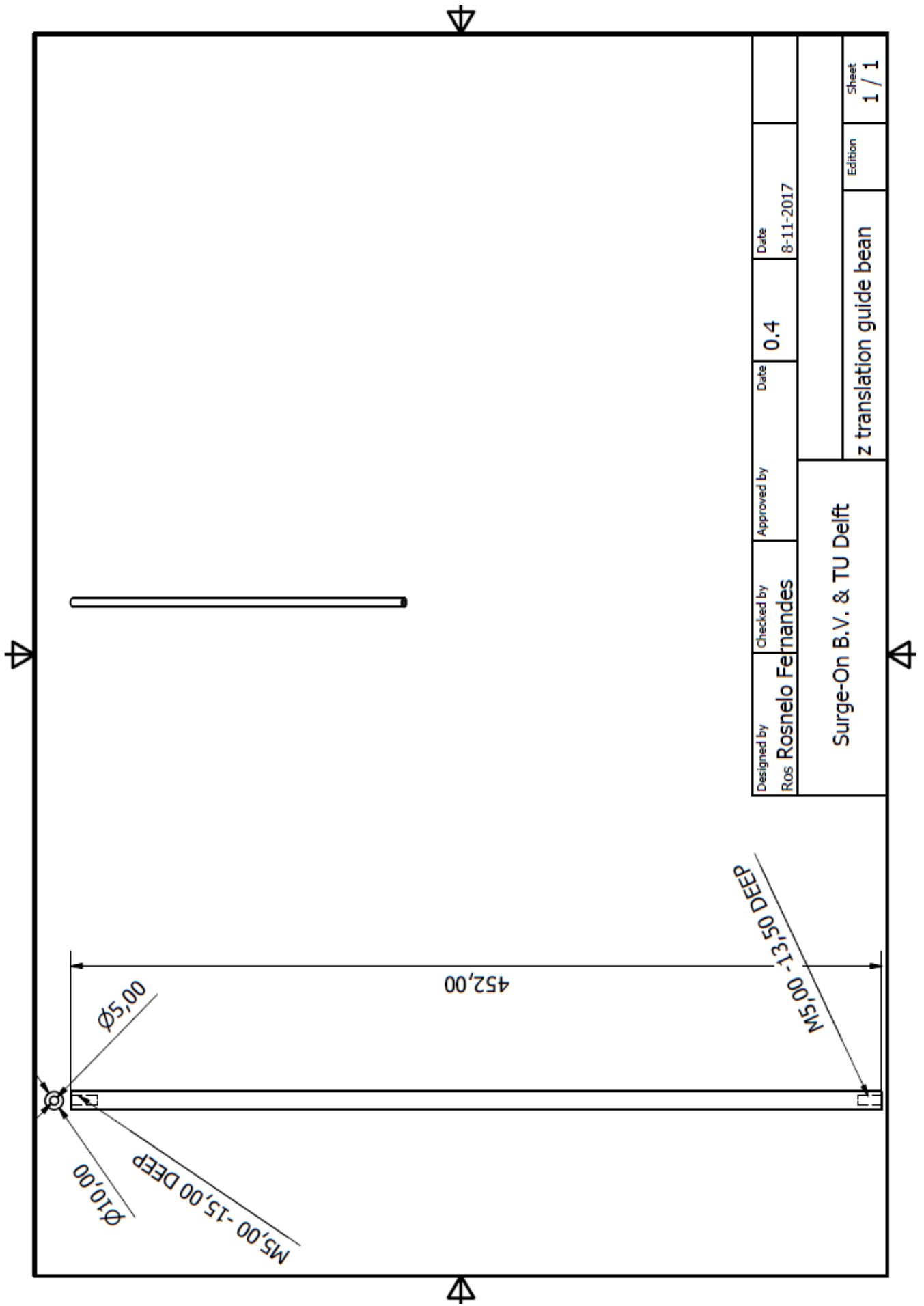


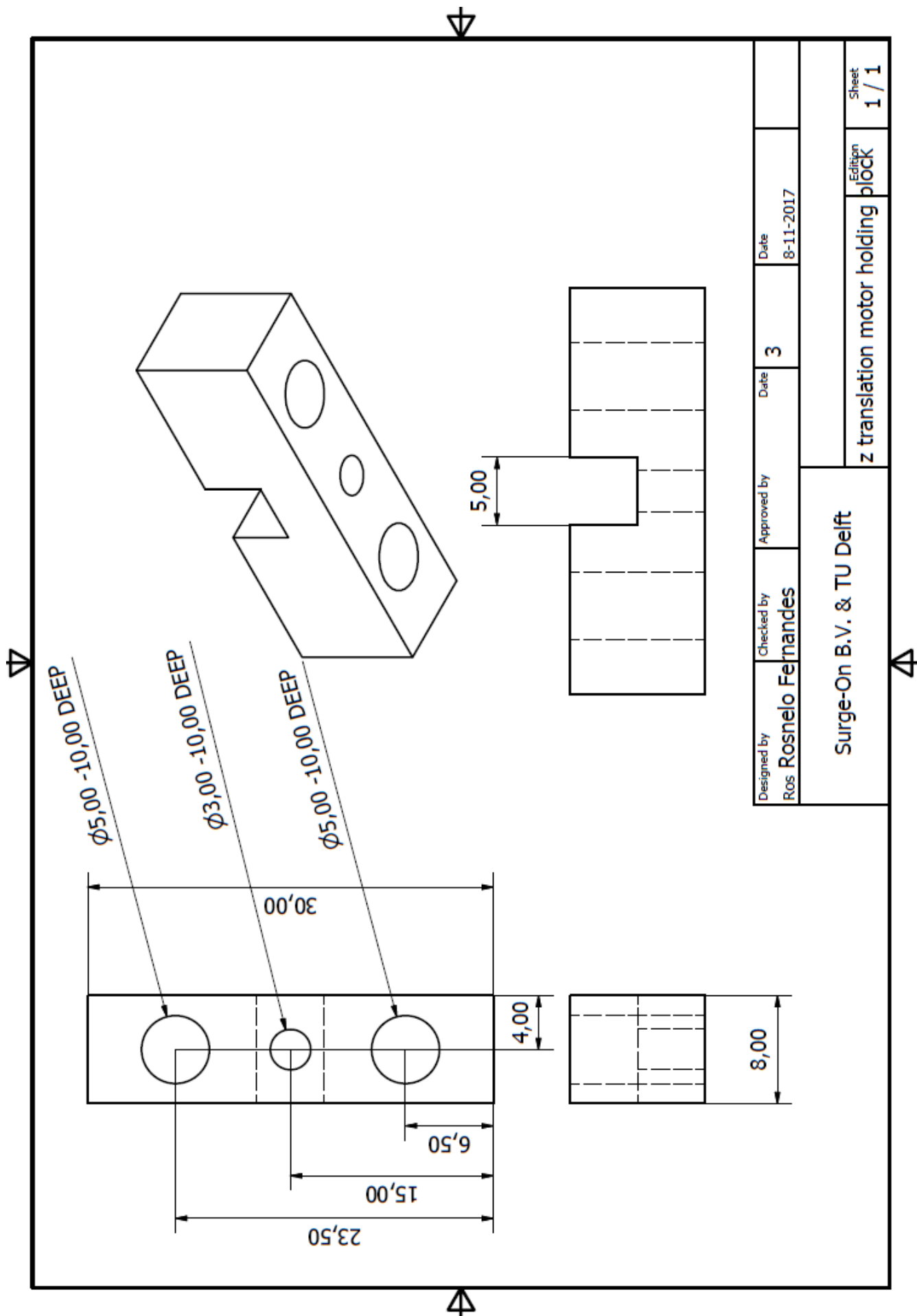


Designed by Ros (Rosnelo Fernandes)	Checked by Ros (Rosnelo Fernandes)	Approved by	Date 08-Nov-17	2 : 1	Date 08-Nov-17	1
Surge-On B.V. & TU Delft						1
support rod z translation over tube						1
Sheet 1 / 1						1









Bibliography

Photonics Media. (2018). Minimally invasive surgery market to double by 2019. [online] Available at: <https://www.photonics.com/Article.aspx?AID=55957> [Accessed 14 Jan. 2018].

Marketsandmarkets.com. (2018). Minimally Invasive Surgical Instruments Market worth 21.47 Billion USD by 2021. [online] Available at: <https://www.marketsandmarkets.com/PressReleases/minimally-invasive-surgical-devices.asp> [Accessed 14 Jan. 2018].

Kuo, C., Dai, J. and Dasgupta, P. (2012). Kinematic design considerations for minimally invasive surgical robots: an overview. *The International Journal of Medical Robotics and Computer Assisted Surgery*, 8(2), pp.127-145.

Walker Reynolds, J., 2001. The first laparoscopic cholecystectomy. *JSL: Journal of the Society of Laparoendoscopic Surgeons*, 5(1), p.89.

Vierra, M.D. (1995). Minimally Invasive Surgery. *Annual Review of Medicine*, 46(1), pp.147-158.

Veteran disability and long term disability Arizona MD + Lawyer. (2017). Complications Of Laparoscopic Surgery. [online] Available at: <https://www.danaise.com/complications-of-laparoscopic-surgery/> [Accessed 15 Jun. 2017].

Jaffray, B. (2005). Minimally invasive surgery. *Archives of Disease in Childhood*, 90(5), pp.537-542.
Fullum, T., Ladapo, J., Borah, B. and Gunnarsson, C. (2009). Comparison of the clinical and economic outcomes between open and minimally invasive appendectomy and colectomy: evidence from a large commercial payer database. *Surgical Endoscopy*, 24(4), pp.845-853.

Guthart, G.S. and Salisbury, J.K., 2000. The Intuitive/sup TM/telesurgery system: overview and application. In *Robotics and Automation, 2000. Proceedings. ICRA'00. IEEE International Conference on* (Vol. 1, pp. 618-621). IEEE.

Benz, S., Barlag, H., Gerken, M., Fürst, A. and Klinkhammer-Schalke, M. (2016). Laparoscopic surgery in patients with colon cancer: a population-based analysis. *Surgical Endoscopy*, 31(6), pp.2586-2595.

Prasad, A., Mukherjee, K., Kaul, S. and Kaur, M. (2010). Postoperative pain after cholecystectomy: Conventional laparoscopy versus single-incision laparoscopic surgery. *Journal of Minimal Access Surgery*, 6(4), p.114.

Pierre, F. and Chapron, C. (2005). Complications of laparoscopy: An inquiry about closed versus open-entry technique. *American Journal of Obstetrics and Gynecology*, 192(4), p.1352.

Jafari, M.D., Stamos, M.J. and Mills, S., (2015). Patient Positioning, Instrumentation, and Trocar Placement. In *Minimally Invasive Approaches to Colon and Rectal Disease* (pp. 15-24). Springer New York.

Harjai, M.M. and Kumar, A., (2015). Comparison of systemic stress response in open surgery versus laparoscopic surgery in children. *Continuing Medical Education (CME)*, 9(2), pp.1-52.

Mack, M. (2001). Minimally Invasive and Robotic Surgery. *JAMA*, 285(5), p.568.

Breedveld, P., Stassen, H., Meijer, D. and Jakimowicz, J. (1999). Manipulation in Laparoscopic Surgery: Overview of Impeding Effects and Supporting Aids. *Journal of Laparoendoscopic & Advanced Surgical Techniques*, 9(6), pp.469-480.

Hadavand, M., Mirbagheri, A., Behzadipour, S. and Farahmand, F. (2013). A novel remote center of motion mechanism for the force-reflective master robot of haptic tele-surgery systems. *The International Journal of Medical Robotics and Computer Assisted Surgery*, 10(2), pp.129-139.

- Wentink, B. (2001). Eye-hand coordination in laparoscopy - an overview of experiments and supporting aids. *Minimally Invasive Therapy & Allied Technologies*, 10(3), pp.155-162.
- Ir.transenterix.com. (2018). TransEnterix Announces US 510(k) FDA Clearance for Senhance Surgical Robotic System. [online] Available at: <http://ir.transenterix.com/releasedetail.cfm?ReleaseID=1043898> [Accessed 16 Jan. 2018].
- Kwoh, Y., Hou, J., Jonckheere, E. and Hayati, S. (1988). A robot with improved absolute positioning accuracy for CT guided stereotactic brain surgery. *IEEE Transactions on Biomedical Engineering*, 35(2): 153–160.
- Taylor, R., Funda, J., Eldridge, B., Gomory, S., Gruben, K., LaRose, D., Talamini, M., Kavoussi, L. and Anderson, J. (1995). A telerobotic assistant for laparoscopic surgery. *IEEE Engineering in Medicine and Biology Magazine*, 14(3): 279–288.
- Rovetta, A., Sala, R., Wen, X. and Togno, A. (1996). Remote control in telerobotic surgery. *IEEE Transactions on Systems, Man, and Cybernetics Part A: Systems and Humans*, 26(4): 438–444
- Madhani, A., Niemeyer, G. and Salisbury, J. (1998). The Black Falcon: a teleoperated surgical instrument for minimally invasive surgery. *Proceedings IEEE/RSJ International Conference on Intelligent Robots and Systems*, vol. 2, pp. 936– 944.
- Lanfranco, A., Castellanos, A., Desai, J. and Meyers, W. (2004). Robotic Surgery. *Annals of Surgery*, 239(1), pp.14-21.
- Lum, M., Friedman, D., Sankaranarayanan, G., King, H., Fodero, K., Leuschke, R., Hannaford, B., Rosen, J. and Sinanan, M. (2009). The RAVEN: Design and Validation of a Telesurgery System. *The International Journal of Robotics Research*, 28(9), pp.1183-1197.
- Ruurda, J., van Vroonhoven, T. and Broeders, I. (2002). Robot-assisted surgical systems: a new era in laparoscopic surgery. *Annals of the Royal College of Surgeons*, 84(4), pp.223-226.
- Cavusoglu, M., Tendick, F., Cohn, M. and Sastry, S. (1999). A laparoscopic telesurgical workstation. *IEEE Transactions on Robotics and Automation*, 15(4), pp.728-739.
- Taylor, R. and Stoianovici, D. (2003). Medical robotics in computer-integrated surgery. *IEEE Transactions on Robotics and Automation*, 19(5), pp.765-781.
- Ghanem, M., Senagore, A.J. and Shaheen, S., 2015. Cost and outcomes in robotic-assisted laparoscopic surgery. In *Robotic Approaches to Colorectal Surgery* (pp. 267-273). Springer International Publishing.
- Hagn, U., Konietzschke, R., Tobergte, A., Nickl, M., Jörg, S., Kübler, B., Passig, G., Gröger, M., Fröhlich, F., Seibold, U., Le-Tien, L., Albu-Schäffer, A., Nothhelfer, A., Hacker, F., Grebenstein, M. and Hirzinger, G. (2009). DLR MiroSurge: a versatile system for research in endoscopic telesurgery. *International Journal of Computer Assisted Radiology and Surgery*, 5(2), pp.183-193.
- Giulianotti, P. (2003). Robotics in General Surgery. *Archives of Surgery*, 138(7), p.777.
- van den Bedem, L., (2010). Realization of a demonstrator slave for robotic minimally invasive surgery. *Praca doktorska*, Technische Universiteit Eindhoven.
- van Aaken, R.J.T. (2006). Design of a 4 DOF slave robot instrument manipulator for MIS.
- Yamanaka, H., Makiyama, K., Osaka, K., Nagasaka, M., Ogata, M., Yamada, T. and Kubota, Y. (2015). Measurement of the Physical Properties during Laparoscopic Surgery Performed on Pigs by Using Forceps with Pressure Sensors. *Advances in Urology*, 2015, pp.1-10.
- Fumagalli, M., 2014. The Role of Force Perception and Backdrivability in Robot Interaction. In *Increasing Perceptual Skills of Robots Through Proximal Force/Torque Sensors* (pp. 3-12). Springer, Cham.

- Hernia.org. (2018). Laparoscopic Inguinal Hernia Repair (Keyhole Surgery) | The British Hernia Centre. [online] Available at: <https://www.hernia.org/laparoscopic-inguinal-hernia-repair-keyhole-surgery/> [Accessed 24 Jan. 2018].
- Rutala, W. and Weber, D. (2013). Disinfection and sterilization: An overview. *American Journal of Infection Control*, 41(5), pp.S2-S5.
- Barrera, K., Chung, P. and Sugiyama, G., 2017. Robotic Approach to Cholecystectomy. In *Updates in Gallbladder Diseases*. InTech.
- Surge-on Medical. (2018). Steerable Punch: the new arthroscopy instrument - Surge-on Medical. [online] Available at: <http://www.surge-on.nl/arthroscopy/> [Accessed 16 Jan. 2018].
- J. Berendsen, 2018. Clinical (re)use of modular robotic surgical system: how to ensure sterility? *Medical Design and Evaluation*, MISIT Lab, TU Delft.
- Alfa-Wali, M. and Osaghae, S. (2017). Practice, training and safety of laparoscopic surgery in low and middle-income countries. *World Journal of Gastrointestinal Surgery*, 9(1), p.13.
- Morad Asaad, A. and Ahmad Badr, S. (2016). Surgical Site Infections in Developing Countries: Current Burden and Future Challenges. *Clinical Microbiology: Open Access*, 05(06).
- Dogra, P.N., (2012). Current status of robotic surgery in India. *J Int Med Sci Acad*, 25, p.145.
- The Economic Times. (2018). India can become second largest market for robotic surgery: Vattikuti Foundation. [online] Available at: <https://economictimes.indiatimes.com/industry/healthcare/biotech/healthcare/india-can-become-second-largest-market-for-robotic-surgery-vattikuti-foundation/articleshow/61712340.cms> [Accessed 14 Feb. 2018].
- Mir, I., Mohsin, M., Malik, A., Shah, A. and Majid, T. (2008). A structured training module using an inexpensive endotrainer for improving the performance of trainee surgeons. *Tropical Doctor*, 38(4), pp.217-218.
- Pahwa, M., Pahwa, A., Girotra, M., Abrahm, R., Kathuria, S. and Sharma, A. (2014). Defining the Pros and Cons of Open, Conventional Laparoscopy, and Robot-Assisted Pyeloplasty in a Developing Nation. *Advances in Urology*, 2014, pp.1-6.
- Lawlor, K.B., 2012. SMART Goals: How the application of SMART goals can contribute to achievement of student learning outcomes. *Developments in Business Simulation and Experiential Learning*, 39.
- Swanson, M., 2016. Implementation of a SMART Goal Intervention for Diabetic Patients: A Practice Change in Primary Care.
- Imasaki, N. and Tomizuka, M., 1995, May. Adaptive control of robot manipulators with anti-backlash gears. In *Robotics and Automation, 1995. Proceedings., 1995 IEEE International Conference on* (Vol. 1, pp. 306-311). IEEE.
- Vahid-Araghi, O. and Golnaraghi, F., 2010. Friction-induced vibration in lead screw drives. *Springer Science & Business Media*.
- Kovacevic, A.. *Mechanical Analysis and Design ME 2104: Mechanical Analysis Belt and chain drives*. [ebook] London: City University London, p.10. Available at: <http://www.staff.city.ac.uk/~ra600/ME2105/Analysis/ME2104-A-3.pdf> [Accessed 20 Jan. 2018].
- Armstrong, P. (2016). *Mechanical Technology*. [ebook] p.20. Available at: <http://slideplayer.com/slide/4773725/> [Accessed 20 Jan. 2018].
- Physics.bu.edu. (2018). *Elasticity*. [online] Available at: <http://physics.bu.edu/~duffy/py105/notes/Elasticity.html> [Accessed 29 Mar. 2018].

PolyFlex™ Technical Data Sheet. (2018). [ebook] Shanghai · New York · Utrecht · Tokyo: Polymaker. Available at: http://www.polymaker.com/wp-content/uploads/2015/06/PolyFlex_TDS-v1.pdf [Accessed 29 Mar. 2018].

CAC.C Studio V. (2018). Design Process. [online] Available at: <https://caccstudiov.com/2015/01/30/design-process/> [Accessed 25 Jan. 2018].

Cervone, H. (2009). Applied digital library project management. OCLC Systems & Services: International digital library perspectives, 25(4), pp.228-232.

EnvisionTEC. (2018). R5 | 3D Printing Materials | EnvisionTEC. [online] Available at: <https://envisiontec.com/3d-printing-materials/perfactory-materials/r5/> [Accessed 13 Feb. 2018].